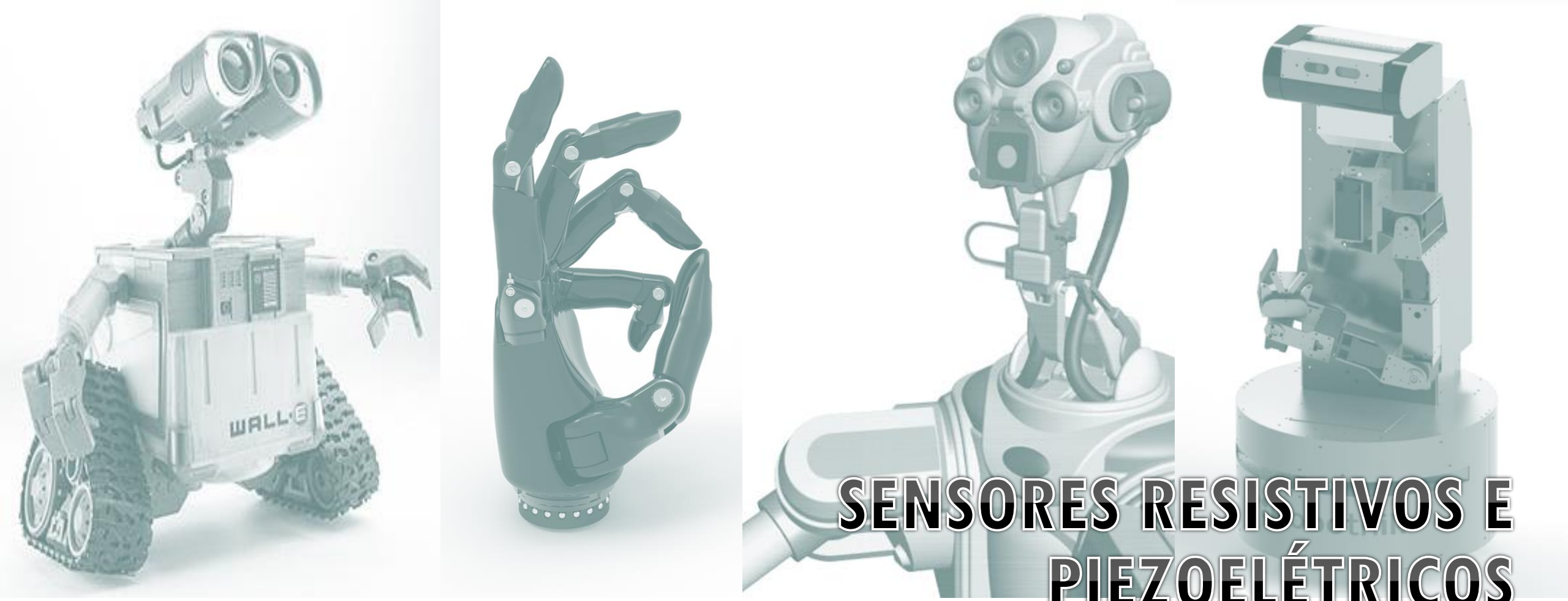

SENSORES RESISTIVOS E PIEZOELÉTRICOS

GMSIE – Grupo de Mecânica dos Sólidos e Impacto em Estruturas

Larissa Driemeier
Marcilio Alves
Rafael T. Moura

Baseado em Resistive, Capacitive, Inductive, and Magnetic Sensor Technologies
WY Du, CRC Press, e outras fontes citadas

RESISTÊNCIA E RESISTIVIDADE

Resistividade elétrica (também resistência elétrica específica) ρ é uma medida da oposição de um material ao fluxo de corrente elétrica. Quanto mais baixa for a resistividade mais facilmente o material permite a passagem de uma carga elétrica. Unidade: ohm metro (Ωm).

A resistência elétrica R de um dispositivo indica as propriedades de um objeto, componente ou corpo feito de determinado material, com dimensões e formato específicos. A resistência elétrica R é dada por:

$$R = \rho \frac{L}{A}$$

Material	Resistividade
Alumínio	0,029
Antimônio	0,417
Bronze	0,067
Chumbo	0,22
Cobre puro	0,0162
Constantan	0,5
Estanho	0,115
Grafite	13
Ferro puro	0,096
Latão	0,067
Mercúrio	0,96
Nicromo	1,1
Níquel	0,087
Ouro	0,024
Prata	0,0158
Tungstêio	0,055
Zinco	0,056

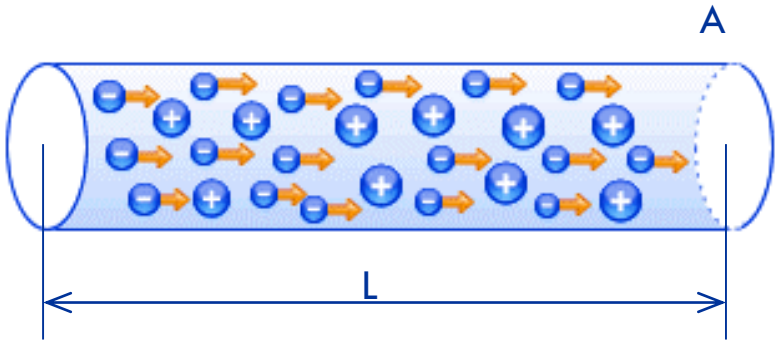

SENSORES RESISTIVOS

$$\frac{1}{R}\frac{\partial R}{\partial X} = \frac{1}{\rho}\frac{\partial \rho}{\partial X} + \frac{1}{L}\frac{\partial L}{\partial X} - \frac{1}{A}\frac{\partial A}{\partial X}$$

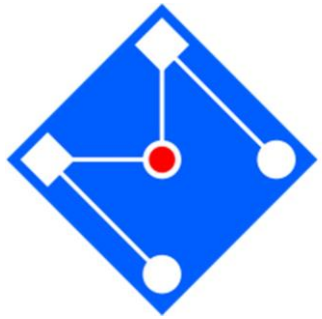

- Sensores potenciométricos: Mudança de resistência devido a mudança de posição linear ou angular
- Sensores resistivos de temperatura (RTS): Mudança da resistência causada por variação de temperatura (efeito termoresistivo)
- Sensores piezorresistivos: Resistência muda quando uma força é aplicada a um condutor piezorresistivo (efeito piezorresistivo)
- Sensores magnetorresistivos: Resistência muda na presença de um campo magnético externo (efeito magnetorresistivo)
- Sensores fotorresistivos: Diminuição da resistência quando a luz atinge um material fotocondutivo (efeito fotorresistivo)
- Sensores quimiorresistivos: Condutividade do material/solução se altera devido a reações químicas que alteram o número de elétrons ou concentração de íons.
- Sensores biorresistivos: Mudança na bioresistência, em proteínas ou células, induzida por variações estruturais e interações biológicas.

SENSORES POTENCIOMÉTRICOS

- Linear
- Angular

1. Noticeable mechanical load (friction)
2. Need for a physical coupling with the object
3. Low speed
4. Friction and excitation voltage cause heating of the potentiometer
5. Low environmental stability

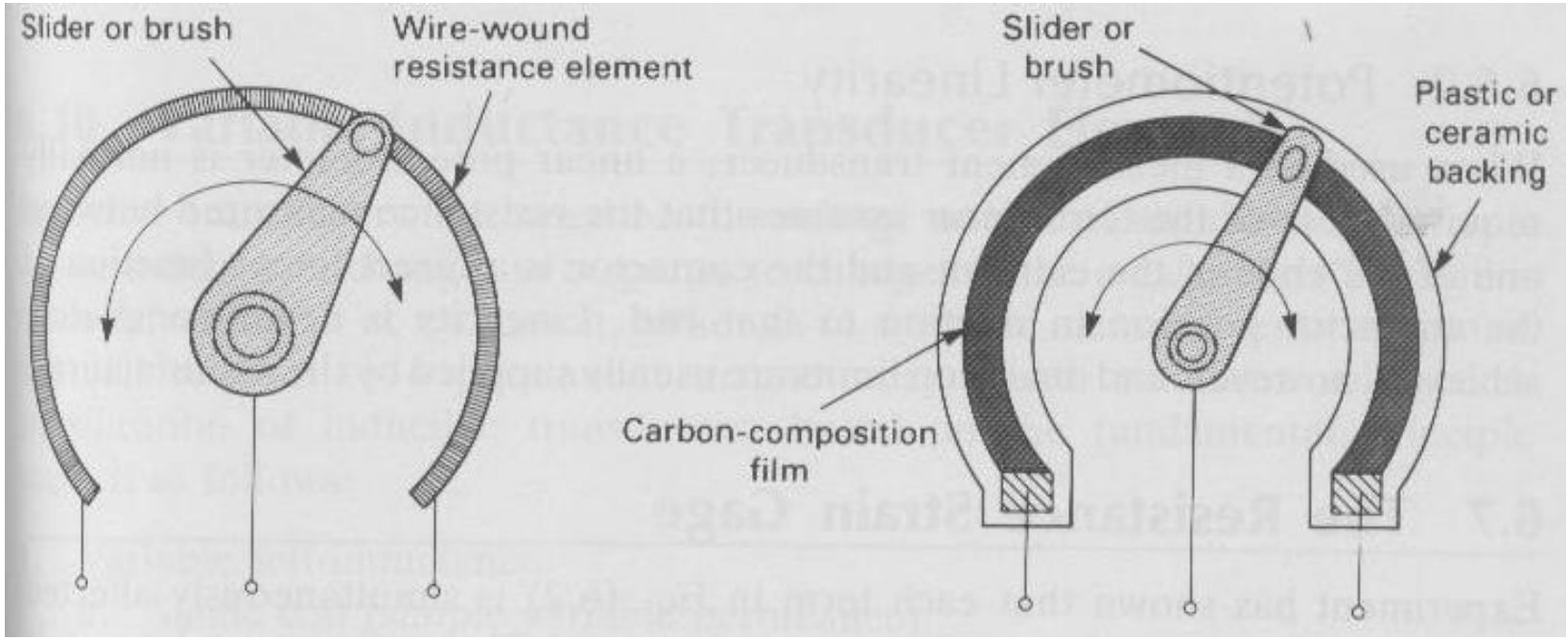

TIPOS DE SENSORES POTENCIOMÉTRICOS

Linear

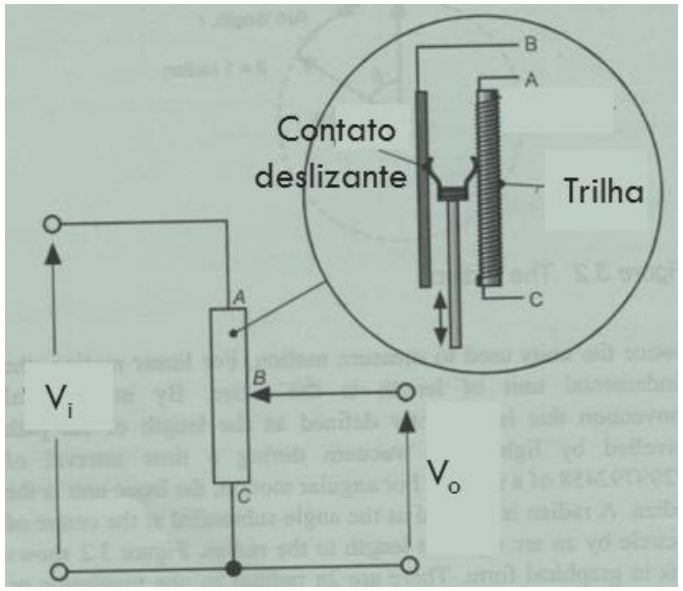

Angular

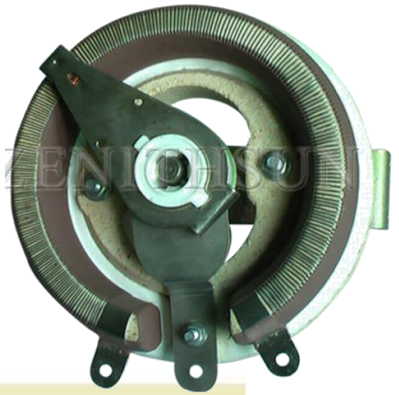

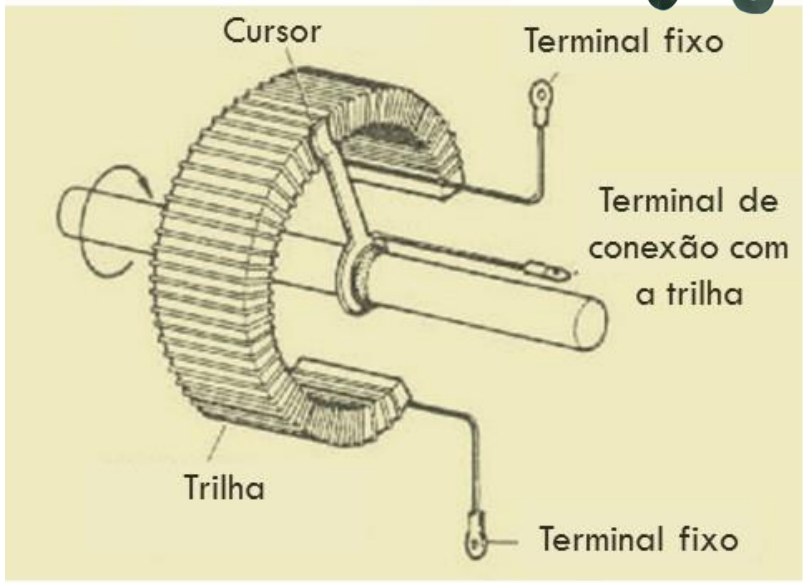

PROJETO

Linear

- Possui **3 terminais;**
- **Banhado a ouro** para evitar a corrosão;
- Resistor de alta qualidade com baixo coeficiente de temperatura (estabilidade e evitar corrosão);
- Trilha com material de boa qualidade (vida longa e pouco ruído);
- Arruelas de pressão para **evitar folgas;**
- Ligado ao objeto que se move por rosca, chanfros ou mola.
- Verificar em projeto: comprimento de curso, valor de resistência, limitações de espaço, qualidade dos elementos, como conectar o sensor ao elemento móvel a ser medido.

Rotacional

- Single-turn: 0 a ~240-330^0 (acima 10% erro, mais econômicos)
- Multi-turn: 5,10,20,25 voltas – maior resolução (1%, controle fino, maior linearidade e estabilidade)
- Possui 3 terminais
- Resistor de alta qualidade com baixo coeficiente de temperatura (estabilidade e evitar corrosão);
- Verificar em projeto: ângulo ou rotação a ser medido, valor de resistência, resolução.

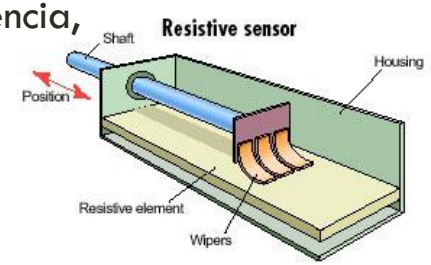


0
10
20
30
40
50
60
70
80
90

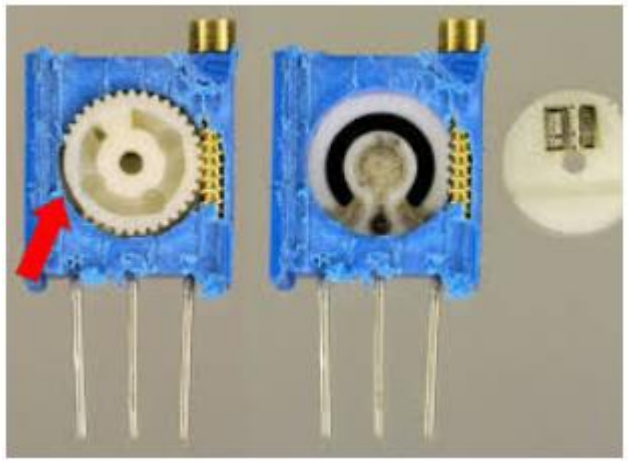


3G3

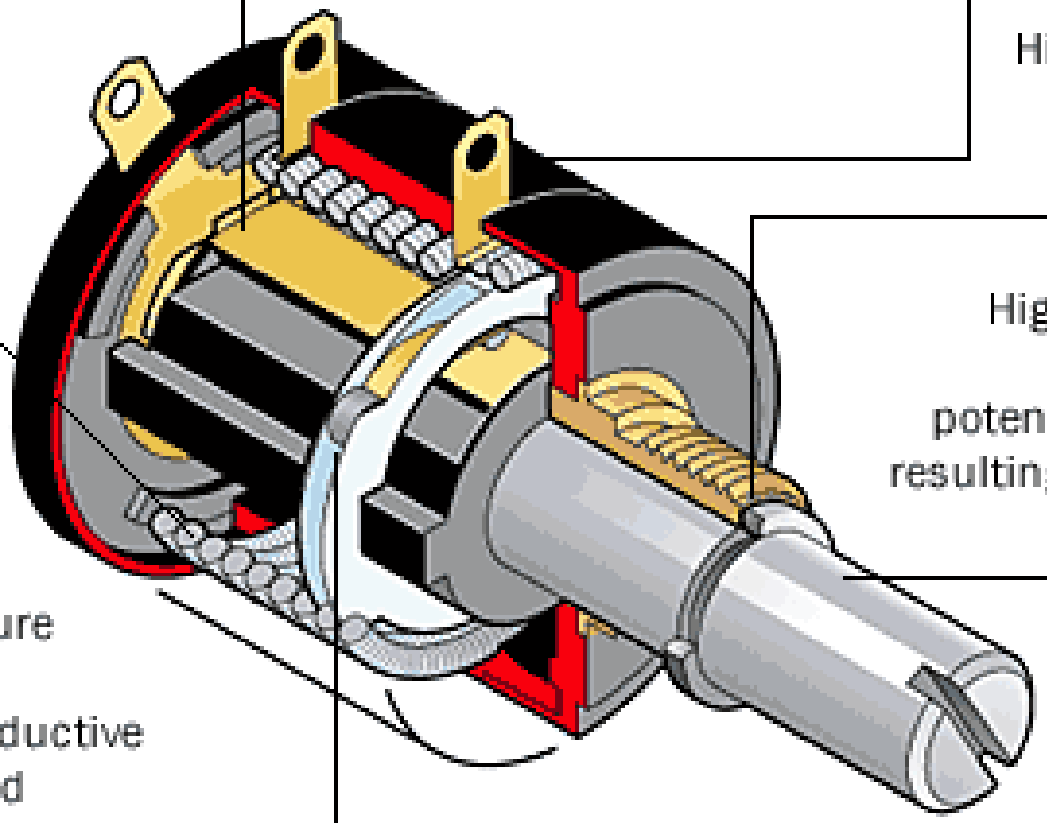

GOLD PLATED TERMINALS AND CONTINUITY BAR:
Do not corrode or tarnish.

HOUSING:
High temp. plastic
Durable in harsh
environments.

BRASS BUSHINGS:
Hign quality brass bushings.
Provde better support for
potentiometer shaft side loads,
resulting in long life expectancies

STAINLESS STEEL SHAFT:
Non-corrosive. Many
modifications available
for ease of linking
to your system

ELEMENT:
Wirewound (shown):
Most commonly used
in multi-turns. Offers
better stability and
linearity. Low temperature
coefficient.
Hybrid: Made with conductive
plastic over a wirewound
element. Lower inductance,
better resolution, and
longer life

PRECIOUS METAL WIPER:
Platinum alloy ensures
long life and low noise.

GOLD PLATED TERMINALS:
Do not corrode or tarnish

STAINLESS STEEL SHAFT:
Non-corrosive. Many modifications available for ease of linking to your system

PRECIOUS METAL SLIP RING CONTACTS:
For low noise and long life

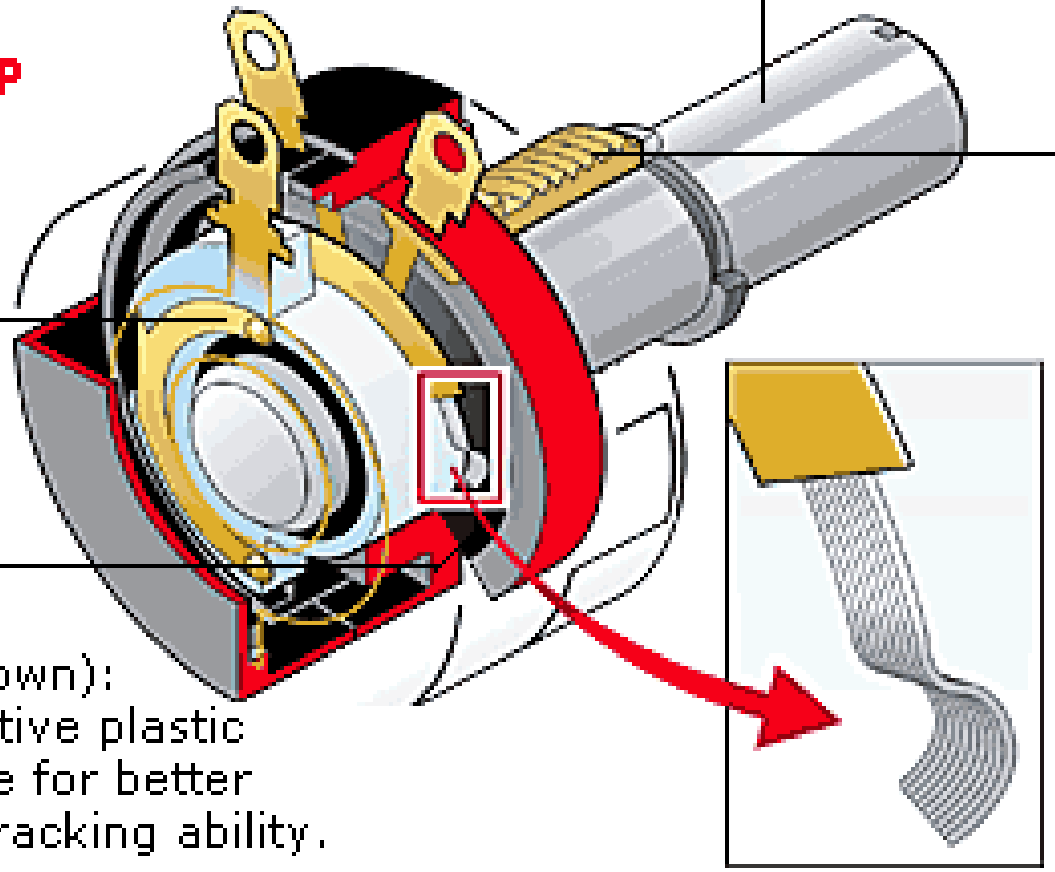

BRASS BUSHINGS:
Provide support for shaft side loads

PATENTED PRECIOUS METAL WIPER:
Platinum alloy wiper for long life and low noise. Conductive plastic models employ multi-finger wipers cut on a bias, preventing intermittants in higher shock and vibration applications.

ELEMENT:
Conductive Plastic (shown): High temperature conductive plastic resin molded on substrate for better reliability, long life, and tracking ability.

Wirewound: Provides better stability and lower temperature coefficients.

CIRCUITO

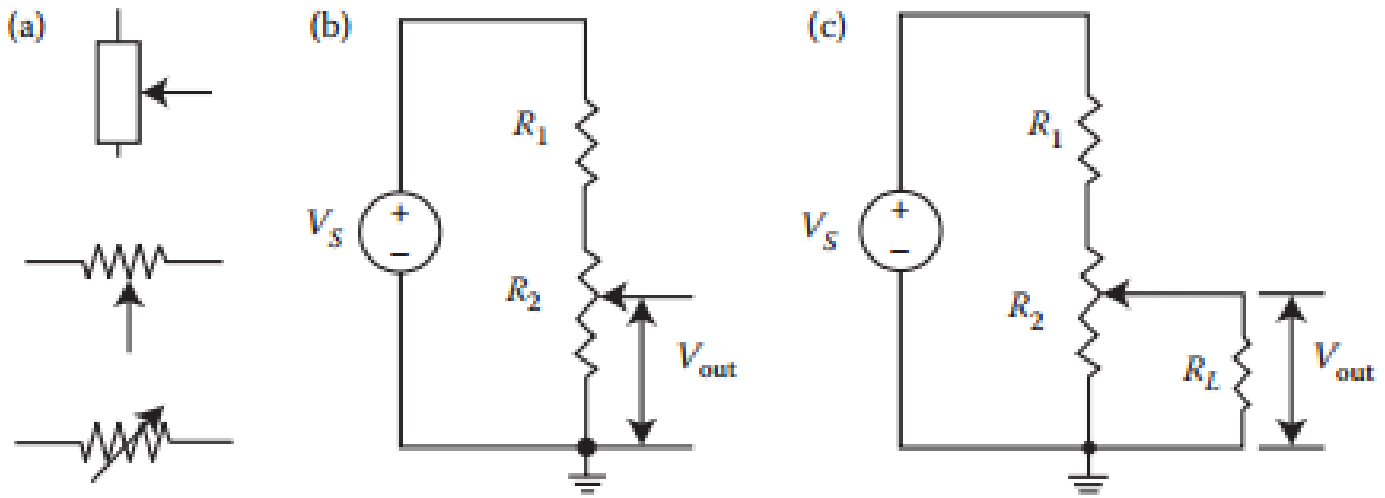

FIGURE 2.2 Potentiometer circuits: (a) circuit symbols; (b) a voltage divider circuit; (c) a voltage divider circuit with a load.

$$V_{out} = \frac{R_2}{(R_1 + R_2)} V_S$$

Não linear

$$V_{out} = \frac{R_2 R_L}{R_1 R_L + R_2 R_L + R_1 R_2} V_S$$

R_L = carga [eg, do osciloscópio]
Se alta impedância > medição mais precisa

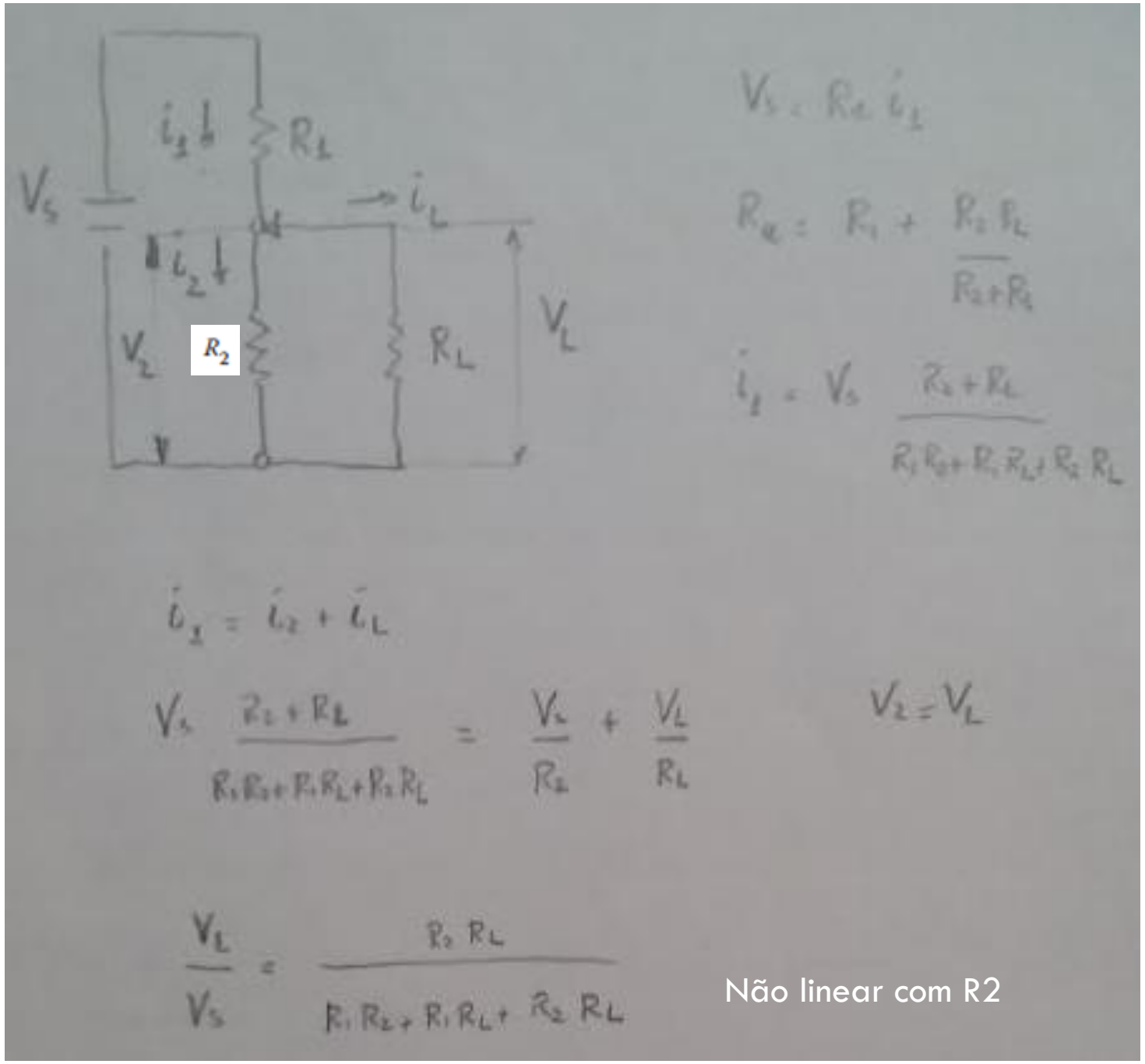

Não linear com R2

An ideal op-amp has infinite input impedance, thus current in both inverting input (–), I_-, and noninverting input (+), I_+, should be zero, that is, $I_- = I_+ = 0$. Also, an ideal op-amp has the same voltage potential at its two inputs, that is, $V_- = V_+$. Apply Kirchhoff's current law at node A:

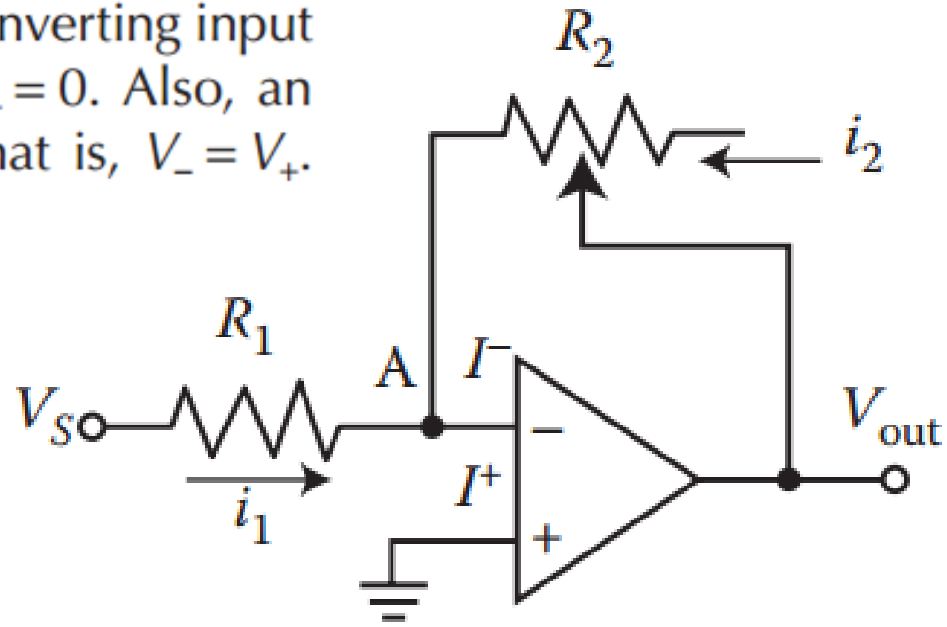

$$i_1 + i_2 = I_- = 0 \Rightarrow \frac{V_S - V_A}{R_1} + \frac{V_{out} - V_A}{R_2} = 0$$

and $V_A = V_- = V_+ = 0$ (since V_+ is grounded), resulting in

$$V_{out} = -\frac{R_2}{R_1} V_S$$

linear com R2

Equation 2.5 provides the linear relationship between V_{out} and R_2. The ratio R_2/R_1 is the gain of the amplifier. The negative sign indicates that it is an inverting amplifier. R_1 is often chosen equal to the sensor's resistance range (i.e., $R_1 = R_{2,Max}$). This op-amp circuit is also applicable to many other resistive sensors.

EXERCÍCIO

Um sensor potenciométrico de medição do nível de água. A resistência muda linearmente de 0 a 2 kΩ com o nível de água, que se altera de 0 a 80mm. (A) Desenvolvam um circuito de medição para fornecer uma saída linear, de 0 a 10 V, com a variação de nível. (B) Se a saída do sensor é de 7,5 V, qual é o nível de água?

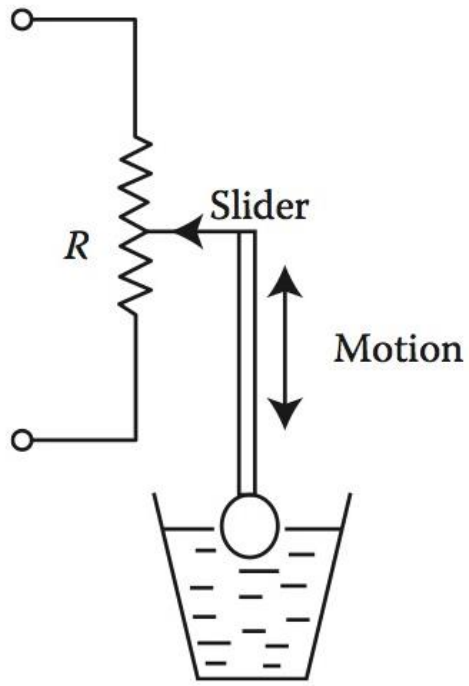

SOLUÇÃO...

Define-se:

$V_s = 10V$ a voltagem de entrada

R_2 o potenciômetro

Porém, a voltagem de saída V_{out} não é linear com a variação da resistência R_2

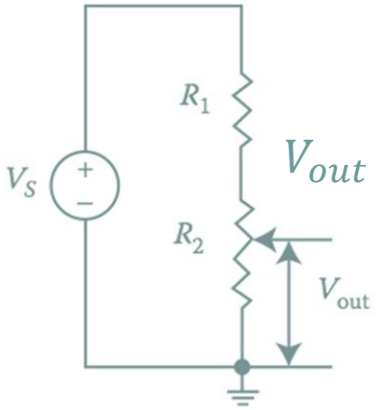

$$V_{out} = \frac{R_2 - R_x}{(R_1 + R_2)} V_S$$

Como resolver?!?!?!?!

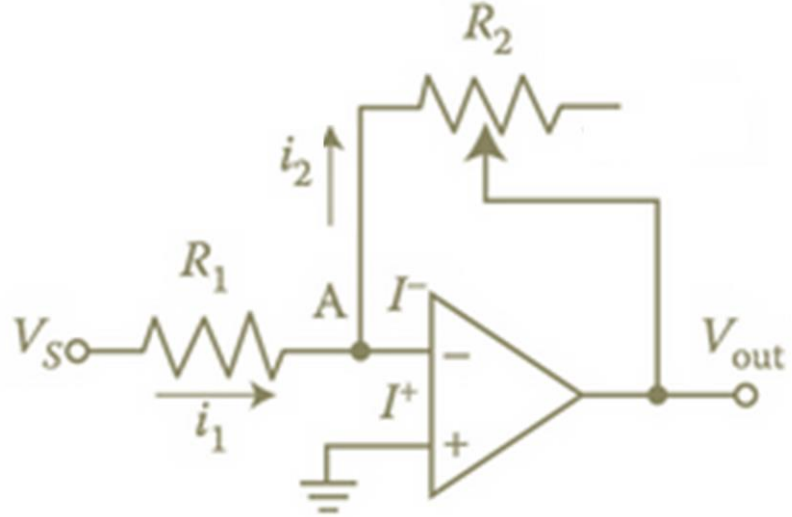

$$i_1 = \frac{V_s - V_A}{R_1}$$

$$i_2 = \frac{V_A - V_{out}}{R_2}$$

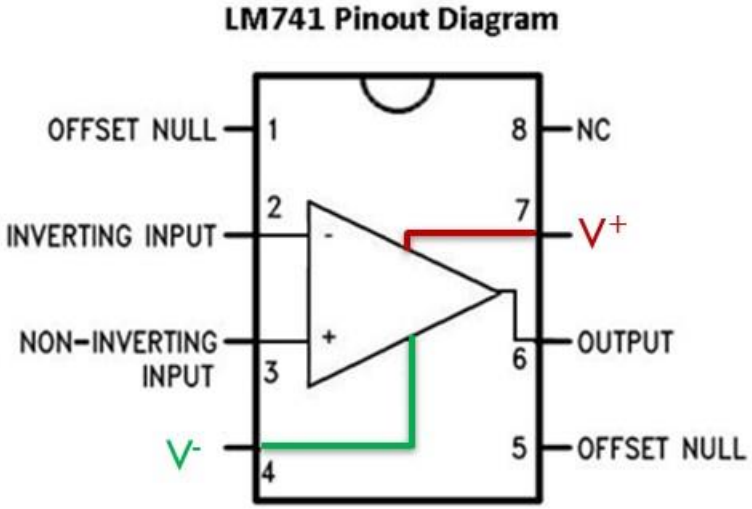

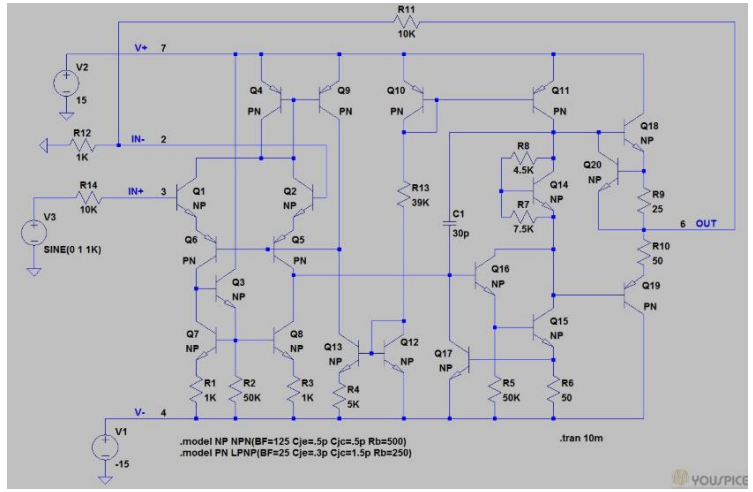

amp op ideal: $i_1 = i_2$ e $V_+ = V_-$

Portanto,

$$\frac{V_s - V_A}{R_1} = \frac{V_A - V_{out}}{R_2}$$

$V_A = 0$ já que $V_- = V_+ = 0$

$$\frac{V_s}{R_1} = \frac{-V_{out}}{R_2} \Longrightarrow V_{out} = -\frac{R_2}{R_1} V_s$$

$\therefore R_1 = 2k\Omega$ (a resistência máxima do potenciômetro)

CONT...

A)Aplicando a equação, porém, considerando um amp op não inversor,

$$V_{out} = \frac{R_2}{R_1} V_S = \frac{R_2}{2000} 10 = 0{,}005 R_2$$

Dessa forma, a medida que R_2 varia de 0-2kΩ, a voltagem de saída V_{out} irá variar linearmente entre 0-10V.

B) Para $V_{out} = 7{,}5V$,

$$R_2 = \frac{V_{out}}{0{,}005} = \frac{7{,}5}{0{,}005} = 1{,}5k\Omega$$

Como o nível de água é proporcional à mudança de resistência R_2,

$$\frac{x - x_{min}}{x_{max} - x_{min}} = \frac{R_2 - R_{min}}{R_{max} - R_{min}} \Longrightarrow \frac{x - 0}{80 - 0} = \frac{R_2 - 0}{2000 - 0} \Longrightarrow$$

$$x = 0{,}04 R_2 = 0{,}04 * 1500 = 60mm$$

EXEMPLOS

Sensor de pressão Rotacional e Linear

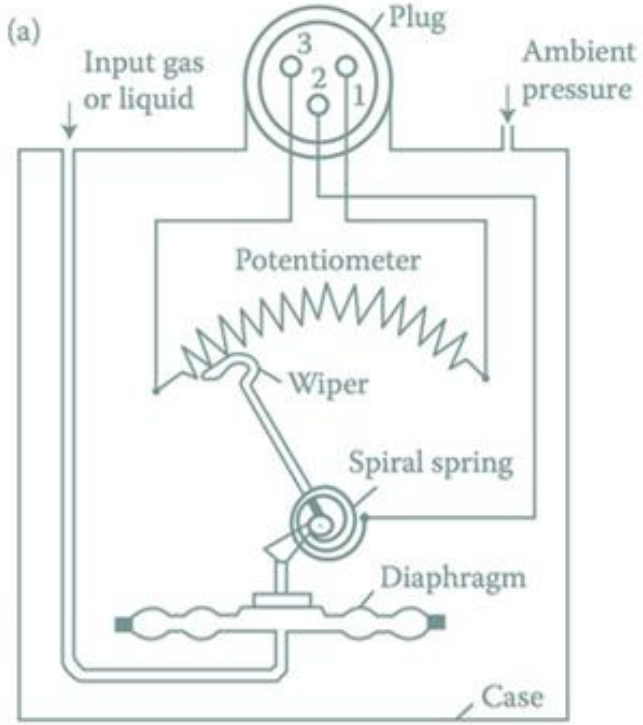

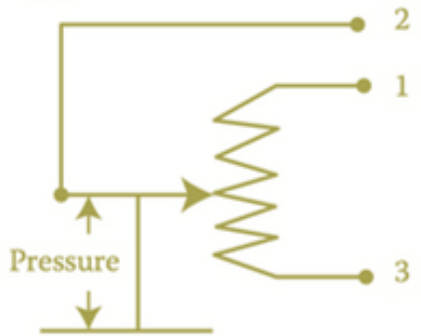

sensor de fluxo de ar

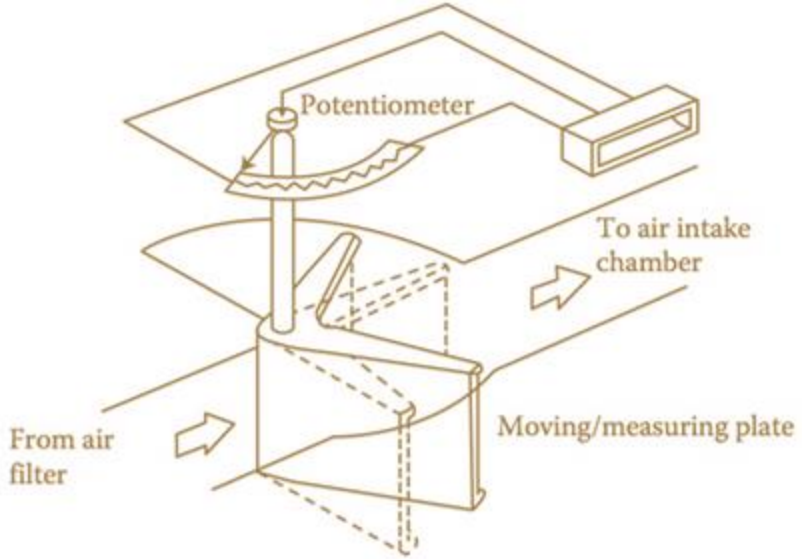

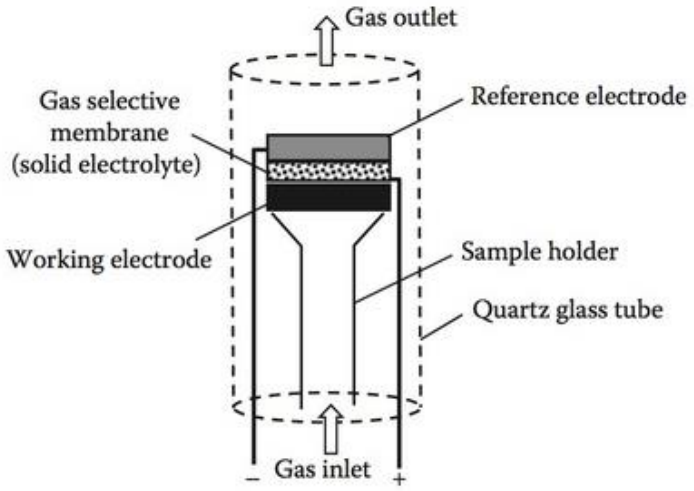

FIGURE 2.7 A potentiometric gas sensor.

TABLE 2.1
Typical Gas Detection Membranes

Membrane	Typical Gas to Be Detected
Glass membrane	CO_2, SO_2, NH_3
Ag_2S membrane	HCN, H_2S
Crystalline LaF_3 membrane	HF

Source: From Bunce, N., *CHEM7234/CHEM 720 Fundamentals of Electrochemistry Lecture Notes*, University of Guelph, Ontario, Canada, Spring 2003. With permission.

The gas selective membrane binds the gas of interest. The bounded gas then reacts with the analyte on each side
of the membrane, causing a change in conductivity of the membrane. This change is indicated by an output voltage change between the two electrodes. By convention,
the measuring electrode is considered as the cathode in potentiometric sensors.

Table 2.1 shows several typical membranes for gas detection [1]

MEDIDOR POTENCIOMÉTRICO DE ESFORÇO

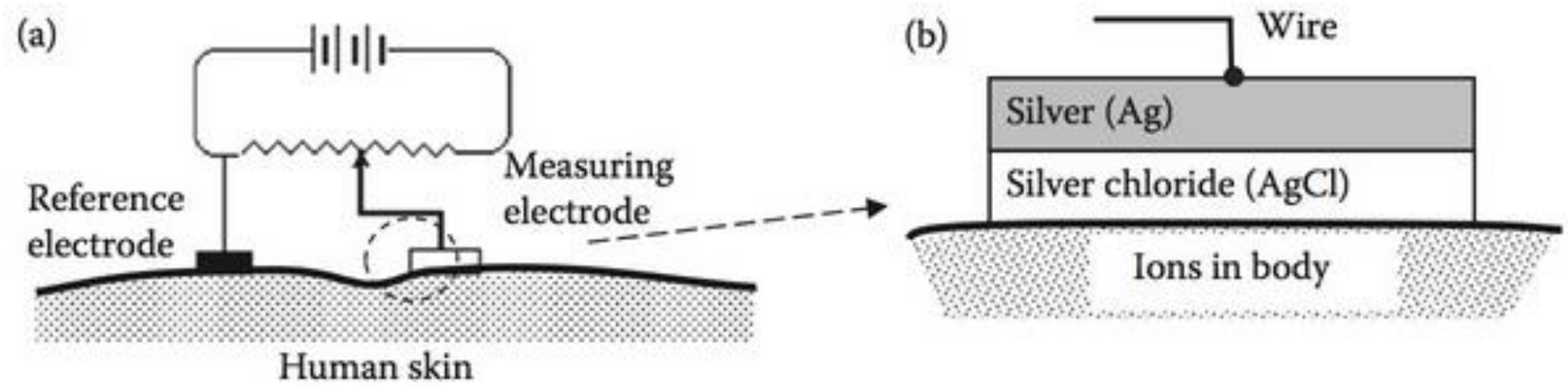

SENSORES TERMORRESISTIVOS

SENSOR TERMO-RESISTIVO

A resistividade ρ de um material depende da temperatura. A esse efeito, dá-se o nome de termo-resistividade. O efeito termo-resistivo de metais e semicondutores é bastante utilizado em sensores, mas seu efeito é diferente em cada um desses materiais...

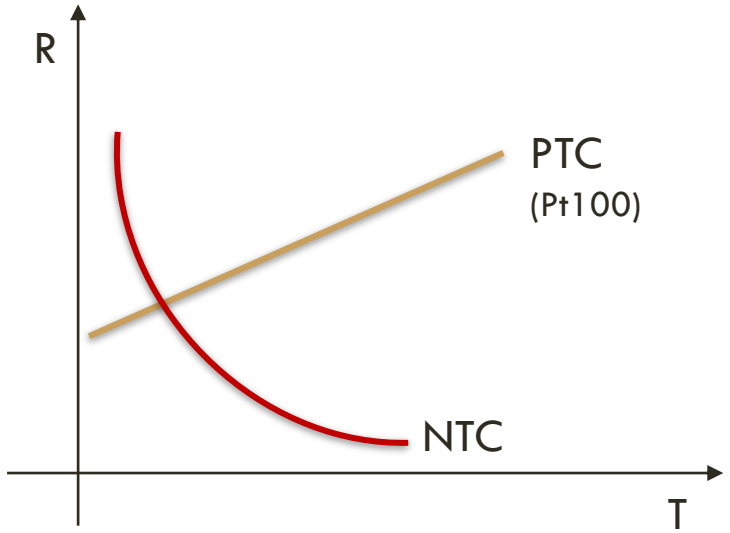

NTC (*Negative Temperature Coefficient*) – Aumento na quantidade de elétrons e lacunas livres gerado por excitação térmica, assim a resistência diminui com o aumento da temperatura.

PTC (Positive Temperature Coefficient) – Aumento da vibração dos átomos, dificultando a movimentação de elétrons e surgimento de lacunas, assim a resistência aumenta com o aumento da temperatura.

2.3.1.1 Thermoresistive Effect for Metals

The electrical resistance of a metal conductor increases as temperature increases. This is because the electrical conductivity of a metal relies on the movement of electrons through its crystal lattice. Due to thermal excitation, the vibration of electrons increases, which slows the electrons' movement, thus causing the resistance to increase. The relationship between resistance R and temperature T can be expressed by a polynomial equation:

$$R_T = R_0[1 + A(T - T_0) + B(T - T_0)^2 + C(T - T_0)^3 + \cdots] \quad (2.6)$$

Its simplified version is

$$R_T = R_0[1 + A(T - T_0)] \quad (2.7)$$

where R_0 is resistance at the reference temperature T_0 (usually either 0°C, 20°C, or 25°C); $A, B, C, \ldots$ are material-dependent temperature coefficients (in $\Omega \cdot \Omega^{-1} \cdot °C^{-1}$). Metals have *positive temperature coefficients* (PTC), because their resistance increases as the temperature increases. All resistance temperature devices (RTDs), made of metals, are PTC sensors. The temperature coefficient for all pure metals is of the order of 0.003–0.007 $\Omega \cdot \Omega^{-1} \cdot °C^{-1}$. Temperature coefficients A for common metals are listed in Table 2.2 [2].

The temperature coefficient of an alloy is often very different from that of the constituent metals. Small traces of impurities can greatly change the temperature coefficients. For example, an alloy of 84% Cu, 12% Mn, and 4% Ni has almost zero response to temperature. Thus, it is used to manufacture precision resistors. Figure 2.9 shows a typical resistance–temperature curve of an RTD.

A relação entre a resistência R e a temperatura T podem ser expressas por uma equação polinomial,

$$R_T = R_0[1 + A(T - T_0) +$$

RTDs E TERMISTORES

Os RTDs (do inglês, Resistance Temperature Devices) são formados por materiais como Platina, Níquel ou ligas de Cobre-Níquel. Estes materiais exibem um coeficiente *positivo* de resistividade e são usados para a fabricação de RTDs porque são estáveis e dotados de capacidade de resposta à uma ampla faixa de variação de temperatura.

Os termistores são sensores fabricados com materiais semicondutores como óxido de magnésio ou cobalto; em aplicações que exigem alta precisão, o semicondutor utilizado pode ser o silício ou o germânio, com algum outro material como o latão ou determinadas ligas de cobre. Por serem construídos de material semicondutor, possuem a grande vantagem de serem fabricados em um tamanho físico muito pequeno.

Medidor elétrico de temperatura por variação de resistência (condutores)

•Termômetros RTD
(Resistance Temperature Detectors)

http://www.branom.com/literature/rtd.html

No mesmo ano em que Seebeck fez sua descoberta sobre a termoeletricidade, Sir Homphrey Dovy descobriu que a resistividade dos metais, apresentava uma dependência física para com a temperatura (a variação do movimento aleatório dos elétrons livres nos metais, varia a resistividade dos mesmo).

Cinqüenta anos depois, Sir William Siemens propôs o uso da platina, como sensor nos termômetros de resistência. Sua escolha mostrou-se bastante apropriada, pois até hoje os resistores de platina são utilizados como elementos primários na medição de temperaturas com alta precisão.

Platina é excelente para este propósito, dado que ela pode resistir altas temperaturas mantendo a sua estabilidade.

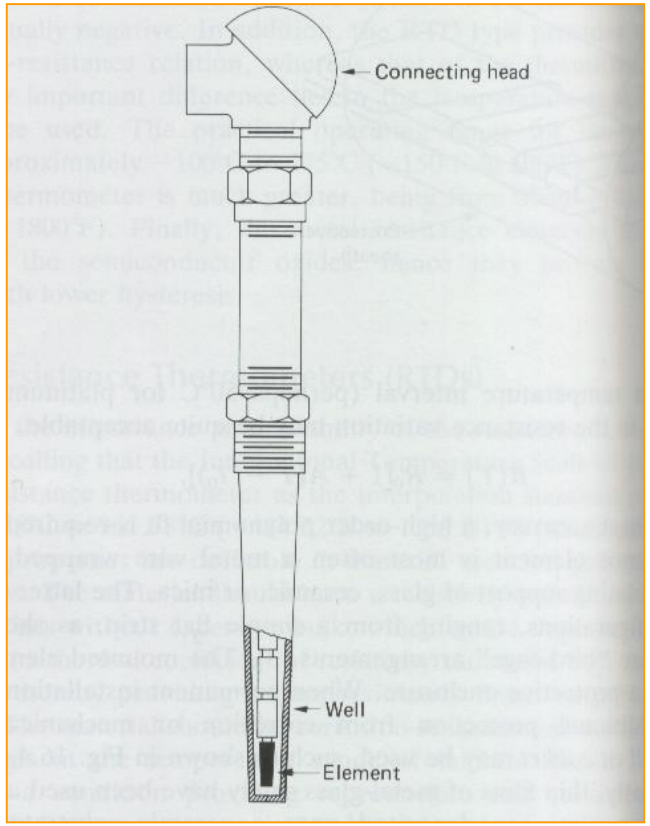

RTD de platina mede com alta precisão entre -259,35°C e 961,78°C

$$R(T) = R_0\left[1 + A(T - T_0) + B(T - T_0)^2\right]$$

Thermistor – Temperature Detection Fire Alarm Example

Thermistors serve a crucial role in temperature detection. For example, thermistor temperature detection can be used in fire alarms to detect fires based on a sudden change in temperature. Unlike photoelectric detectors or ionization alarms, thermistors only require heat to activate.

> *Thermistors are temperature-sensing elements made of semiconductor material that displays large changes in resistance in proportion to small changes in temperature.*

https://www.ametherm.com/blog/thermistors/thermistor-temperature-detection-fire-alarm-example/

PTC DE METAIS

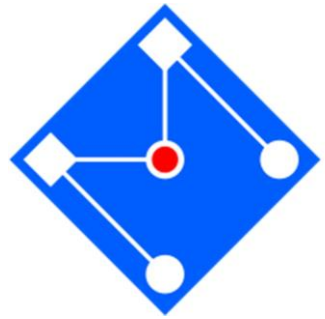

MATERIAL	COEFICIENTE TEMPERATURA (A_{20})
prata	$3{,}819\ 10^{-3}$
cobre	$4{,}041\ 10^{-3}$
ouro	$3{,}715\ 10^{-3}$
alumínio	$4{,}308\ 10^{-3}$
tungstênio	$4{,}403\ 10^{-3}$
níquel	$5{,}866\ 10^{-3}$
ferro	$5{,}671\ 10^{-3}$
platina	$3{,}850\ 10^{-3}$

O coeficiente de temperature de uma liga é, em geral, muito diferente daquele dos metais constituintes. Pequenos traços de impureza podem alterar muito o A. Por exemplo, uma liga de 84%Cu, 12%Mn, 4% Ni tem resposta praticamente nula com a temperatura.

RTDs

Qualquer metal pode ser usado para medir temperatura, mas um RTD deve utilizar metais com as seguintes características:

- Alto ponto de fusão;
- Resistência à corrosão;
- Estabilidade química até altas temperaturas;
- Viabilidade na forma quase pura (garantia de consistência no processo de manufatura);
- Repetibilidade;
- Previsível e relação R-T o mais linear possível.

Common RTD Sensor Materials and Their Characteristics

Metal	Temperature Range (°C)	A ($\Omega \cdot \Omega^{-1} \cdot °C^{-1}$)	Comments
Platinum (Pt)	–240 ~ +850	0.00385	Good precision, broad temperature range
Nickel (Ni)	–80 ~ +260	0.00672	Low cost, limited temperature range
Copper (Cu)	–200 ~ +260	0.00427	Low cost, applied in measuring the temperature of electric motor and transformer windings
Molybdenum (Mo)	–200 ~ +200	0.00300 or 0.00385	Lower cost, alternative to platinum in the lower temperature ranges, ideal material for film-type RTDs

PLATINA VS NÍQUEL

Platina é o material mais comum em RTDs porque:

- Estável
- Larga faixa de temperatura
- Fácil fabricação
- Custo razoável

RTDs de platina estão disponíveis com valores nominais de resistência R_0 (a 0 ^{0}C) de 10, 25 e 100 Ω. Pt100 é o modelo dominante na prática, com variação de temperatura entre -240 ^{0}C a 850 ^{0}C.

RTDs de platina são oficialmente utilizados para medir os 16 valores fixos definidos na IPTS (International Practical Temperature Scale, de 1968 e revisada em 1990)

EQUALIBIRIUM STATE	K	^{0}C
Triple point of hydrogen	13.8033	-259.3467
Boiling point of hydrogen at pressure of 33321.3Pa	17.035	-256.115
Boiling point of hydrogen at pressure of 101292Pa	20.27	-252.88
Triple point of neon	24.5561	-248.5939
Triple point of oxygen	54.3584	-218.7916
Triple point of argon	83.8058	-189.3442
Triple point of mercury	234.3156	-38.8344
Triple point of water	273.16	0.01
Melting point of gallium	302.9146	29.7646
Freezing point of indium	429.7485	156.5985
Freezing point of tin	505.078	231.928
Freezing point of zinc	692.677	419.527
Freezing point of aluminium	933.473	660.323
Freezing point of silver	1234.93	961.78
Freezing point of gold	1337.33	1064.18
Freezing point of copper	1357.77	1084.62

RTDs de níquel são preferidos em aplicações de baixo custo, como ar condicionado. Produzidos com valores mais altos de resistência de referência (1 ou 2k Ω). Menos inerte quimicamente que a platina, portanto, menos estável que a platina a altas temperaturas.

EQUAÇÃO DE CALLENDAR-VAN DUSEN

Um RTD Pt100 tem sua relação R-T descrita pela equação de Callendar-Van Dusen, válida para temperaturas entre -200 ^{0}C e 850 ^{0}C:

$$R_T = R_0[1 + A'T + B'T^2 + C'(T - 100)T^3]$$

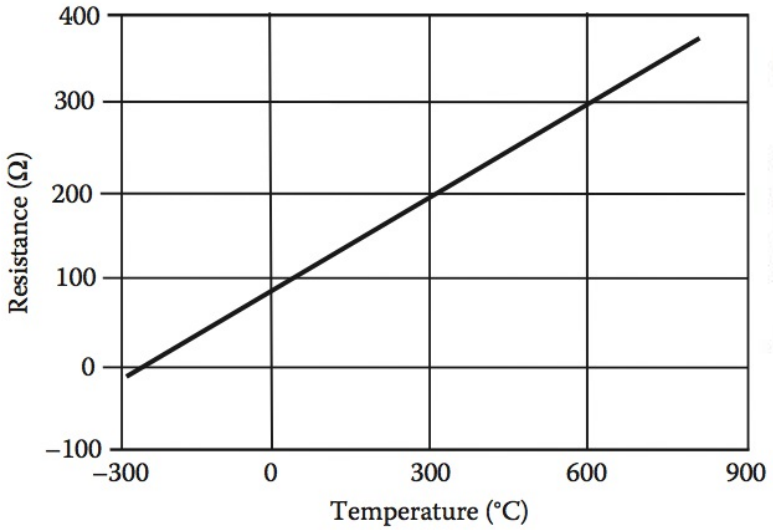

Callendar–Van Dusen Coefficients Corresponding to Standard RTDs

Standard	A'	B'	C' ($C' = 0$ for $T > 0$°C)
DIN 43760	3.9080×10^{-3}	-5.8019×10^{-7}	-4.2735×10^{-12}
American	3.9692×10^{-3}	-5.8495×10^{-7}	-4.2325×10^{-12}
ITS-90	3.9848×10^{-3}	-5.8700×10^{-7}	-4.0000×10^{-12}

Source: From Measuring temperature with RTDs—A tutorial, Application Note 046, National Instruments Corporation, Austin, Texas, USA, 1996. With permission.

Fonte: livro texto

PROJETO DE UM RTD

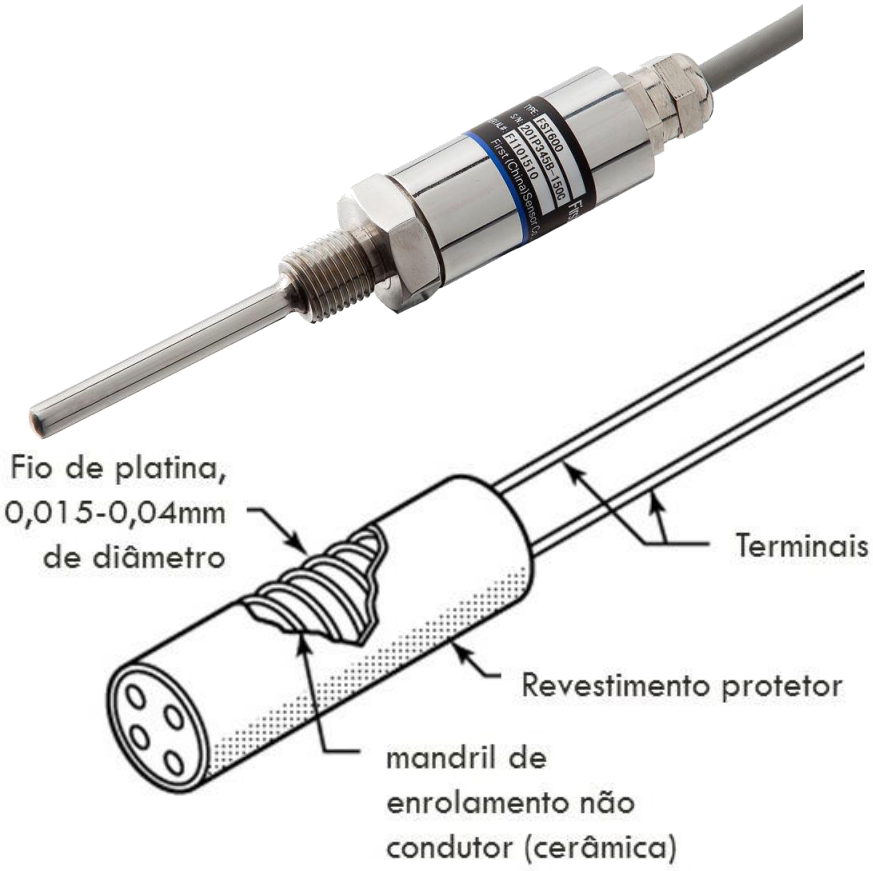

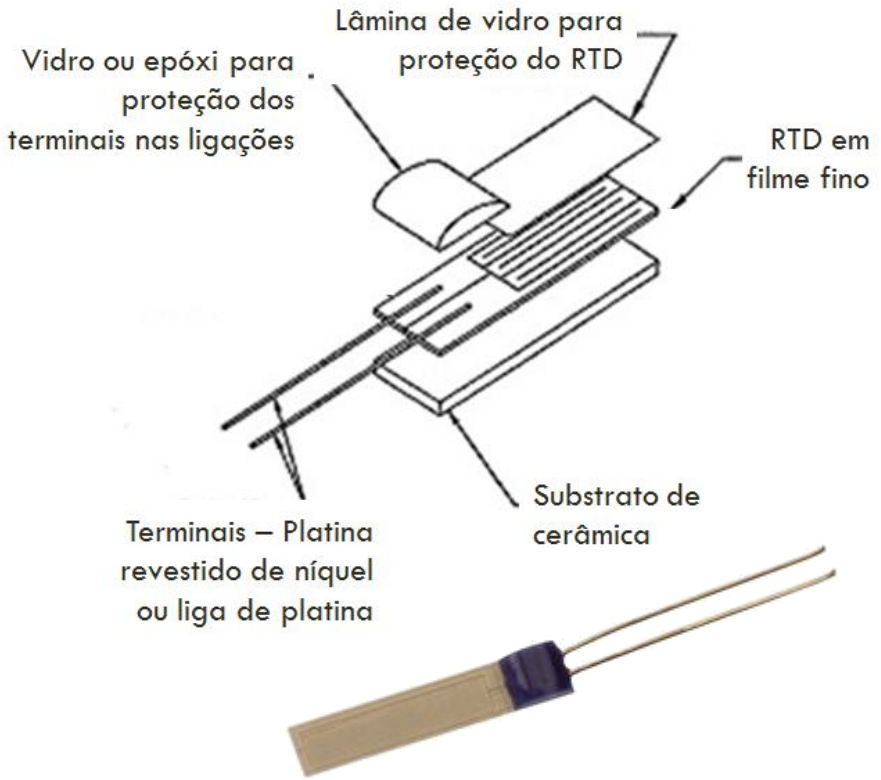

EFEITO DOS FIOS DOS TERMINAIS

Some resistive temperature sensors, such as RTDs, are difficult to measure due to their low resistance (e.g., 100 Ω) that changes only slightly with temperature ($< 0.4\ \Omega \cdot {}^{\circ}C^{-1}$). To accurately measure these small changes in resistance, special configurations should be used to minimize errors from lead wire resistance. Figure 6.6 shows the three common RTD wirings (the arrow "→" across the resistors means that the resistors are variable or adjustable resistors):

Two-wire RTD connection (Figure 6.6a). The actual resistance that causes V_{out} change is the total resistance of the sensor R_T and the two lead wires ($L_1 + L_2$). If the lead wire resistance is constant, it introduces an offset error and can be easily compensated. However, as temperature varies, the wire resistance also changes, which creates errors in measurement, especially when the wires are long. Thus, two-wire RTD connection is only used with very short lead wires or with a high resistance (e.g., 1 kΩ) sensor.

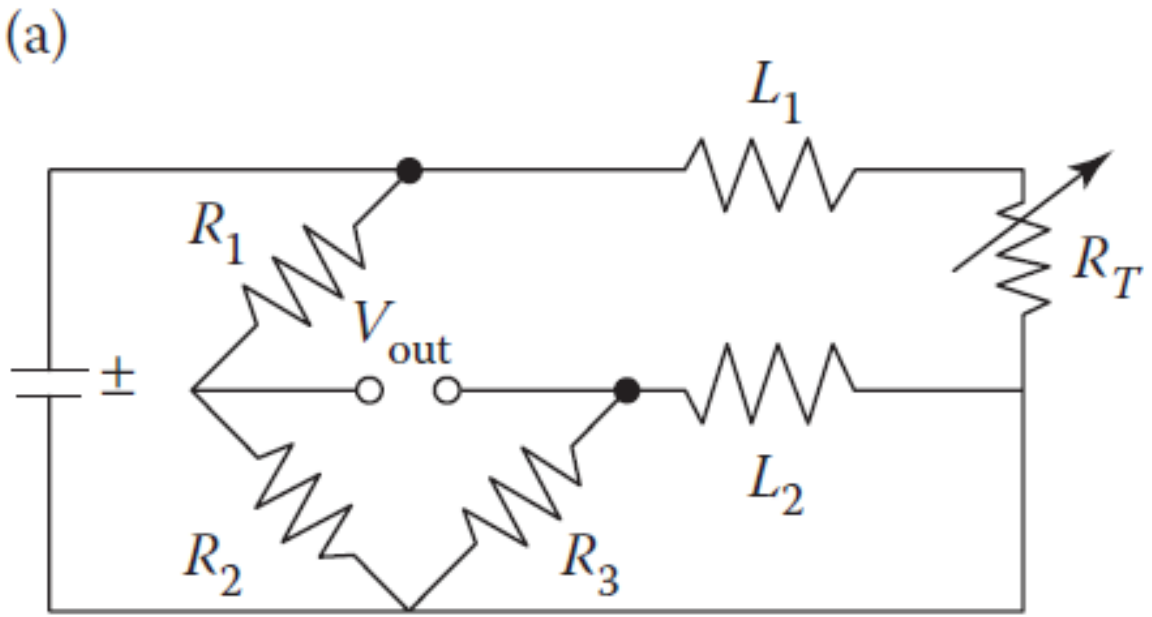

Three-wire RTD connection (Figure 6.6b). In this connection, L_1 and L_3 carry the measuring current, while L_2 acts as a potential or reference lead only. If the resistances of L_1 and L_3 are perfectly matched, their affects on the temperature measurement will be cancelled. Thus, L_1 and L_3 can lead up to tens of feet long and usually work well for 100 Ω RTDs.

(b)

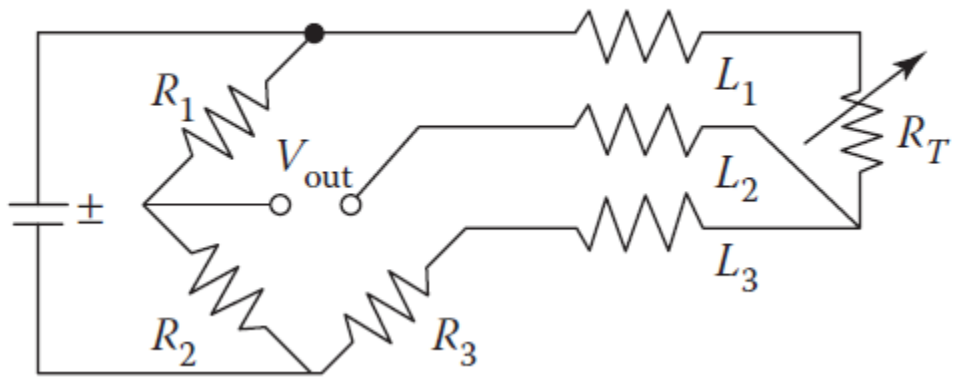

Four-wire connection (Figure 6.6c). This is the optimum wiring form for RTDs. It removes the error caused by mismatched lead wires resistance. A constant current is passed through L_1 and L_4; while L_2 and L_3 measure the voltage drop across the RTD. With a constant current, the voltage is strictly a function of the resistance R_T and a true measurement is achieved. This connection provides a high degree of accuracy although it is more expensive than two- or three-wire connections.

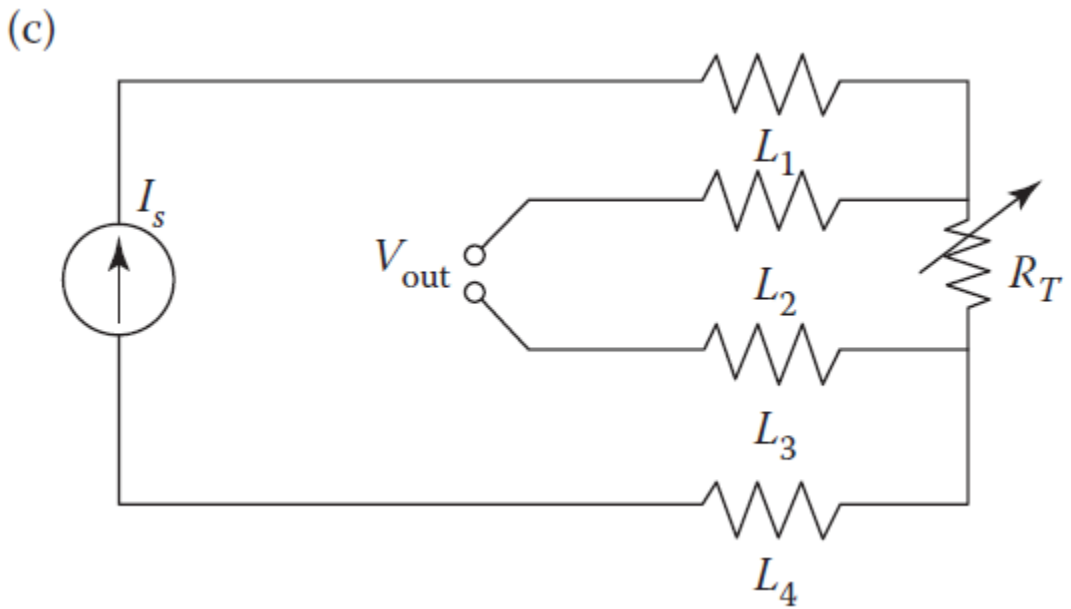

TERMISTORES – TERMORRESISTIVIDADE EM SEMICONDUTORES

A relação entre R e T é exponencial,

$$R_T = R_0 e^{\left[\beta\left(\frac{1}{T}-\frac{1}{T_0}\right)\right]}$$

R_0 resistência de referência em T_0 (em K, usualmente 298K=25 0C).
β é um NTC.

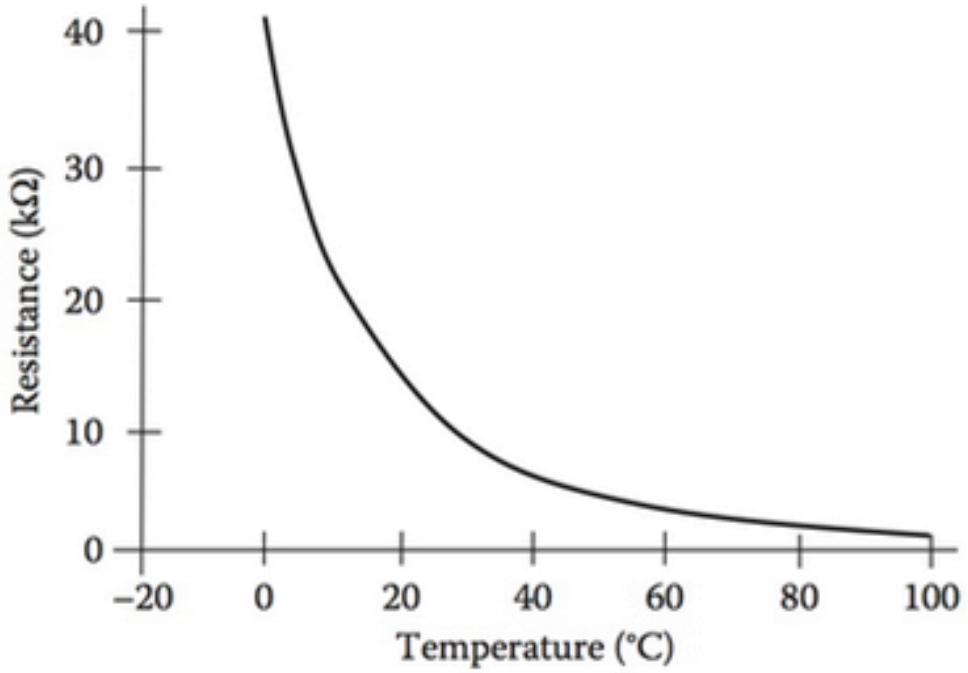

Medidor elétrico de temperatura (semi-condutor)

Termistor

Semi-condutor cerâmico: diminui sua resistência elétrica com o aumento da temperatura

Bastante sensível

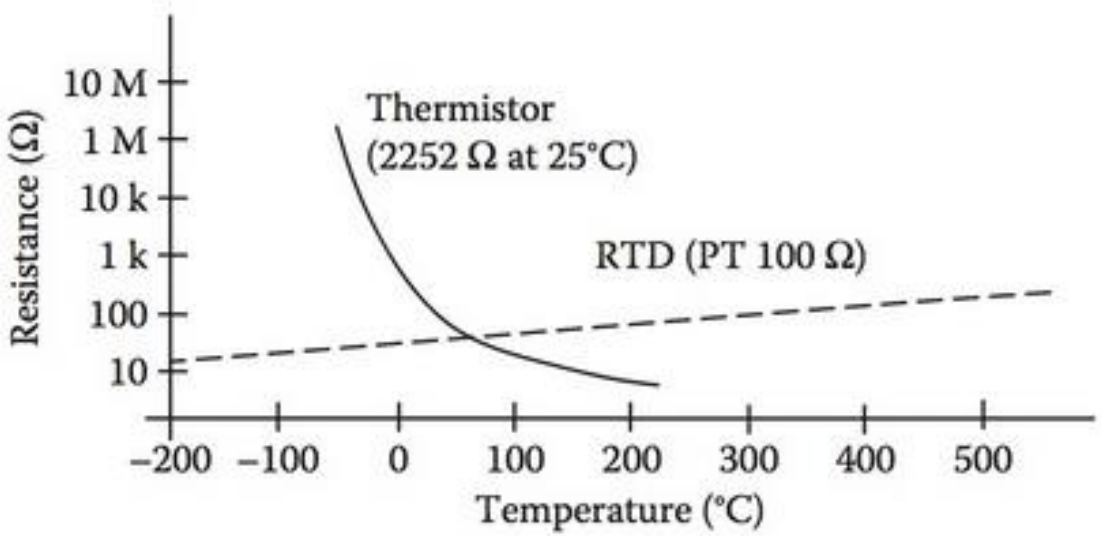

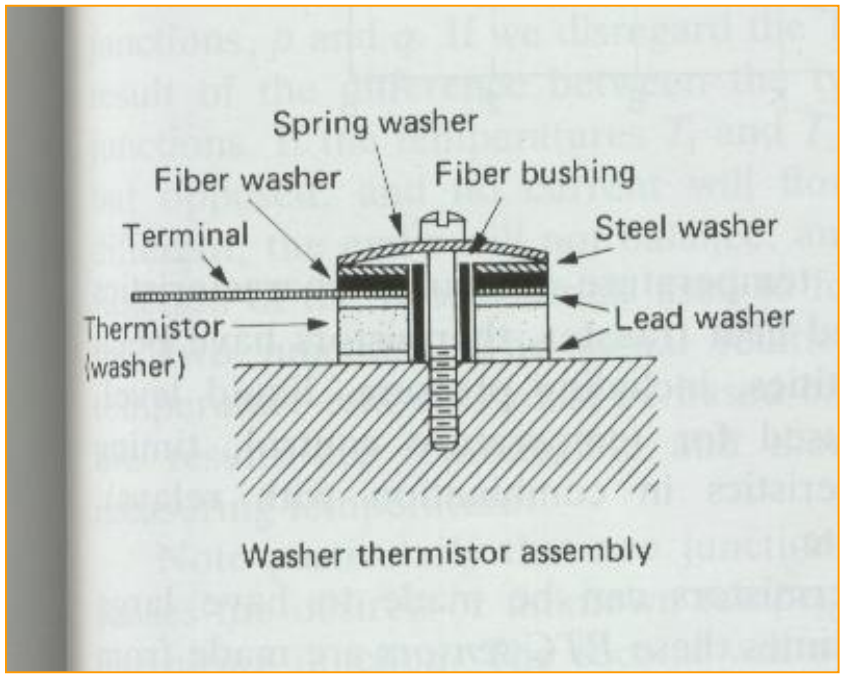

$$R(T) = R_0 \exp\left[\beta(1/T - 1/T_0)\right]$$

https://br.omega.com/prodinfo/termistores.html

VANTAGENS DOS TERMISTORES

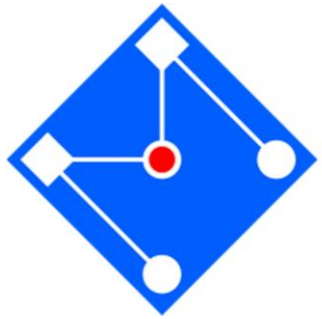

As principais vantagens de termistores para a medição de temperatura são:

Pt100 apresenta sensibilidade de apenas 0,4 Ω/°C

- Sensibilidade extremamente elevada. Um termistor 2252Ω tem uma sensibilidade de -100 Ω/°C à temperatura ambiente. Termistores resistência mais elevada pode exibir uma sensibilidade de -10 kΩ/°C ou mais.
- Resposta rápida às mudanças de temperatura.
- Resistência relativamente elevada, variando de centenas a milhões de ohms.
- São bem mais econômicos que RTDs

Elevada resistência diminui o efeito de fios condutores que pode causar erros significativos com dispositivos de baixa resistência como RTD

As principais desvantagens de termistores são sua alta não-linearidade e faixa de temperatura limitada (tipicamente abaixo de 300 °C).

RTD VS TERMISTOR VS TERMOPAR

Comparison of Characteristics for RTDs, NTC Thermistors, and Thermocouples

Characteristics	RTD	NTC Thermistor	Thermocouple
Measured parameters	Resistance	Resistance	Voltage
Resolution	Poor	Good	Moderate
Linearity	Linear	Nonlinear	Nonlinear
Temperature range	–250°C ~ 850°C	–100°C ~ 300°C	0°C ~ 1600°C
Current source	Necessary	Necessary	Not necessary
Compensation for environments	Not necessary	Not necessary	Necessary
Response	Relatively slow	Fast	Fast
Cost	Expensive	Inexpensive	Varies

Source: The data in the table are compiled based on several manufacturers' data sheets.

ANEMÔMETRO VIA SENSOR DE TEMPERATURA

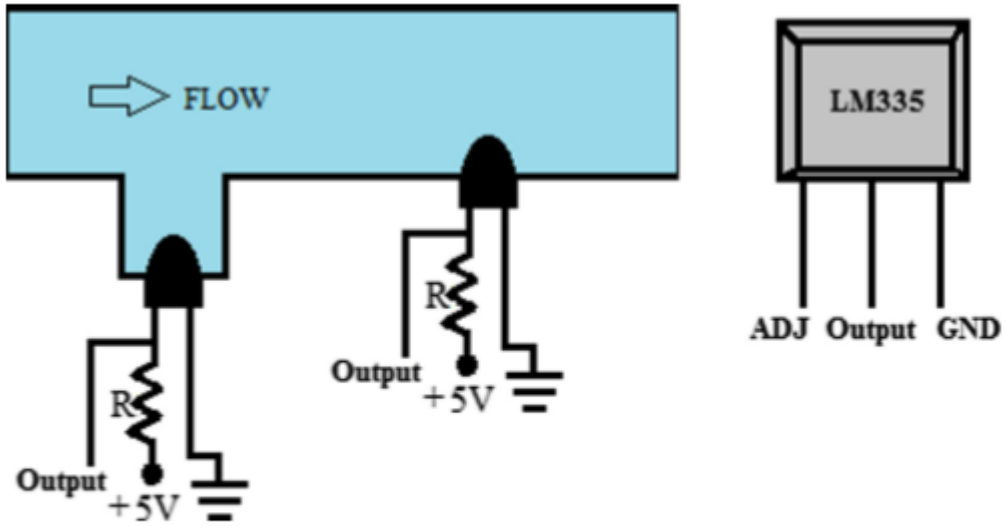

Fig. 1. (a) Mounting of LM335 in the flow head (b) LM335 pin configuration.

Contents lists available at ScienceDirect

Measurement

journal homepage: www.elsevier.com/locate/measurement

Anemometric type flow transmitter using LM335 – A temperature sensing IC

G. Rajita, A. Lata, N. Mandal *

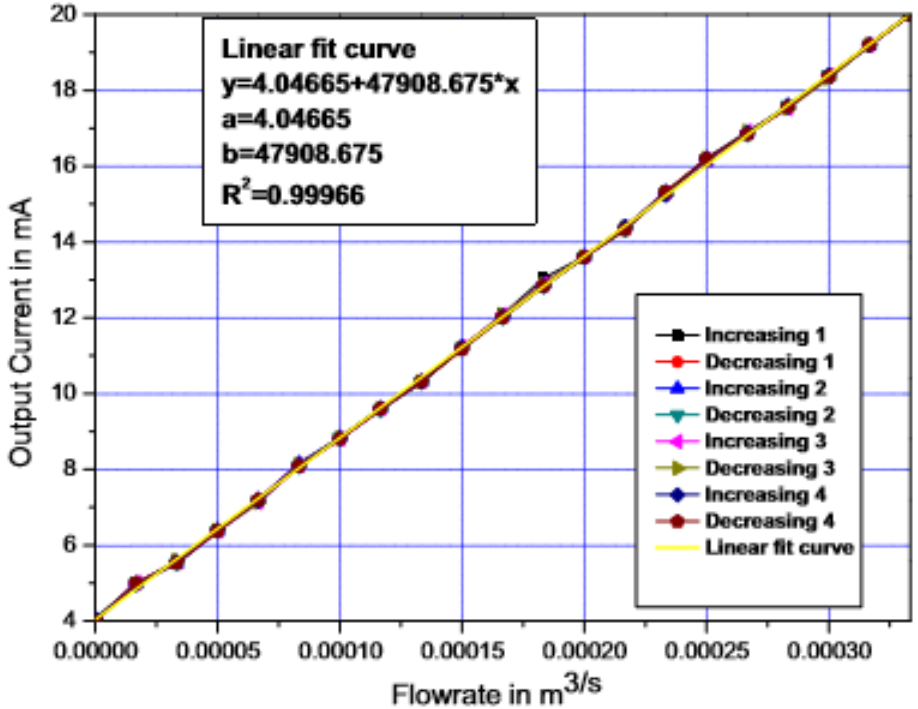

(a) Flow transmitter characteristic

not produce any obstruction to the flowing fluid. Two IC units are supplied from the same stabilized 5 V DC source. LM335 is a 2-terminal zener and provides a break down voltage directly proportional to absolute temperature. The device operates over a current range of 400 μA–5 mA with less than 1 Ω dynamic impedance. The DC voltage developed from the IC has been found to be related with fluid flow rate. The voltage signals developed for two horizontal IC's has been subtracted from each other and this voltage is assumed to be a function of fluid flow rate. The differential op-amp output voltage is of mV signal range. An instrumentation amplifier along with signal conditioning circuit converts this into 1–5 V signal. The function of the flow sensor has been theoretically analyzed and its characteristic equations have been derived. To find the characteristics of the flow sensor experiment has been performed. The analysis of operation of the system is described below.

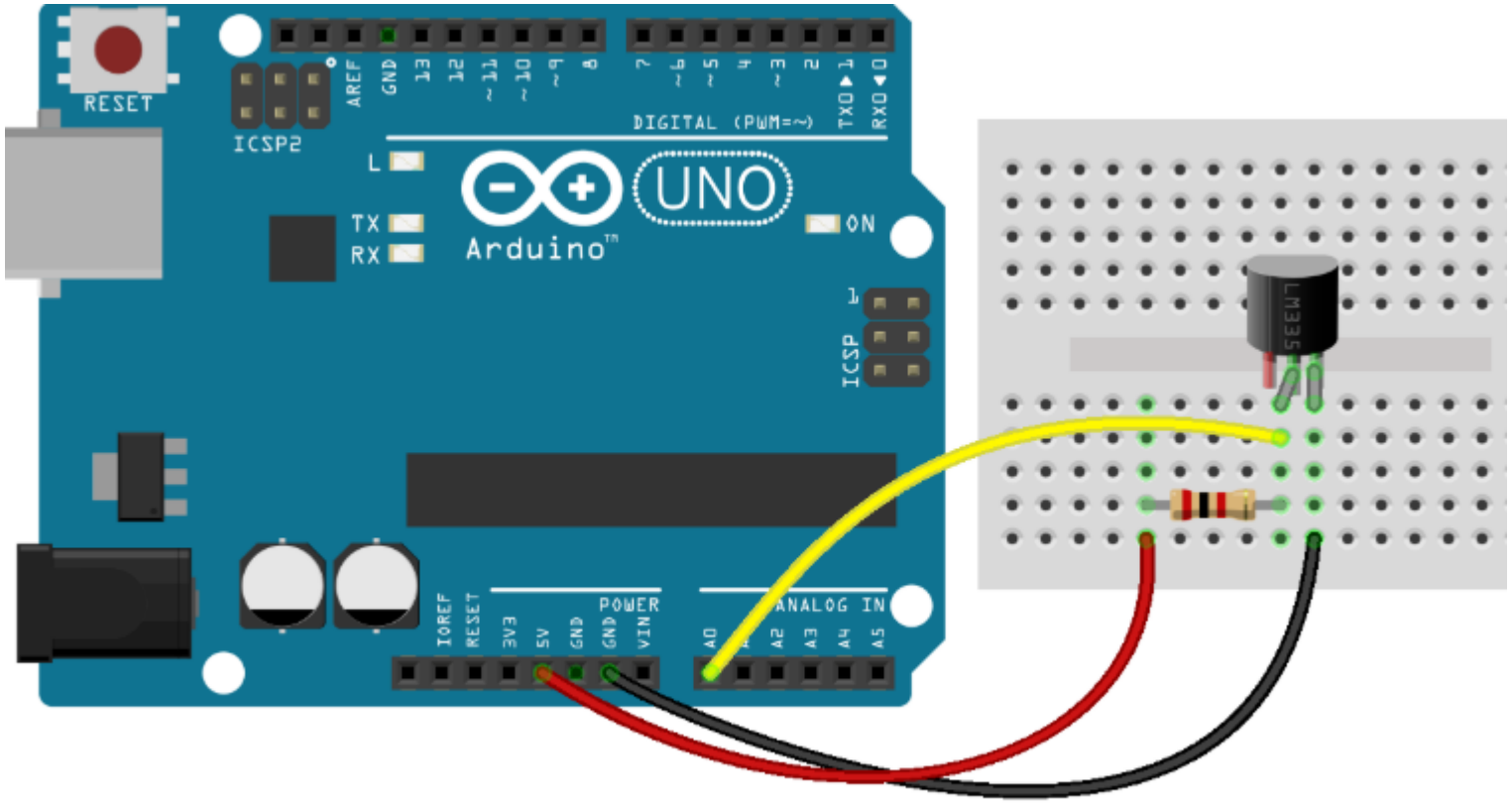

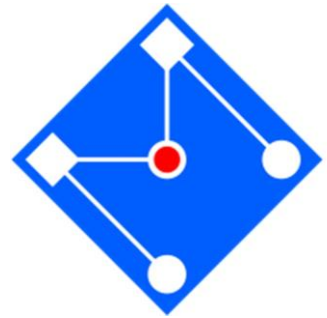

LM335 Pinout

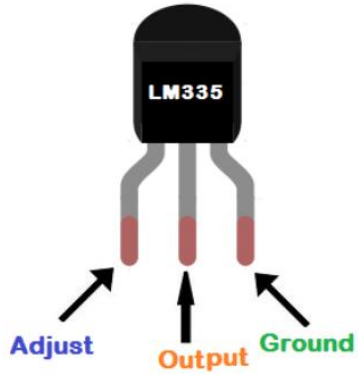

LM335 Animation

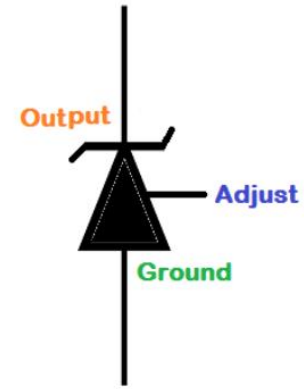

Symbolic Representation

LM335

A. Um RTD possui A = 0,004/°C e R=100 Ω a 20°C, encontre a resistência a 25°C.

B. Considere depois o RTD conectado a um braço da ponte de Wheatstone. A 20^0C o circuito está balanceado e a voltagem de alimentação é 10V. Determine a variação mínima da voltagem de saída para uma variação de temperatura de 1 ^{0}C.

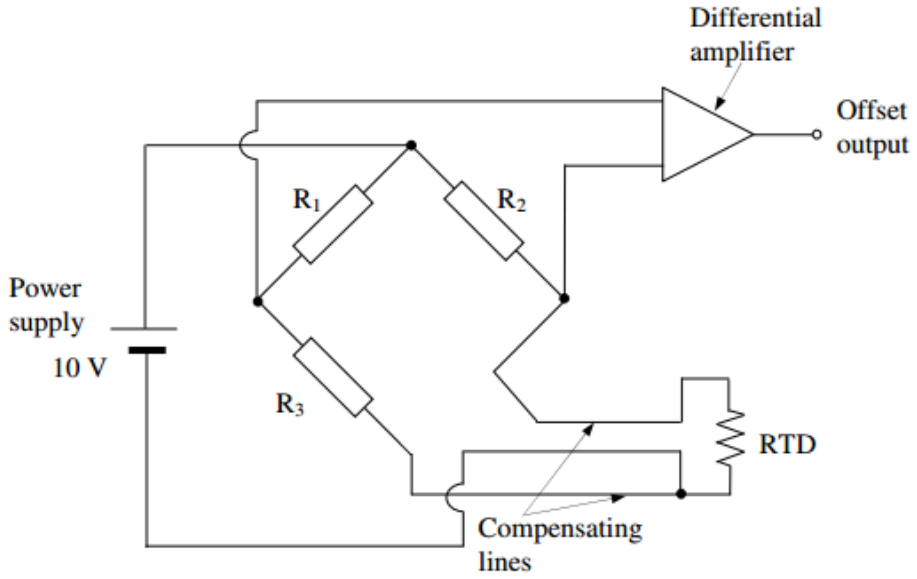

A. A relação polinomial entre R e T é dada por,

$$R_T = R_0[1 + A(T - T_0)]$$

Portanto,

$$R_T = 100[1 + 0{,}004(25 - 20)] = 102\Omega$$

B. **RTD Condicionamento de sinais**: Tendo em vista as alterações mínimas de resistência com a temperatura (0,4%), o RTD é geralmente utilizado num circuito de ponte. A figura ilustra as características essenciais de tal sistema. A compensação na perna R_3 da ponte é necessária quando os fios são tão longos que gradientes térmicos ao longo do RTD podem causar alterações na resistência. Ao utilizar a linha de compensação, as mesmas alterações de resistência aparecem no lado de R_3 e causam mudança líquida nula na ponte.

$$R_T = 100[1 + 0{,}004(21 - 20)] = 100{,}4\Omega$$

$$\therefore \Delta R = 0{,}4\Omega$$

$$V_o = \frac{\Delta R}{4(R + \Delta R/2)} V_0 = \frac{0{,}4}{4(100 + 0{,}4/2)} 10 = 0{,}01V$$

Um RTD tem A_0=0,005/^{0}C a 20^{0}C e uma taxa de dissipação constante de P=30mW/^{0}C. O RTD usa a ponte de Wheatstone conforme figura. R_1= R_2= R=500Ω e R_3 é variável, usado para equilibrar a ponte. Se a tensão fornecida é de 10V e o RTD é imerso no gelo a 0 ^{0}C:

A. Encontre o valor de R_3 para equilibrar a ponte;
B. Encontre a voltagem de saída medida pelo voltímetro (R_v=∞) com o valor de R_3 obtido no item A para uma temperatura de 100^{0}C. Considere o efeito do auto-aquecimento e calcule o erro do RTD.

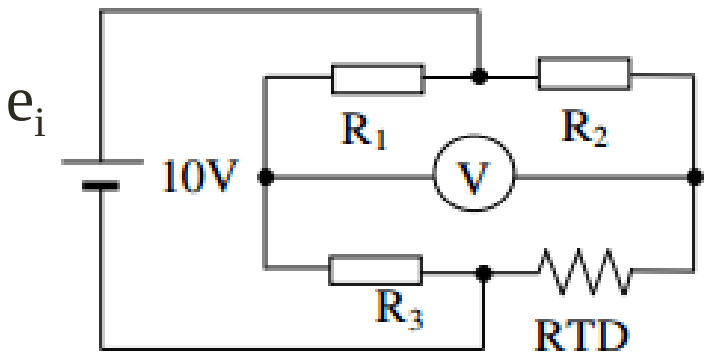

A. O RTD é uma resistência, e, portanto, uma energia $W = i^2R$ é dissipada pelo próprio dispositivo e provoca um pequeno efeito de aquecimento, um auto-aquecimento.

Isso também pode causar uma leitura errônea ou até mesmo prejudicar o ambiente em uma condição delicada de medição. Assim, a corrente através do RTD deve ser mantida suficientemente baixa e constante para evitar a auto-aquecimento. Geralmente, uma constante de dissipação é fornecida nas especificações de IDT. Este número refere-se a energia necessária para elevar a temperatura RTD por um grau de temperatura. Assim, a constante dissipação $25\ mW/\ ^0C$ mostra que, se a perda de energia i^2R no RTD for de $25\ mW$, este será aquecida de $1{,}0\ ^\circ C$.

A constante de dissipação é normalmente especificada sob duas condições: ar livre e em banho de óleo. Isto é devido à diferença na capacidade do meio para transportar o calor para fora do dispositivo. O aumento da temperatura de auto-aquecimento pode ser encontrado a partir da potência dissipada pelo RTD e a constante de dissipação, como:

$$\Delta T = \frac{P}{P_D}$$

onde ΔT é a elevação de temperatura por causa do auto-aquecimento, em °C; P é a potência dissipada no RTD do circuito, em W; e P_D é a constante dissipação do IDT em $W/\ ^0C$.

Portanto,

$$R = 500[1 + 0{,}005(0 - 20)] = 450\Omega$$

Desprezando-se os efeitos de auto-aquecimento, esperara-se que a ponte balanceasse para $R_3 = 450\Omega$. Agora, verifica-se a influência do auto-aquecimento neste problema. Primeiro, encontra-se a potência dissipada no RTD do circuito, assumindo a resistência ainda é 450Ω. A potência vale:

$$W = i^2 R$$

O valor da corrente, com três algarismos significativos, vale:

$$i = \frac{10}{500 + 450} = 0{,}011\ A = 11\ mA$$

De modo que a potência vale:

$$W = 0{,}011^2 450 = 0{,}054W$$

O aumento de temperatura será de,

$$\Delta T = \frac{0{,}054}{0{,}030} = 1{,}8\ ^0C$$

Assim, o RTD não está, na verdade, à temperatura de $0\ ^0C$ mas a uma temperatura de $1{,}8\ ^0C$. Portanto, a resistência do RTD será de,

$$R = 500[1 + 0{,}005(1{,}8 - 20)] = 454{,}5\Omega$$

Portanto, a ponte estará balanceada para uma resistência $R_3 = 454{,}5\Omega$

B. Para temperatura de 100 a resistência do RTD será de,

$$R = 500[1 + 0{,}005(100 - 20)] = 700\Omega$$

Calcula-se a corrente,

$$i = \frac{10}{700 + 500} = 0{,}0083\ A = 8{,}3\ mA$$

De modo que a potência e aumento de temperatura valem, respectivamente:

$$W = 0{,}0083^2 700 = 0{,}048W \qquad \Delta T = \frac{0{,}048}{0{,}030} = 1{,}6\ ^0C$$

Portanto,

$$R = 500[1 + 0{,}005(101{,}6 - 20)] = 704\Omega$$

Daí,

$$V_0 = \frac{R_2 R_{RTD}}{(R_2 + R_{RTD})^2}\left[\frac{dR_3}{R_3} - \frac{dR_1}{R_1} + \frac{dR_2}{R_2} - \frac{dR_{RTD}}{R_{RTD}}\right] V_i(1 - \eta)$$

, para $\eta = \frac{1}{1 + \frac{1 + R_{RTD}/R_2}{\frac{dR_2}{R_2} + \frac{dR_1}{R_1} + \frac{R_{RTD}}{R_2}\left[\frac{dR_3}{R_3} + \frac{dR_{RTD}}{R_{RTD}}\right]}}$

Para $dR_1 = dR_2 = dR_3 = 0$ e $dR_{RTD} = 204\Omega$,

$$\eta = \frac{dR_{RTD}}{dR_{RTD} + R_2 + R_{RTD}} = 0{,}170$$

$$V_0 = \frac{R_2 R_{RTD}}{(R_2 + R_{RTD})^2}\left[-\frac{dR_{RTD}}{R_{RTD}}\right] V_i(1 - \eta) = 3{,}06V$$

O erro do RTD será dado por,

$$e = \frac{\Delta T}{T} = \frac{1{,}6}{100} = 0{,}016 = 1{,}6\%$$

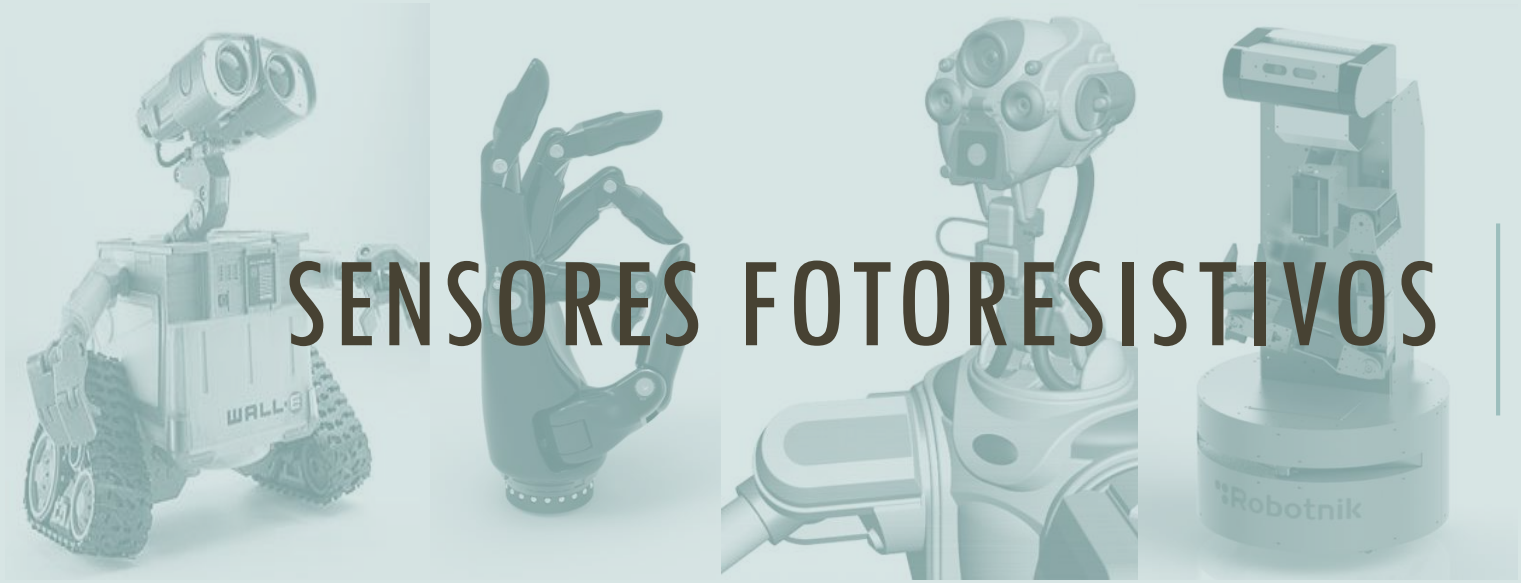

SENSORES FOTORESISTIVOS

PHOTORESISTOR

A photoresistor is also called a *light-dependent resistor* (LDR), *photoconductor*, or *photocell* since its resistance changes as incident light intensity changes. The relationship between the resistance and light intensity can be described by the characteristic curve of a photoresistive sensor (see Figure 2.20a, for an ISL2902 CdS photoresistor from *Festo Didactic*, Hauppauge, NY). The sensor's spectral response (see Figure 2.20b) is about 550 nm (yellow to green region of visible light). When placed in the dark, its resistance is as high as 1 MΩ and then falls to 400 Ω when exposed to bright light. Table 2.9 shows the ISL2902 CdS photoresistor's datasheet. CdS sensors are of very low cost. They are often used in autodimming, darkness, or twilight detection for turning street lights ON and OFF, and for photographic exposure meters.

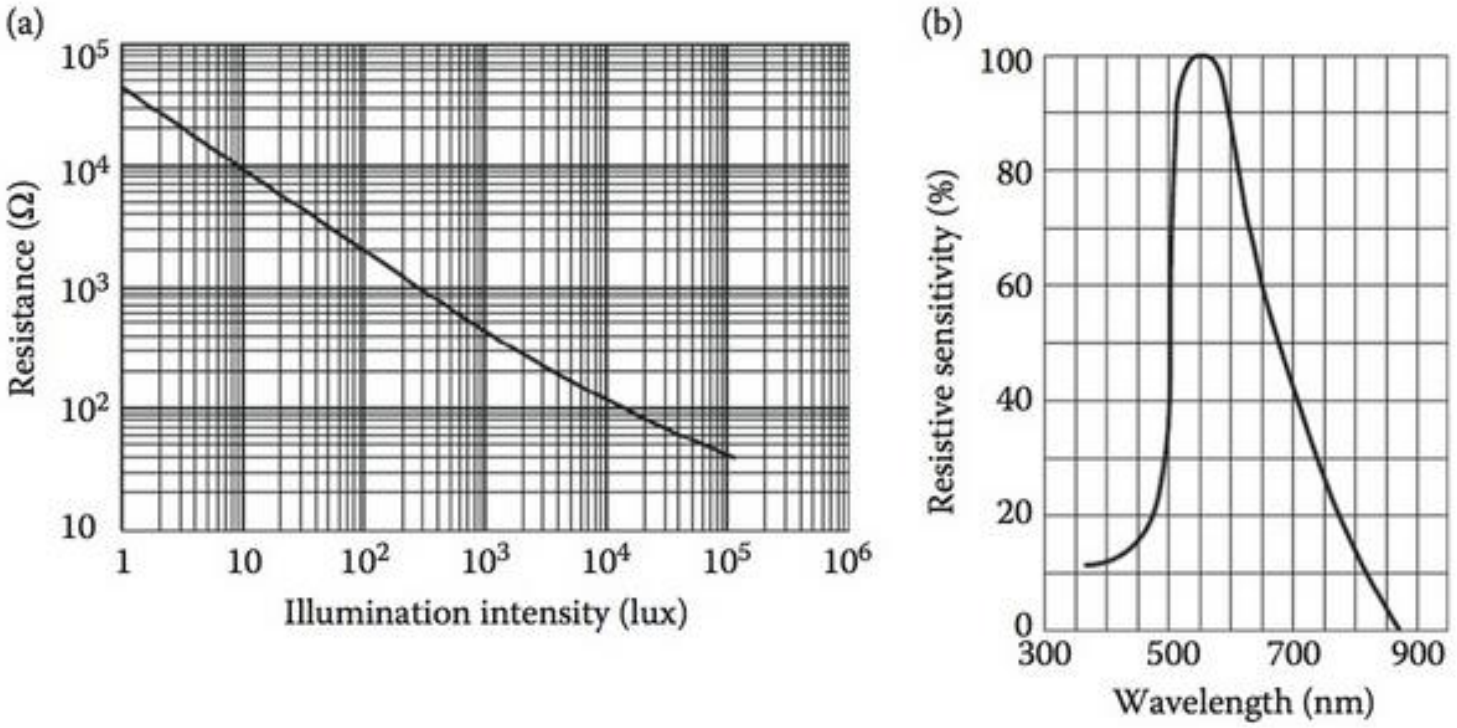

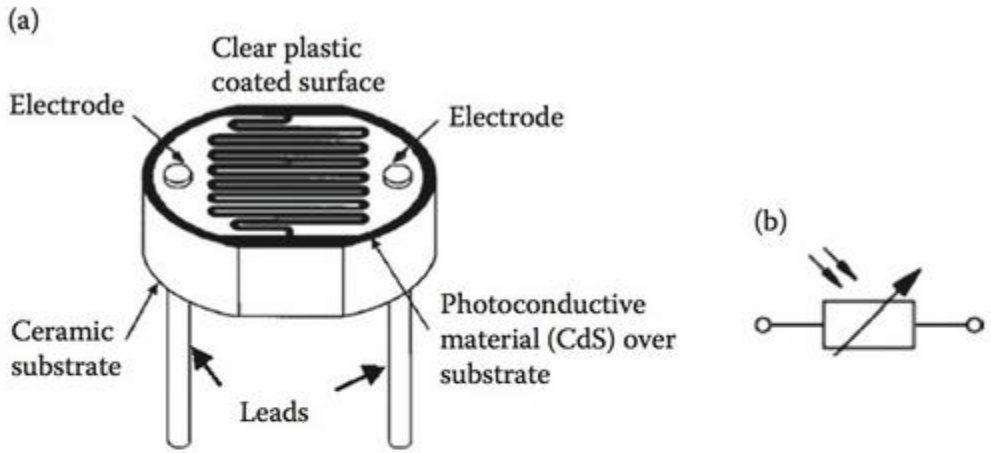

FIGURE 2.21 A typical construction (a) and circuit symbols (b) of a photoresistor.

TABLE 2.10
Characteristics of PGM1200 CdS Photoresistor

Ambient temperature	–30°C ~ +70°C
Spectral peak	560 nm
Photo (light) resistance (at 10 lux)	2 kΩ ~ 5 kΩ
Dark resistance	1.0 MΩ
Response time (rise/decay)	30 ms/40 ms
Dimension (diameter)	5 mm

TABLE 2.11
Application Examples of Photoresistive Sensors

Light control	Automatic gain control
Position sensor	Automatic rear view mirror
Automatic iris control in camera	Automatic headlight dimmer
Camera exposure control	Night light control
Auto slide focus	Oil burner flame out indicator
Colorimetric test equipment	Absence/presence (beam breaker)
Densitometer	Isolated circuit
Electronic scales—dual cell	Photocopy machine—density of toner

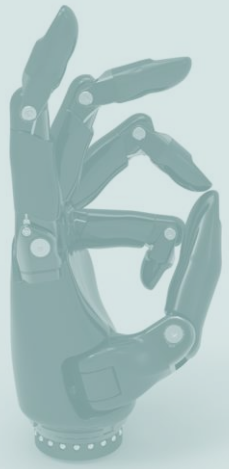

EXTENSÔMETROS

SENSIBILIDADE DA RESISTÊNCIA

Lord Kelvin, em 1856, foi quem primeiro percebeu que condutores metálicos sujeitos a deformações mecânicas exibem mudança em sua resistência elétrica.

$$R = \rho \frac{L}{A}$$

Deformação altera a geometria de um condutor e, por consequência, sua resistência.

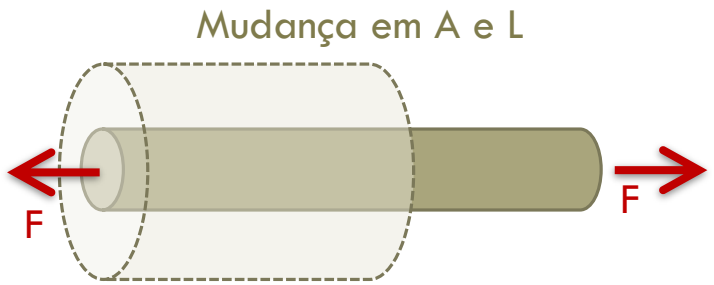

$$\frac{dR}{R} = \frac{d\rho}{\rho} + \frac{dL}{L} - \frac{dA}{A}$$

Variações de resistividade (termo piezoresistivo)

Variação da área de seção transversal A se relaciona com a deformação transversal ε_t

$$\frac{dA}{A} = \frac{2dD}{D} = 2\varepsilon_t$$

Variação do comprimento L se relaciona com a deformação axial do condutor ε_a

$$\frac{dL}{L} = \varepsilon_a$$

FATOR DE GANHO OU GAGE FACTOR

$$\frac{dR}{R} = \frac{d\rho}{\rho} + \frac{dL}{L} - \frac{dA}{A}$$

$$\frac{dR}{R} = \frac{d\rho}{\rho} + \varepsilon_a - 2\varepsilon_t$$

Coeficiente de Poisson: $\nu = -\frac{\varepsilon_t}{\varepsilon_a}$

$$\frac{dR}{R} = \frac{d\rho}{\rho} + (1 + 2\nu)\varepsilon_a$$

$$\frac{dL}{L} = \varepsilon_a$$

$$\frac{dA}{A} = \frac{2dD}{D} = 2\varepsilon_t$$

$$GF = \frac{dR/R}{\varepsilon_a} = \frac{d\rho/\rho}{\varepsilon_a} + (1 + 2\nu)$$

$$1 \leq GF \leq 2$$

Problema para se pensar!!!
Dada a ordem de grandeza do gage fator, as mudanças de resistência devem ser da mesma ordem que as mudanças na deformação! Em materiais de engenharia este nível de deformação é, tipicamente, de 0,000002 - 0,01. Assim, alterações na resistência de não mais do que l% devem ser detectadas! **Aqui reside o desafio na concepção de circuitos de medição e um problema em instalações práticas.**

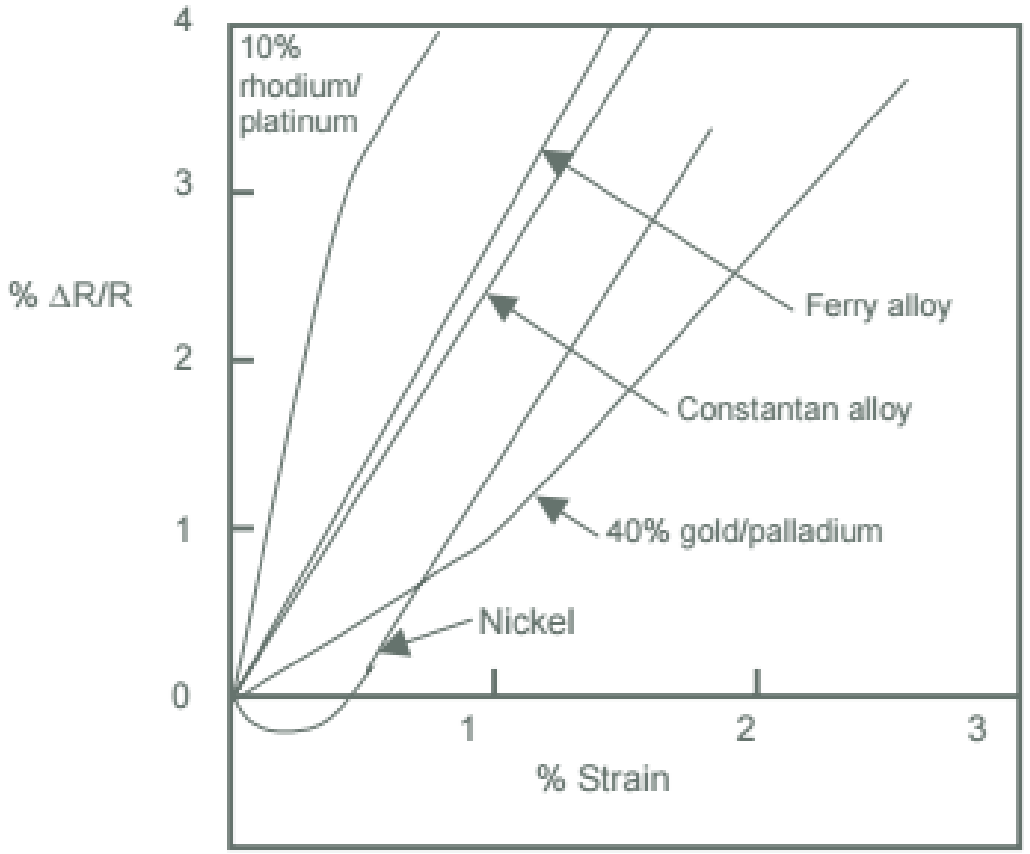

Gauge Factor and Ultimate Elongation for Several Materials

Material	Gauge Factor (GF)		Ultimate Elongation (%)
	For Low Strain	For High Strain	
Copper	2.6	2.2	0.5
Constantan	2.1	1.9	1.0
Platinum	6.1	2.4	0.4
Silver	2.9	2.4	0.8
40% Gold/palladium	0.9	1.9	0.8

Source: From Craig, J.I., *AE3145 Resistance Strain Gage Circuits, Course Materials*, Georgia Institute of Technology, Atlanta, 2000. With permission.

Um sensor tem GF=2,0 e resistência de 120Ω e é usado para medir a deformação de uma estrutura de alumínio. Encontre dR quando a estrutura está sujeita a

A. 5μ de deformação

B. 5m de deformação

Respostas:

0,0012Ω

1,2Ω

EXTENSOMETERS (STRAIN GAUGES)

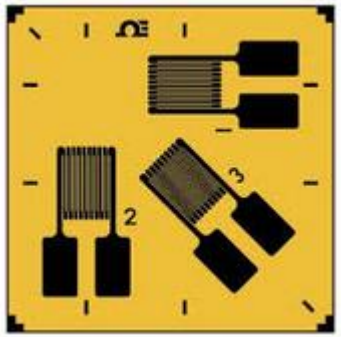

$$R = \frac{\rho l}{A}$$

$$\varepsilon = \frac{1}{G.F.}\frac{\Delta R}{R}$$

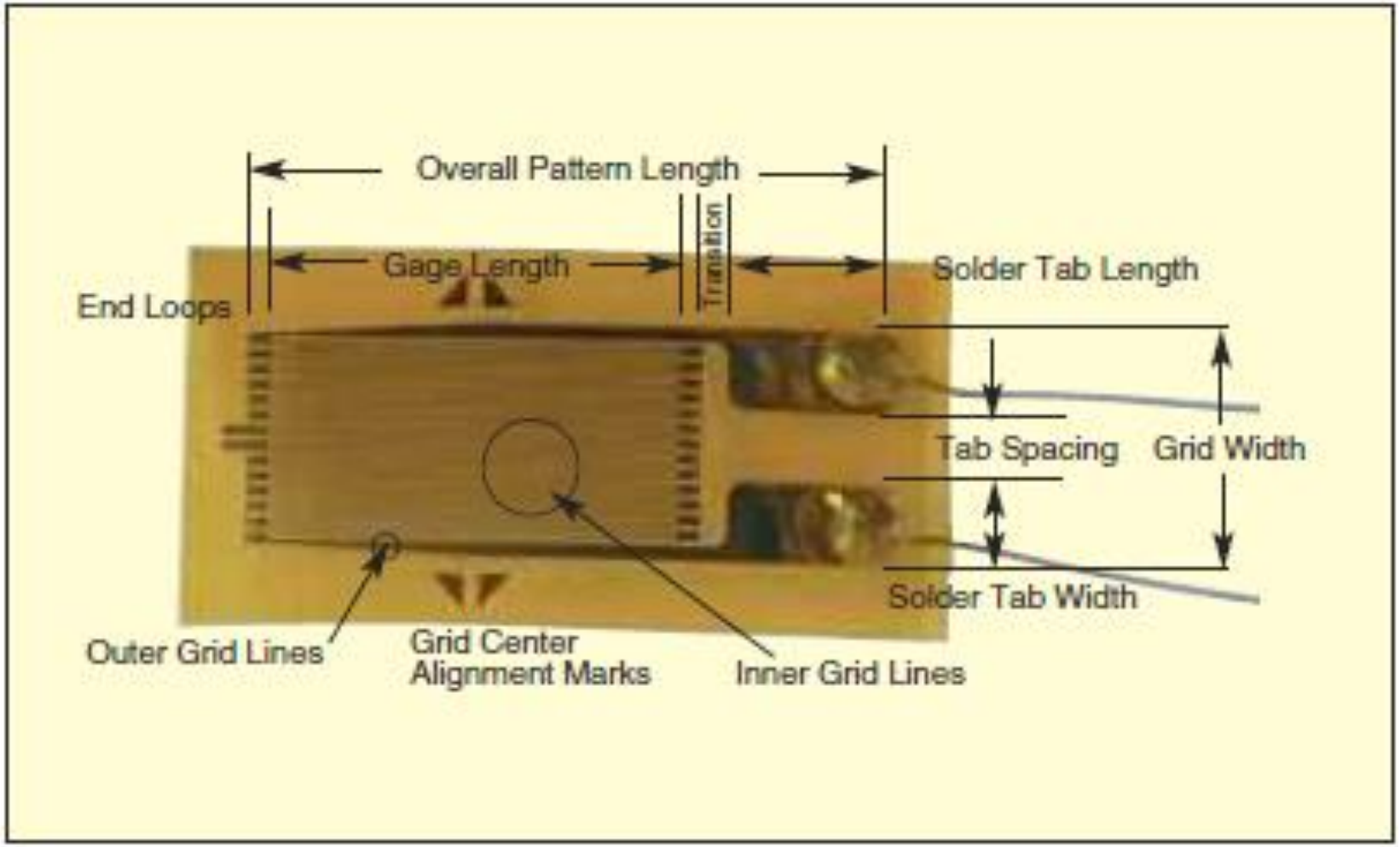

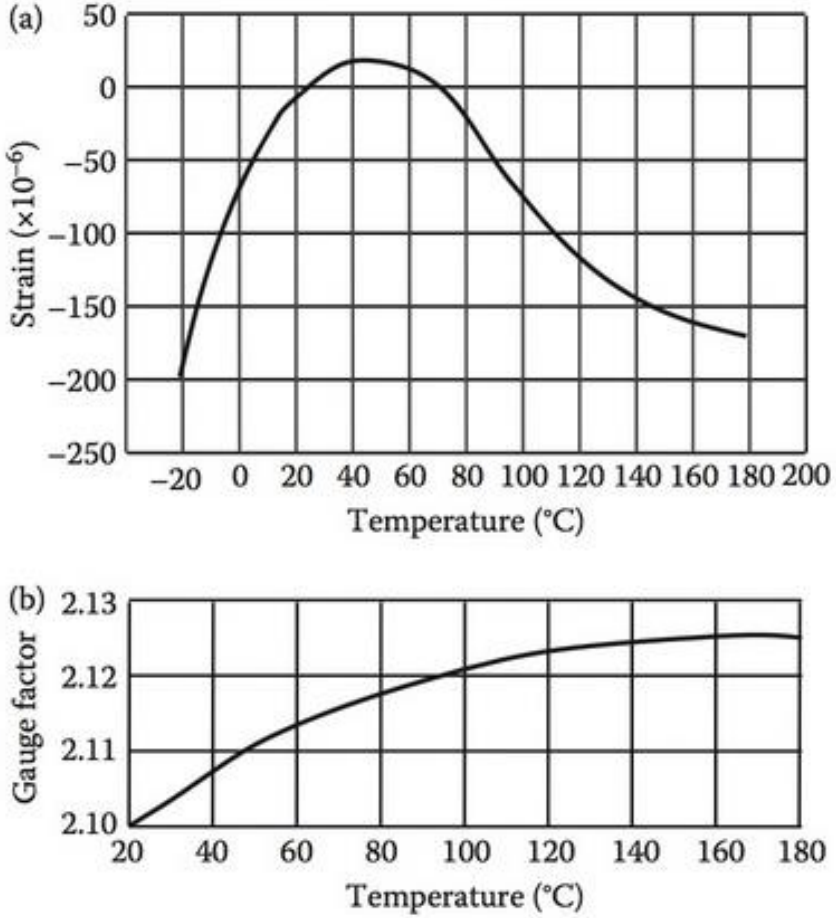

FIGURE 2.28 A foil strain gauge's (a) strain–temperature curve; (b) gauge factor–temperature curve.

2.5.4.1.2 *Metal Foil Strain Gauges*

A foil strain gauge (see Figure 2.29) is the most widely used type. A very thin metal foil pattern (2~5 μm thick, usually Constantan or Nichrome V) is deposited onto a thin insulating backing or carrier (10~30 μm thick, usually epoxy, polyimide, or polycarbonate). The measuring grid pattern including the metallic terminal tabs is produced by the photoetching process. The entire gauge is typically 5~15 mm long.

The main advantages of foil strain gauges over wire gauges are their better heat dissipation, low transverse sensitivity, better flexibility (the smallest bending radius is 0.3 mm), and easy creep compensation (the positive creep of the elastic sensing element can be compensated by the negative creep of the carrier material of the gauge). The disadvantages include limited working temperature due to properties of the carrier materials and adhesives, as well as technical limitations in miniaturization.

2.5.4.1.3 *Single-Crystal Semiconductor Strain Gauges*

This type of strain gauge is manufactured from a thin strip of semiconductor cut from a single crystal of silicon or germanium, doped with accurate amounts of impurities to obtain either *n*- or *p*-type. The output of a semiconductor gauge is very high compared to a wire or foil gauge. Semiconductor gauges can provide both positive and negative gauge factors depending on whether the gauges are *n*-type or *p*-type. The typical gauge factor of a semiconductor is −100 ~ +170, although −115 ~ +205 are achievable. The output of semiconductor gauges is usually nonlinear with strain (*p*-type gauges have better linearity in tension while *n*-type gauges are more linear in compression), but they exhibit no creep or hysteresis and have an extremely long fatigue life. Semiconductor gauges are highly sensitive to temperature; thus they require a high level of temperature compensation. They also present large TCR due to their specific resistance–temperature curves. Semiconductor gauges are widely used in small sensors such as force, acceleration, and pressure sensors since their sensing elements can be micromachined out of a single piece of silicon. Figure 2.30 illustrates a semiconductor strain gauge—a resistance strip (fabricated from a semiconductor single crystal) fixed on an insulating substrate that supports both the strip and the terminals on its surface.

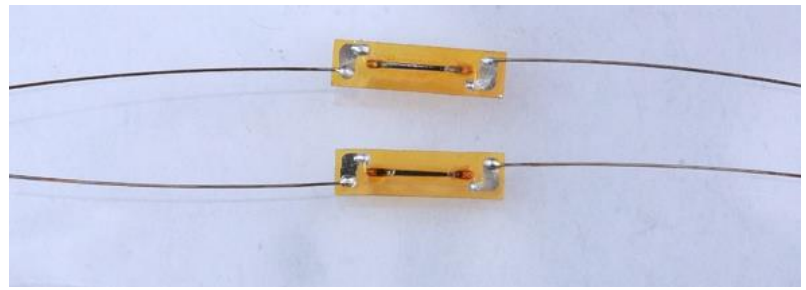

Strain gauges: características

- Ligas de constantan e níquel-cromo
- Preço acessível
- Não reutilizável
- Preciso
- Boa resposta em frequência
- Resistividade transversal é reduzida com aumento da área da grade em seus extremos
- Resistividade transversal = G_F transversa/ G_F longitudinal=[0:10%]
- Uso de resistores de precisão para completar a ponte
- Dissipação de calor por efeito Joule pode afetar balanceamento
- Limitar voltagem de alimentação: [3-10V]

VISHAY PRECISION GROUP

GAGE PATTERN AND MATRIX (1X SIZE)	GAGE LENGTH in (mm)	OVERALL LENGTH in (mm)	GRID WIDTH in (mm)	OVERALL WIDTH in (mm)	GAGE DESIGNATION	RES. IN OHMS	STD. CREEP CODE
Full-Bridge Patterns							
S5027 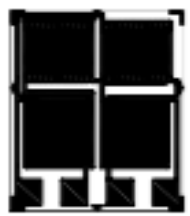	0.033 (0.86)	0.1515 (3.85)	0.056 (1.43)	0.127 (3.21)	N2K-XX-S5027P-10C/DG/E3 N5K-XX-S5027P-10C/DG/E3	1000 ±0.2% 1000 ±0.2%	P* P*
	1K Full bridge gage. Bridge is balanced to ±0.4 mV/V, but RG is 1000 ohms ±0.2%.						
S5020 	0.028 (0.71)	0.147 (3.73)	0.044 (1.12)	0.137 (3.48)	N2K-XX-S5020Q-50C/DG/E3 N5K-XX-S5020Q-50C/DG/E3	5000 ±0.2% 5000 ±0.2%	Q* Q*
	Full bridge gage for bending beam transducers. Bridge is balanced to ±0.4 mV/V, but RG is 5000 Ω ±0.2%.						

Linear strain gauges with 1 measurement grid

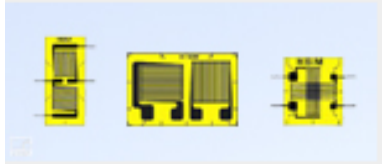

T rosettes with 2 measuring grids for analyzing biaxial stress states with known principal directions

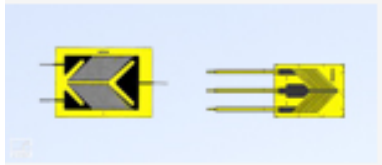

Torsion/shear strain gauges with 2 measuring grids for measurements on torsion bars and determining shear stresses

Strain gauge rosettes with 3 measuring grids for analyzing biaxial stress states with unknown principal strain directions

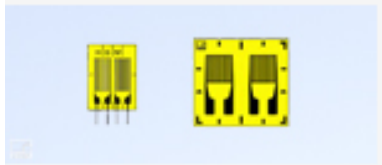

Strain gauge with 2 parallel measurement grids

Full bridge strain gauges with 4 measuring grids for measurements on tension/compression bars

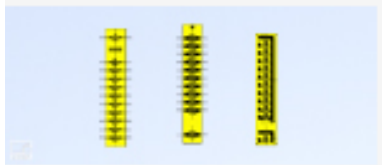

Strain gauge chains for determining strain gradients

The Specialist for extreme Temperatures

http://www.hbm.com/en/menu/products/strain-gages-accessories/strain-gauges-for-stress-analysis/

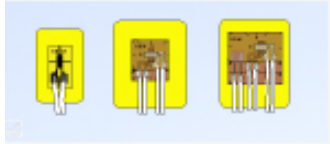

Encapsulated strain gages with 3m stranded connection wire

Strain gauges for determining residual stress

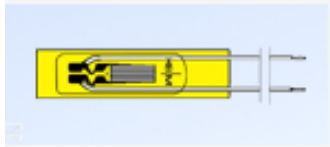

Weldable strain gauge for measurements at elevated temperatures

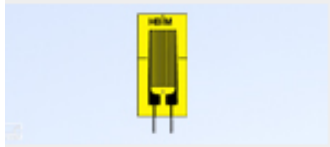

Strain gauges for high strains or compression greater than 5 %

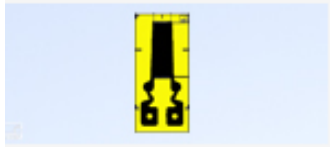

Strain gauge for integration into fiber composites

Crack propagation gauges for determining crack propagation

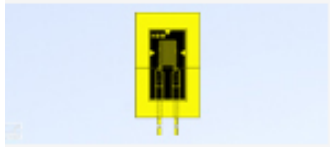

Encapsulated / Waterproof Strain Gauge

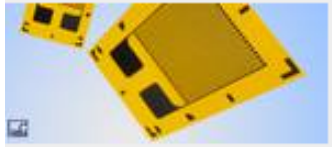

The temperature sensor that is installed as easily as a strain gauge

Measurement gauge for transient pressure measurement

KFH-C1 Series
R$ 690,00 | Saiba mais
Strain Gages com Fios Soldados, Lineares, Rosetas Planas X-Y (Roseta T), Rosetas Planas 0°/45°/90°

KFH-C1 Series
R$ 505,00 | Saiba mais
Strain Gages com Fios Soldados, Lineares, Rosetas Planas X-Y (Roseta T), Rosetas Planas 0°/45°/90°

KFH-C1 Series
R$ 625,00 | Saiba mais
Strain Gages com Fios Soldados, Lineares, Rosetas Planas X-Y (Roseta T), Rosetas Planas 0°/45°/90°

KFH-D16 Series
R$ 1.230,00 | Saiba mais
Strain Gages com Fios Soldados, Lineares, Rosetas Planas X-Y (Roseta T), Rosetas Planas 0°/45°/90°

KFH-D17 Series
R$ 1.845,00 | Saiba mais
Strain Gages com Fios Soldados, Lineares, Rosetas Planas X-Y (Roseta T), Rosetas Planas 0°/45°/90°

OMEGA/HBM M Series
R$ 995,00 | Saiba mais
OMEGA/HBM Strain Gages | High Temperature and Resistance to Alternating Loads

SGD-1000-LY Series
R$ 670,00 | Saiba mais
Extensômetro de Precisão
Padrão Linear de Precisão para Aplicações Dinâmicas e Estáticas

SGD-LY Series
R$ 308,00 | Saiba mais
Extensômetro de Precisão
Padrão Linear de Precisão para Aplicações Dinâmicas e Estáticas

SGD-LY Series
R$ 344,00 | Saiba mais
Extensômetro de Precisão
Padrão Linear de Precisão para Aplicações Dinâmicas e Estáticas

SGD-LY Series
R$ 420,00 | Saiba mais
Extensômetro de Precisão
Padrão Linear de Precisão para Aplicações Dinâmicas e Estáticas

SGD-LY40 Series
R$ 1.045,00 | Saiba mais
Precision Strain Gauges Extra-Long Grid Pattern for Inhomogeneous Materials

https://br.omega.com/

EXEMPLO

Objetivo

Um recipiente de bebida não alcoólica de alumínio será usado para modelar um cilindro de pressão de parede fina, com pressão interna desconhecida. A superfície da lata será instrumentada com strain gages. Quando a lata é aberta a ponte de Wheatstone deverá registrar a deformação. A pressão dentro da lata é, então, calculada.

Material and Equipamentos:

- Lata de alumínio
- Strain gages (você deve saber o valor da sensibilidade);
- Resistências, trimpots;
- Tesoura, cola superbonder ou similar;
- Lápis, compasso, régua, calculadora e papel milimetrado.

Figuras extraídas da internet

INSTALAÇÃO DOS EXTENSÔMETROS

- Lixar a superfície com uma lixa média e depois com uma lixa muito fina até ficar perfeitamente lisa;
- Marcar a posição do extensômetro;
- Limpar a região onde o extensômetro será colado com acetona para que impurezas não prejudiquem a aderência da cola;
- Com um pedaço de fita, colar o extensômetro com a resistência para cima, passando a cola vagarosamente;
- Pressionar o extensômetro por cima da fita por um tempo razoável;
- Retirar a fita “durex”;
- Colagem do material isolante para apoio dos fios
- Soldagem dos fios para posterior ligação no equipamento de aquisição de dados
- Colocação da pasta (borracha) isolante para proteger o extensômetro.

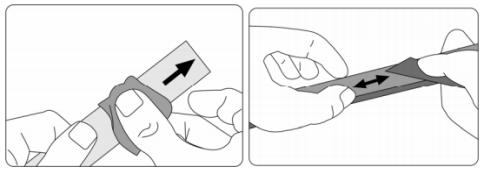

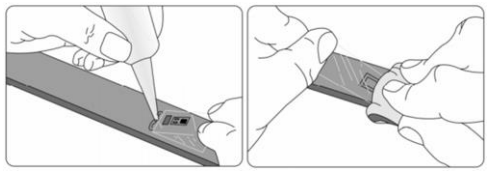

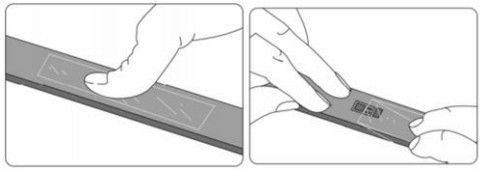

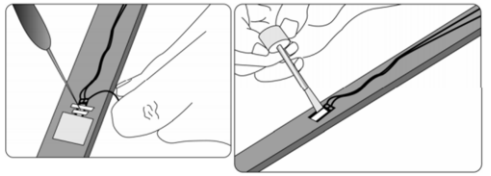

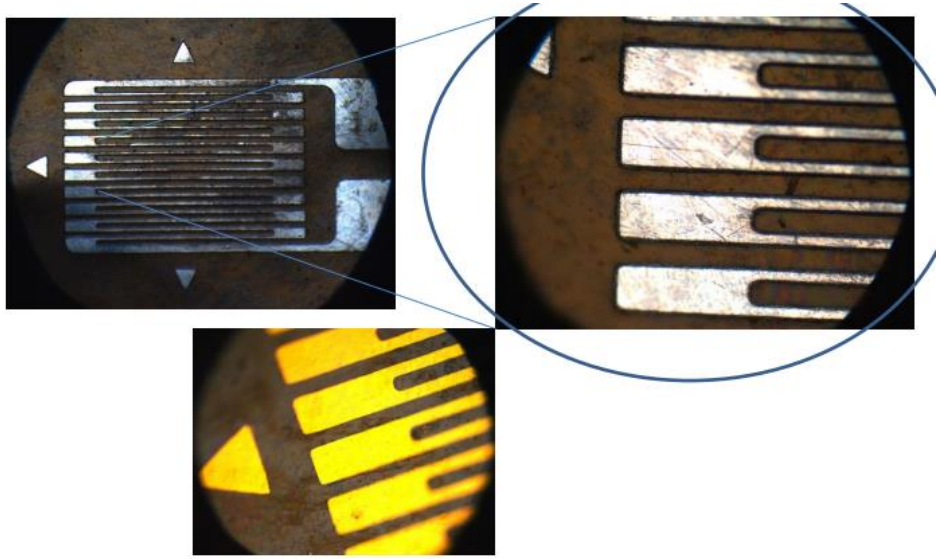

- lixamento
- Limpeza [álcool]
- alinhamento
- Superbond
- Pressão
- Cabeamento
- Testes preliminares

Strain gauges: cabeamento

- Densidade de potência = potência dissipada pelo sg / área do sg [com grade] [de 1 a 10 mW/mm^2]
- Sg tem resolução em torno de 1 micro-strain para ¼ de ponte a 2V e voltímetro de resolução 1mV
- Corrente de 10 a 30 mA
- Aterramento
- Magnetismo

Ex.- Resolução de 1 passo em 1000 km

Exemplo: variação de resistência em um fio de cobre ao pesar uma pessoa

E=100GPa

Rho=2E-8 Ohm.m

Sig_r=200MPa

PONTE DE WHEATSTONE

One advantage of a Wheatstone bridge is that the temperature effect can be directly eliminated. If R_1 is a strain gauge bonded to a specimen and R_2 is a strain gauge held onto a different specimen with heat sink compound, then R_1 will respond to strain plus temperature, and R_2 will only respond to temperature. Since the bridge subtracts the output of R_1 from that of R_2, the temperature effect is cancelled. The typical full-scale bridge output is 10–100 mV.

Variações de resistência de um extensômetros são pequenas

Em 1843, Sir Charles Wheatstone projetou um circuito em ponte que capaz de medir pequenas variações de resistência elétrica [baseado no trabalho de Samuel Hunter Christie, 1833]

O circuito pode ser montado com um ou mais de seus resistores sendo extensômetros, de forma a se obter uma voltagem V_{out} que indique a deformação imposta ao sensor

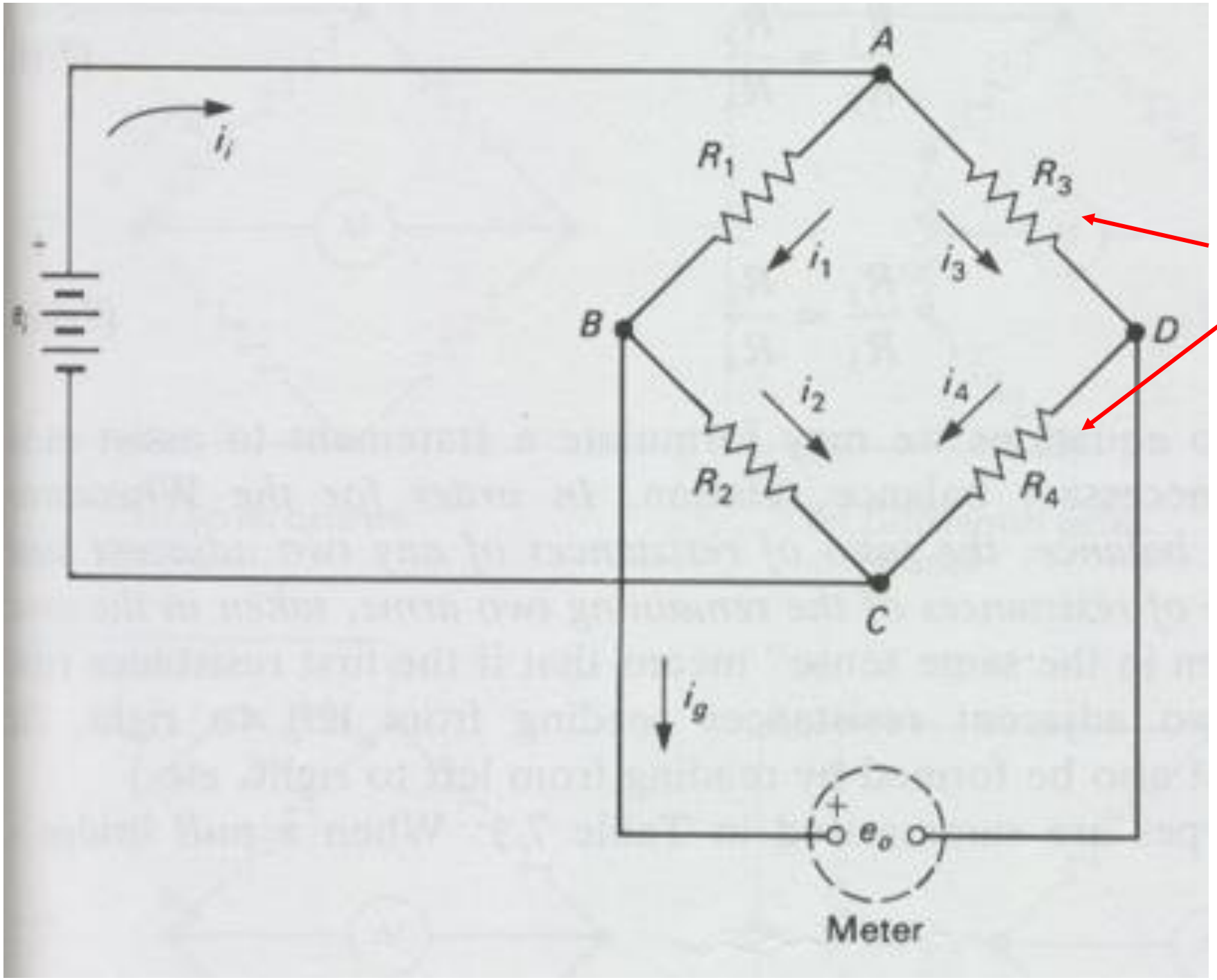

Ramos adjacentes

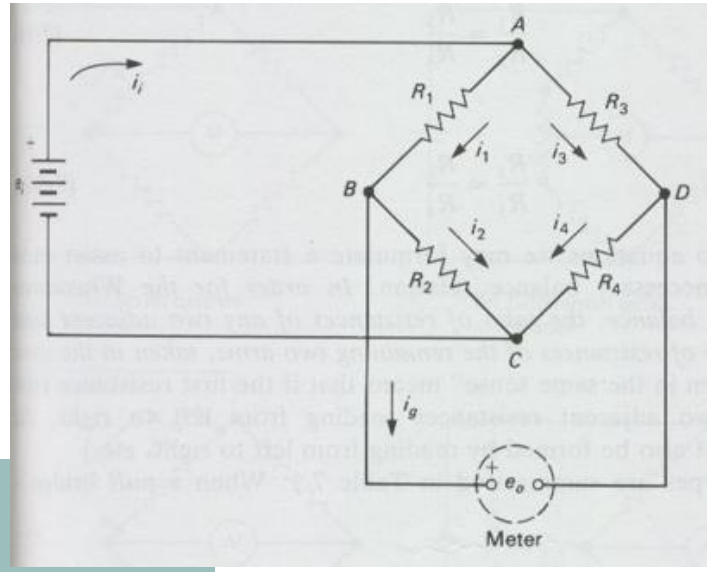

Para a ponte estar balanceada :

$$e_0 = 0 \rightarrow i_g = 0 \rightarrow i_1 = i_2, i_3 = i_4$$

$$e_0 = 0 \rightarrow V_{BD} = 0 \rightarrow V_{BA} = V_{DA} \rightarrow V_{BC} = V_{DC}$$

$$i_1 R_1 = i_3 R_3 \rightarrow i_2 R_2 = i_4 R_4$$

$$i_1 R_2 = i_3 R_4 = i_1 \frac{R_1}{R_3} R_4$$

$$\frac{R_2}{R_4} = \frac{R_1}{R_3}$$

Voltagem induzida pela deformação :

$$i_1 = \frac{e_i}{R_1 + R_2}$$

$$e_{BC} = R_2 i_1 \rightarrow e_{BC} = \frac{R_2}{R_1 + R_2} e_i$$

$$e_{DC} = \frac{R_4}{R_3 + R_4} e_i$$

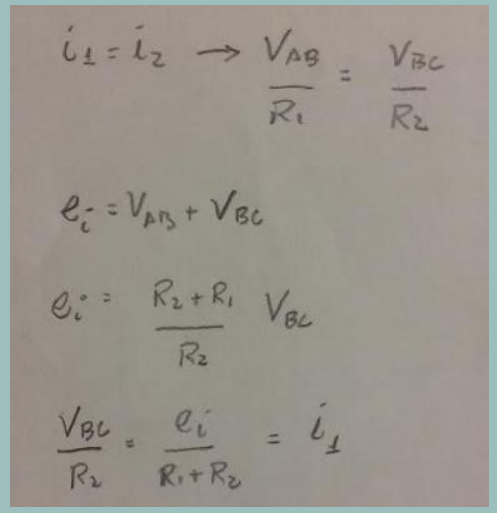

Voltagem de saída da ponte :

$$e_0 = e_{BC} - e_{DC} = \left(\frac{R_2}{R_1 + R_2} - \frac{R_4}{R_3 + R_4} \right) e_i = \left(\frac{R_2 R_3 - R_1 R_4}{(R_1 + R_2)(R_3 + R_4)} \right) e_i$$

Se cada resistência variar ΔR_i, segue que :

$$e_0 = e_i \frac{R_3 R_4}{(R_3 + R_4)^2} \left(\frac{\Delta R_2}{R_2} - \frac{\Delta R_1}{R_1} + \frac{\Delta R_3}{R_3} - \frac{\Delta R_4}{R_4} \right) (1 - \eta)$$

$$\eta = \frac{1}{1 + \dfrac{1 + R_4 / R_3}{\dfrac{\Delta R_3}{R_3} + \dfrac{\Delta R_1}{R_1} + \dfrac{R_4}{R_3} \left(\dfrac{\Delta R_4}{R_4} + \dfrac{\Delta R_2}{R_2} \right)}}$$

Não linearidade pequena

6.5.3.1 Wheatstone Bridge Driven by a Constant Voltage

There are four basic Wheatstone bridge configurations for resistive sensors driven by a constant voltage:

- *Single-element variation* (Figure 6.7a). This configuration is suited for a single sensor (a thermistor, an RTD, or a strain gauge). All the resistances are nominally equal, except the sensor that varies by an amount ΔR. V_{out} is nonlinearly related to ΔR by

$$V_{out} = \frac{\Delta R}{4(R + \Delta R/2)} V_{ex} \tag{6.20}$$

- *Two-diagonal-element variation* (Figure 6.7b). This configuration is used for two identical sensors mounted diagonally to each other. For example, strain gauges with their axes in parallel, pressure or flow meters that have one for sensing and the other for reference. In this case, the bridge output is twice that of the single-element varying bridge:

$$V_{out} = \frac{\Delta R}{2(R + \Delta R/2)} V_{ex} \tag{6.21}$$

- *Two-adjacent-element variation* (Figure 6.7c). This structure contains two adjacently mounted elements, but they vary in opposite directions (e.g., two identical strain gauges: one mounted on the top of a flexing surface, and the other on the bottom). In this case, V_{out} and ΔR are linearly related, and the bridge output is:

$$V_{out} = \frac{\Delta R}{2R} V_{ex} \tag{6.22}$$

- *Four-element variation* (Figure 6.7d). This bridge produces the largest output for resistance changes and is inherently linear. It becomes an industry-standard configuration for load cells which are constructed from four identical strain gauges. The bridge output is:

$$V_{out} = \frac{\Delta R}{R} V_{ex} \tag{6.23}$$

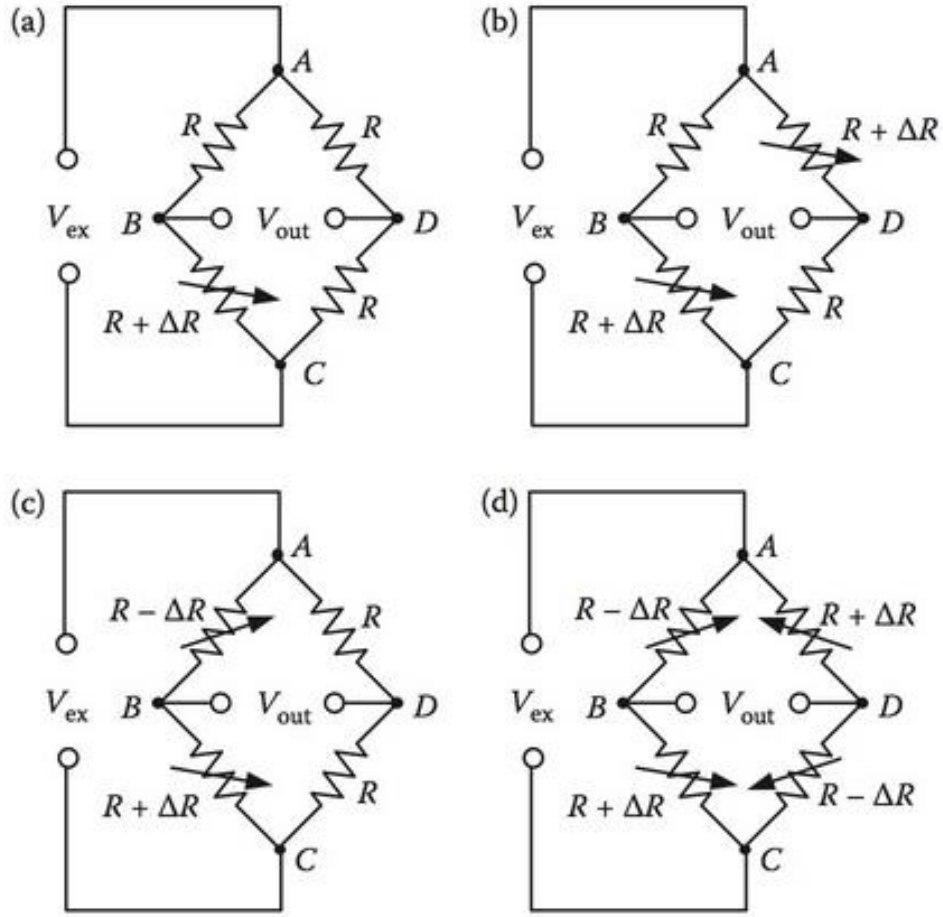

FIGURE 6.7 Four common Wheatstone bridge configurations under a constant voltage drive: (a) single-element; (b) two-diagonal-element; (c) two-adjacent-element; and (d) four-element variations.

6.5.3.2 Wheatstone Bridge Driven by a Constant Current

A Wheatstone bridge can also be driven by a constant current source. A constant current-driven Wheatstone bridge requires an accurate current source since any change in the current will be interpreted as a resistance change. In addition, the drive current must be small to minimize the error caused by power dissipation or self-heating in the resistive sensor. The current drive, though not as popular as the voltage drive, has two advantages:

- The measurement will not be affected by the voltage drop in wire or excitation line resistance. Thus, the bridge can be located remotely from the source of excitation.
- The bridge output is more linear over a large range of ΔR than that of the voltage drive.

Similar to the constant voltage drive, there are four common configurations (see Figure 6.8):

- *Single-element variation* (Figure 6.8a). All the resistances are nominally equal except the sensor's resistance that varies. The output V_{out} is

$$V_{out} = \frac{I_{ex}}{4} \frac{R\Delta R}{(R + \Delta R/4)} \tag{6.24}$$

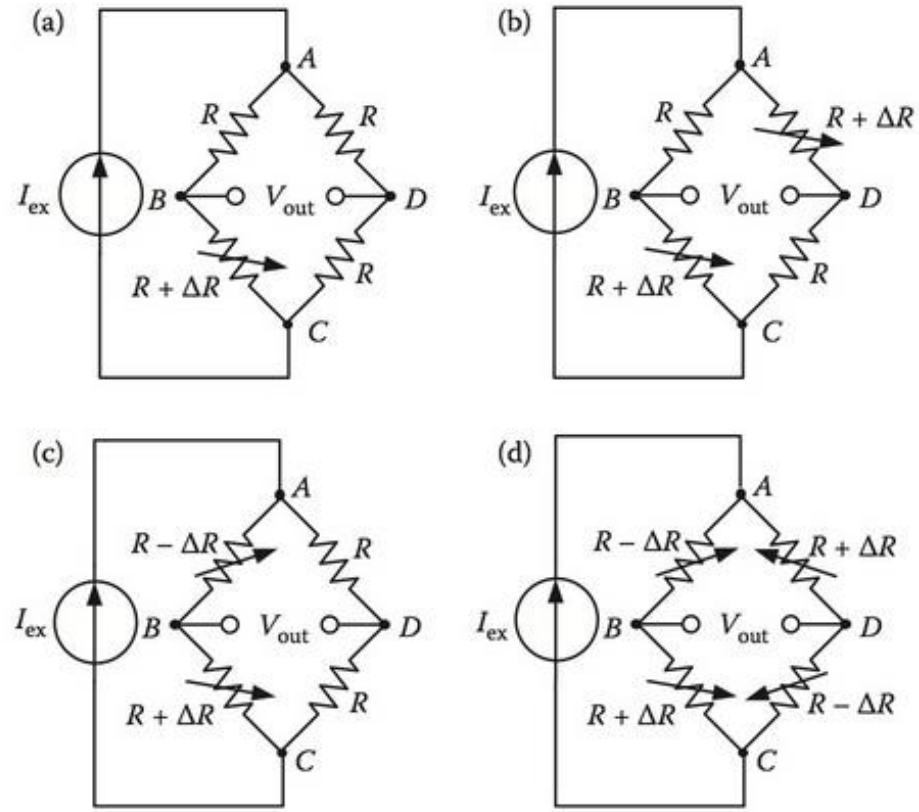

FIGURE 6.8 Four common Wheatstone bridge configurations under a constant current drive: (a) single-element; (b) two-diagonal-element; (c) two-adjacent-element; and (d) four-element variations.

- *Two-diagonal-element variation*. Two identical sensors are mounted diagonally to each other (Figure 6.8b). V_{out} is proportional to ΔR and has a bigger magnitude than that of the single-element varying bridge:

$$V_{out} = \frac{I_{ex}}{2}\Delta R \tag{6.25}$$

- *Two-adjacent-element variation*. Two identical but varying *oppositely* sensors are mounted adjacently to each other (Figure 6.8c). V_{out} is related to ΔR by

$$V_{out} = \frac{I_{ex}}{2}\Delta R \tag{6.26}$$

- *All-element variation* (Figure 6.8d). This bridge configuration has the largest output for the resistance change and is inherently linear.

$$V_{out} = I_{ex}\Delta R \tag{6.27}$$

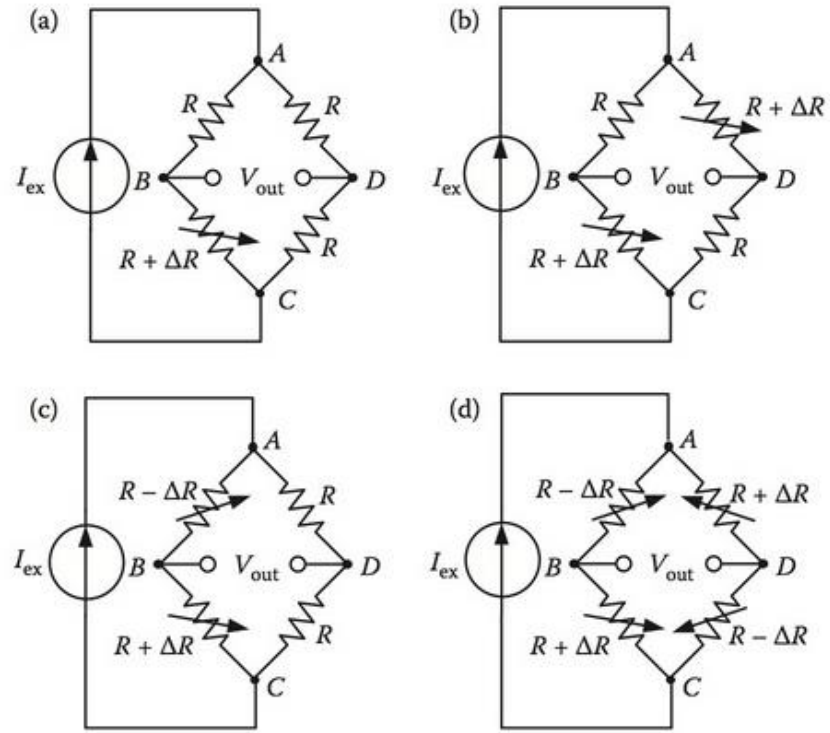

FIGURE 6.8 Four common Wheatstone bridge configurations under a constant current drive: (a) single-element; (b) two-diagonal-element; (c) two-adjacent-element; and (d) four-element variations.

No.	Name	Sample Application	Circuit	Output	Remarks
1	1-active-gage 2-wire system Number of gages: 1	 Uniaxial stress (Uniform tension/compression)	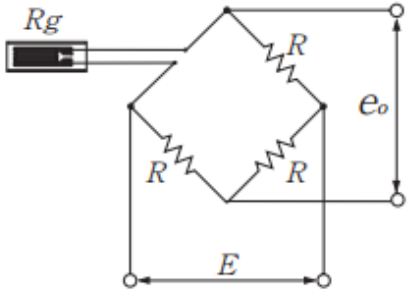	$e_o = \frac{E}{4} K_S \cdot \varepsilon_o$ K_S : Gage factor ε_o : Strain E : Excitation voltage e_o : Output voltage Rg : Gage resistance R : Fixed resistance	Suitable for use under environment of less ambient temperature changes; no temperature compensation. x 1 output
2	1-active-gage 3-wire system Number of gages: 1	 Uniaxial stress (Uniform tension/compression)	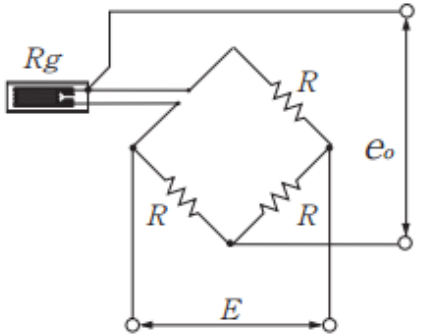	$e_o = \frac{E}{4} K_S \cdot \varepsilon_o$	No temperature compensation; thermal effect of leadwires canceled. x 1 output
3	1-active-gage (dual series gages) 2-wire system for (for cancel bending strain) Number of gages: 2	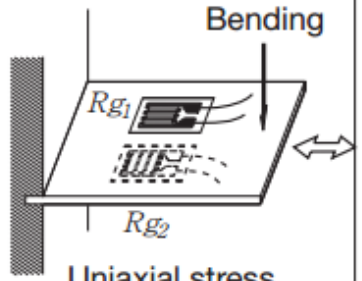 Uniaxial stress (Uniform tension/compression)	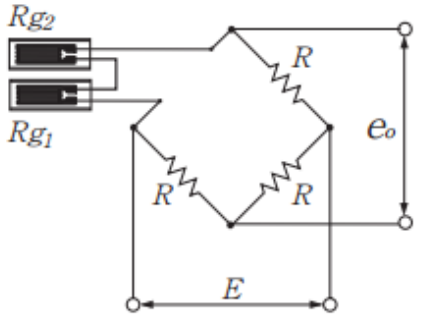	$e_o = \frac{E}{4} K_S \cdot \varepsilon_o$ Rg_1 ·····Strain : ε_1 Rg_2 ·····Strain : ε_2 $\varepsilon_o = \frac{\varepsilon_1 + \varepsilon_2}{2}$ R : Fixed resistance $R = Rg_1 + Rg_2$ ※	No temperature compensation; bending strain canceled. x 1 output

●Relation between strain and voltage

The output of a strain gage bridge is expressed as a strain quantity (μm/mm/m) or an output voltage (mV/V or μV/V) against the bridge voltage. The strain quantity and the output voltage have the following relation:

$$e_o = \frac{E}{4} K_S \cdot \varepsilon_o$$

If the bridge voltage E = 1 V and the gage factor Ks = 2.00, $2e_o = \varepsilon_o$.
Thus, a strain output is always 2 times larger than a bridge output voltage.

e.g. 3000 μm/m → 1500 μV/V = 1.5 mV/V

4	1-active-gage (dual series gages) 3-wire system for (for cancel bending strain) Number of gages: 2	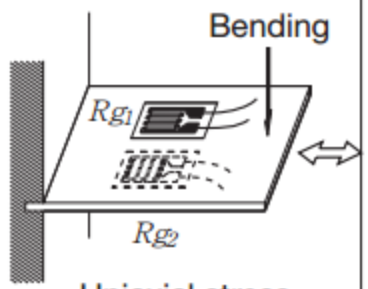 Uniaxial stress (Uniform tension/compression)	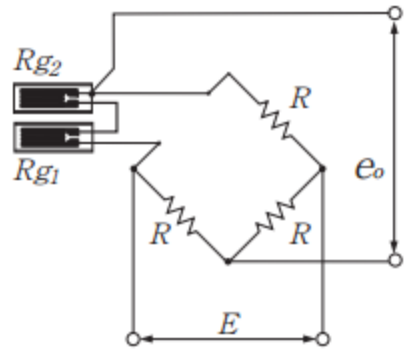	$e_o=\frac{E}{4}K_S \cdot \varepsilon_o$ Rg_1 ·····Strain : ε_1 Rg_2 ·····Strain : ε_2 $\varepsilon_o=\frac{\varepsilon_1+\varepsilon_2}{2}$ R : Fixed resistance $R=Rg_1+Rg_2$ ※	No temperature compensation; bending strain canceled; thermal effect of leadwires canceled. x 1 output
5	Active-dummy 2-gage method Number of gages: 2	Active gage 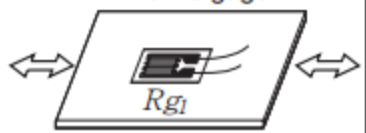 Uniaxial stress (Uniform tension/compression) Dummy gage 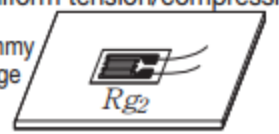	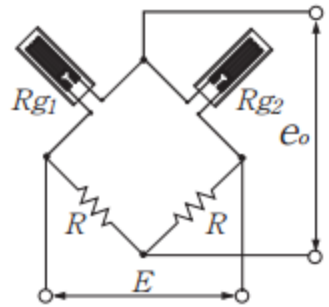	$e_o=\frac{E}{4}K_S \cdot \varepsilon_o$ K_S : Gage factor ε_o : Strain E : Excitation voltage e_o : Output voltage Rg_1 : Strain: ε_o R : Fixed resistance Rg_2 ·····Strain: 0	Temperature compensation; thermal effect of leadwires canceled. x 1 output
6	Orthogonal 2-active-gage method Number of gages: 2	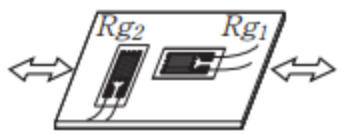 Uniaxial stress (Uniform tension/compression)	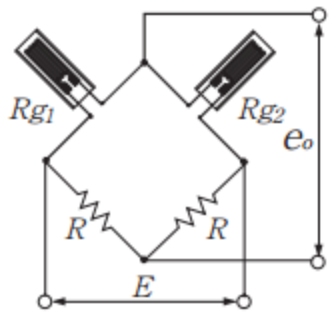	$e_o=\frac{(1+\nu)E}{4}K_S \cdot \varepsilon_o$ ν : Poisson's ratio Rg_1, Rg_2 : Gage resistance Rg_1 ·····Strain : ε_o Rg_2 ···Strain : $-\nu\varepsilon_o$ R : Fixed resistance	Temperature compensation; thermal effect of leadwires canceled. x (1+ν) output

7	2-active-gage method (for bending strain measurement) Number of gages: 2	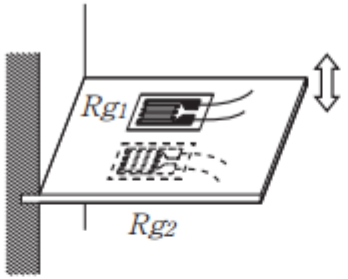 Bending stress	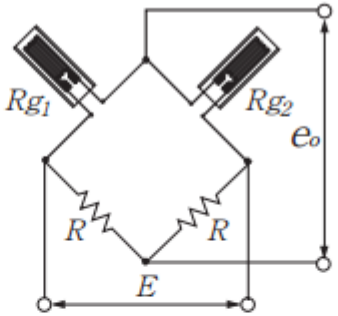	$e_o = \frac{E}{2} K_S \cdot \varepsilon_o$ Rg_1 ·····Strain : ε_o Rg_2 ···Strain : $-\varepsilon_o$ R : Fixed resistance	Temperature compensation; thermal effect of leadwires canceled; compressive/ tensile strain cancelled x 2 output
8	Opposite side 2-active-gage 2-wire system Number of gages: 2	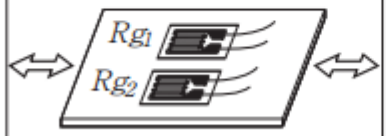 Uniaxial stress (Uniform tension/compression)	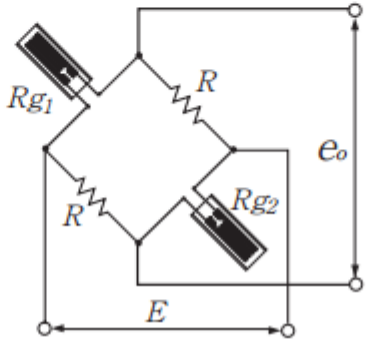	$e_o = \frac{E}{2} K_S \cdot \varepsilon_o$ Rg_1 ·····Strain : ε_o Rg_2 ·····Strain : ε_o R : Fixed resistance	No temperature compensation; bending strain canceled by bonding to the front and rear. x 2 output
9	Opposite side 2-active-gage 3-wire system Number of gages: 2	 Uniaxial stress (uniform tension/compression)	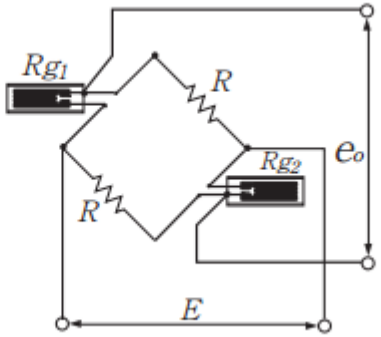	$e_o = \frac{E}{2} K_S \cdot \varepsilon_o$ Rg_1·····Strain : ε_o Rg_2·····Strain : ε_o R: Fixed resistance	No temperature compensation; thermal effect of leadwires canceled; bending strain canceled by bonding to the front and rear. x 2 output

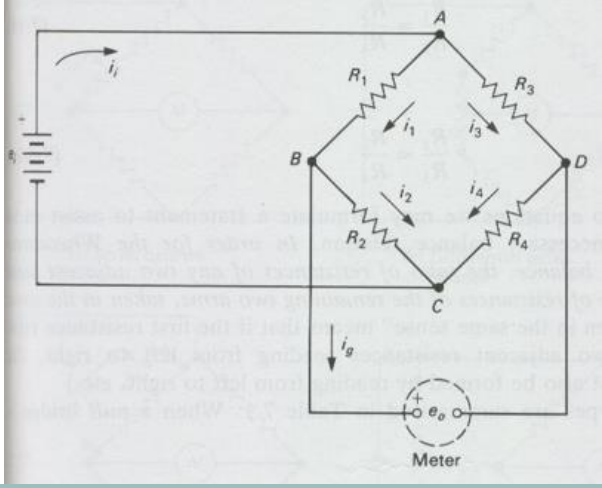

$$e_0 = e_i \frac{R_3 R_4}{(R_3 + R_4)^2}\left(\frac{\Delta R_2}{R_2} - \frac{\Delta R_1}{R_1} + \frac{\Delta R_3}{R_3} - \frac{\Delta R_4}{R_4}\right)$$

$$e_0 = e_i \frac{R^2}{4R^2}\left(\frac{\Delta R_3}{R_3} - \frac{\Delta R_4}{R_4}\right)$$

$$e_0 = e_i \frac{R^2}{4R^2}\left(\frac{\Delta R}{R} - \frac{-\Delta R}{R}\right)$$

$$e_0 = e_i \frac{\Delta R}{2R}$$

$$GF = \frac{\Delta R / R}{\varepsilon}$$

$$e_0 = e_i GF \varepsilon / 2$$

10	4-active-gage system (for bending strain measurement) Number of gages: 4	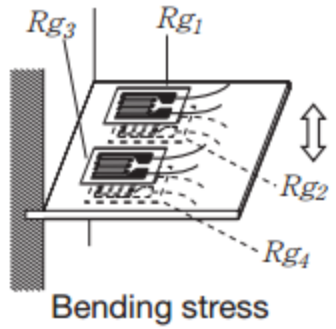	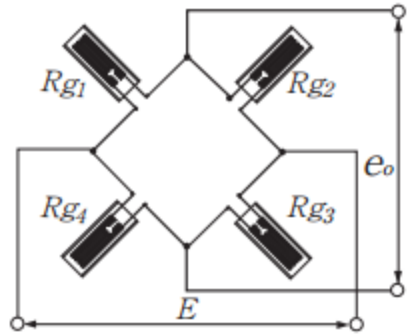	$e_o = \mathrm{Ks} \cdot \varepsilon_o \cdot E$ Rg_1, Rg_3…… Bending strain : ε_o Rg_2, Rg_4 …… Bending strain : $-\varepsilon_o$	Temperature compensation; thermal effect of leadwires canceled; compressive/ tensile strain canceled. x 4 output
11	Orthogonal 4-active-gage system Number of gages: 4	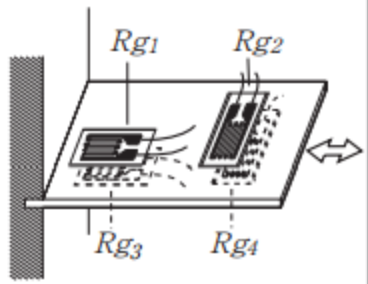	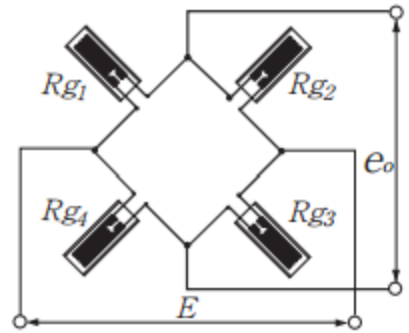	$e_o = \frac{(1+\nu)E}{2} \mathrm{Ks} \cdot \varepsilon_o$ ν : Poisson's ratio Rg_1, Rg_3…… Strain : ε_o Rg_2, Rg_4…… Strain : $-\nu\,\varepsilon_o$	Temperature compensation; thermal effect of leadwires canceled. x 2(1+ν) output
12	Active-dummy 4-gage system Number of gages: 4	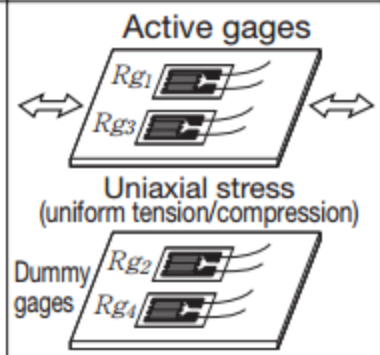	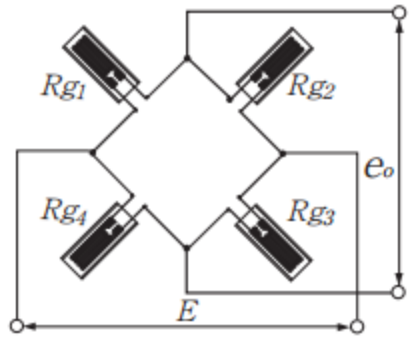	$e_o = \frac{E}{2} \mathrm{Ks} \cdot \varepsilon_o$ Rg_1, Rg_3…… Strain : ε_o Rg_2, Rg_4…… Strain : 0	Temperature compensation; thermal effect of leadwires canceled; bending strain canceled by bonding to the front and rear. x 2 output

13	2-active-gage system (for twisting strain measurement) Number of gages: 2	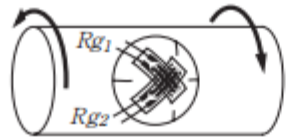	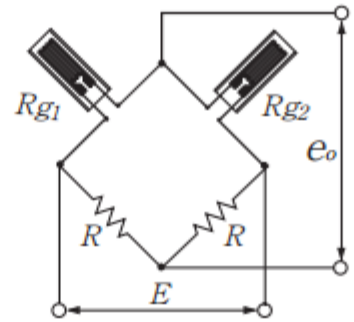	$e_o = \frac{E}{2} K_S \cdot \varepsilon_0$ Rg_1…… Twisting strain : ε_0 Rg_2…… Twisting strain : $-\varepsilon_0$ R : Fixed resistance	Temperature compensation; thermal effect of leadwires canceled. x 2 output
14	4-active-gage system (for twisting strain measurement) Number of gages: 4	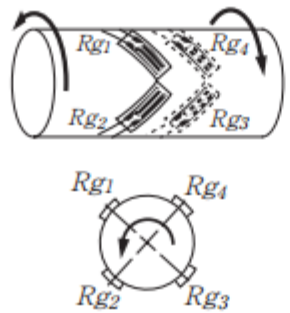	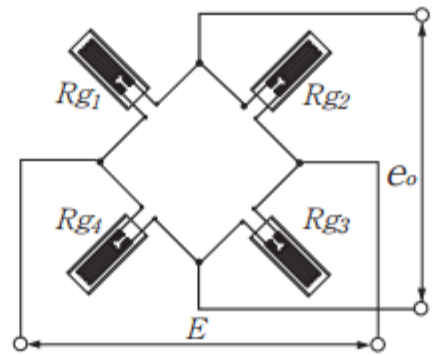	$e_o = K_S \cdot \varepsilon_0 \cdot E$ Rg_1, Rg_3 …… Twisting strain : ε_0 Rg_2, Rg_4…… Twisting strain : $-\varepsilon_0$	Temperature compensation; thermal effect of leadwires canceled. x 4 output
15	4-active-1-gage system (for average strain measurement) Number of gages: 4	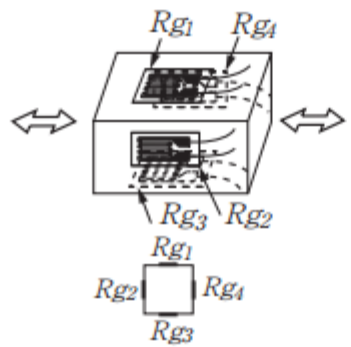	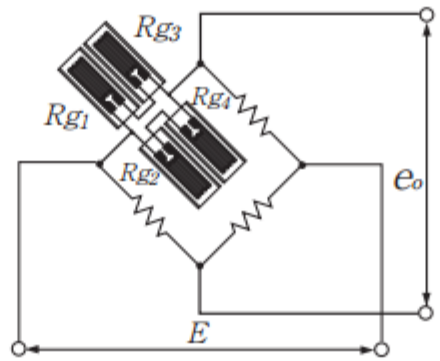	$e_o = \frac{E}{4} K_S \cdot \varepsilon_0$ $\varepsilon_0 = \frac{\varepsilon_1 + \varepsilon_2 + \varepsilon_3 + \varepsilon_4}{4}$ R : Fixed resistance $Rg = R$ $R = Rg_1 = Rg_2 = Rg_3 = Rg_4$	No temperature compensation; average strain x 1 output

Full-Bridge Configurations (BENDING) (AXIAL)

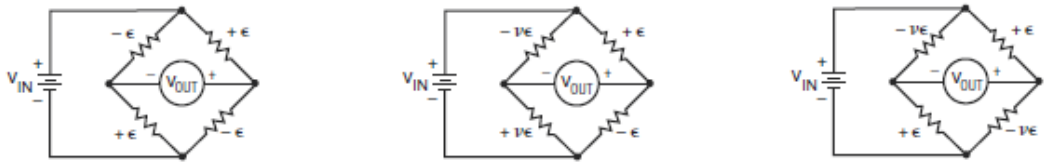

$$\epsilon = \frac{-V_r}{GF} \qquad \epsilon = \frac{-2V_r}{GF(\nu + 1)} \qquad \epsilon = \frac{-2V_r}{GF[(\nu + 1) - V_r(\nu - 1)]}$$

APPENDIX C: EQUATIONS

BIAXIAL STRESS STATE EQUATIONS

$$\epsilon_x = \frac{\sigma_x}{E} - \nu\frac{\sigma_y}{E} \qquad \epsilon_z = -\nu\frac{\sigma_x}{E} - \nu\frac{\sigma_y}{E} \qquad \sigma_y = \frac{E}{1-\nu^2}(\epsilon_x + \nu\,\epsilon_x)$$

$$\epsilon_y = \frac{\sigma_y}{E} - \nu\frac{\sigma_x}{E} \qquad \sigma_x = \frac{E}{1-\nu^2}(\epsilon_x + \nu\,\epsilon_y) \qquad \sigma_z = 0$$

ROSETTE EQUATIONS

Rectangular Rosette:

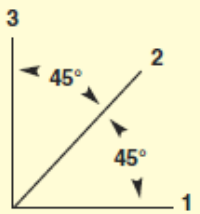

$$\epsilon_{p,q} = \frac{1}{2}\left[\epsilon_1 + \epsilon_3 \pm \sqrt{(\epsilon_1 - \epsilon_3)^2 + (2\epsilon_2 - \epsilon_1 - \epsilon_3)^2}\right]$$

$$\sigma_{p,q} = \frac{E}{2}\left[\frac{\epsilon_1 + \epsilon_3}{1-\nu} \pm \frac{1}{1+\nu}\sqrt{(\epsilon_1 - \epsilon_3)^2 + (2\epsilon_2 - \epsilon_1 - \epsilon_3)^2}\right]$$

$$\Theta_{p,q} = \frac{1}{2}\,\text{TAN}^{-1}\frac{2\epsilon_2 - \epsilon_1 - \epsilon_3}{\epsilon_1 - \epsilon_3}$$

Delta Rosette:

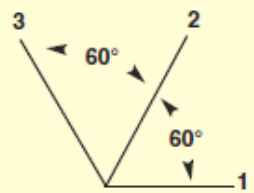

$$\epsilon_{p,q} = \frac{1}{3}\left[\epsilon_1 + \epsilon_2 + \epsilon_3 \pm \sqrt{2[(\epsilon_1 - \epsilon_2)^2 + (\epsilon_2 - \epsilon_3)^2 + (\epsilon_3 - \epsilon_1)^2]}\right]$$

$$\sigma_{p,q} = \frac{E}{3}\left[\frac{\epsilon_1 + \epsilon_2 + \epsilon_3}{1-\nu} \pm \frac{1}{1+\nu}\sqrt{2[(\epsilon_1 - \epsilon_2)^2 + (\epsilon_2 - \epsilon_3)^2 + (\epsilon_3 - \epsilon_1)^2]}\right]$$

$$\Theta_{p,q} = \frac{1}{2}\,\text{TAN}^{-1}\frac{\sqrt{3}\,(\epsilon_2\ \epsilon_3)}{2\epsilon_1 - \epsilon_2 - \epsilon_3}$$

WHERE:

$\epsilon p,q$ = Principal strains

$\sigma p,q$ = Principal stresses

$\Theta p,q$ = the acute angle from the axis of gage 1 to the nearest principal axis. When positive, the direction is the same as that of the gage numbering and, when negative, opposite.

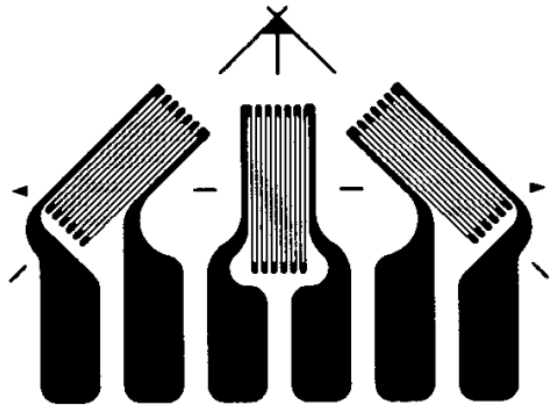

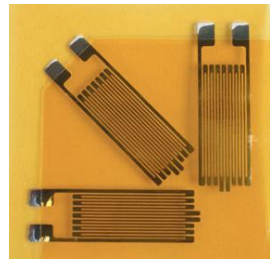

SG PARAFUSOS E PINOS HBM

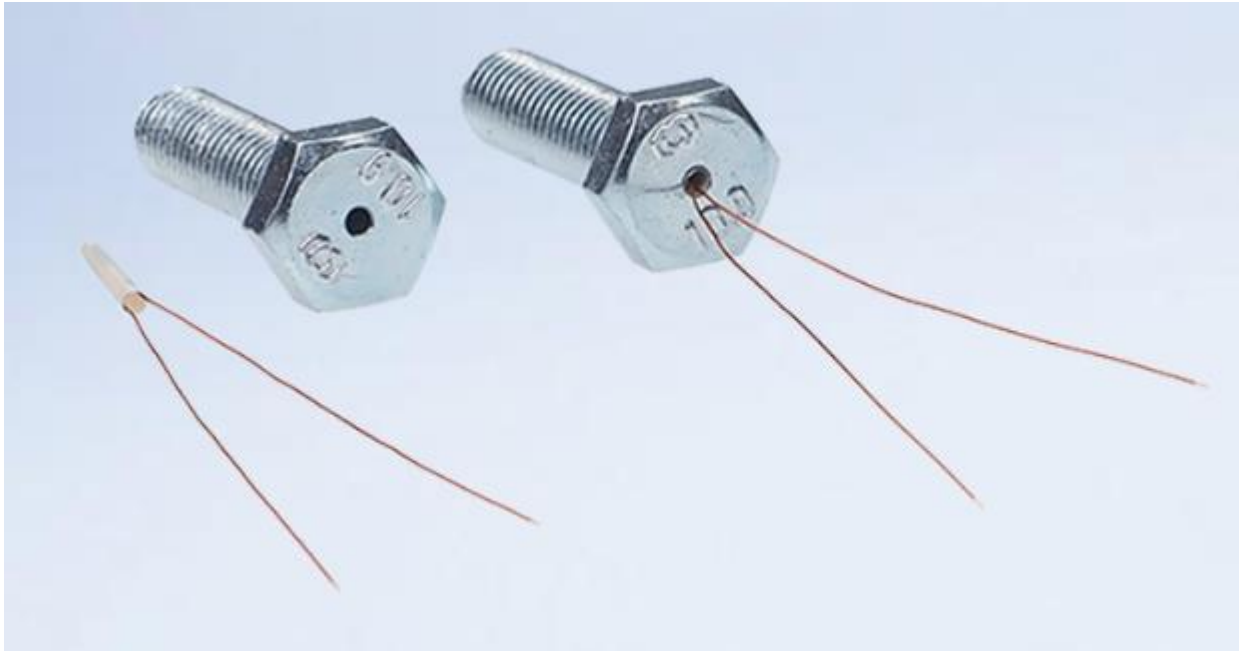

Amplificadores

741

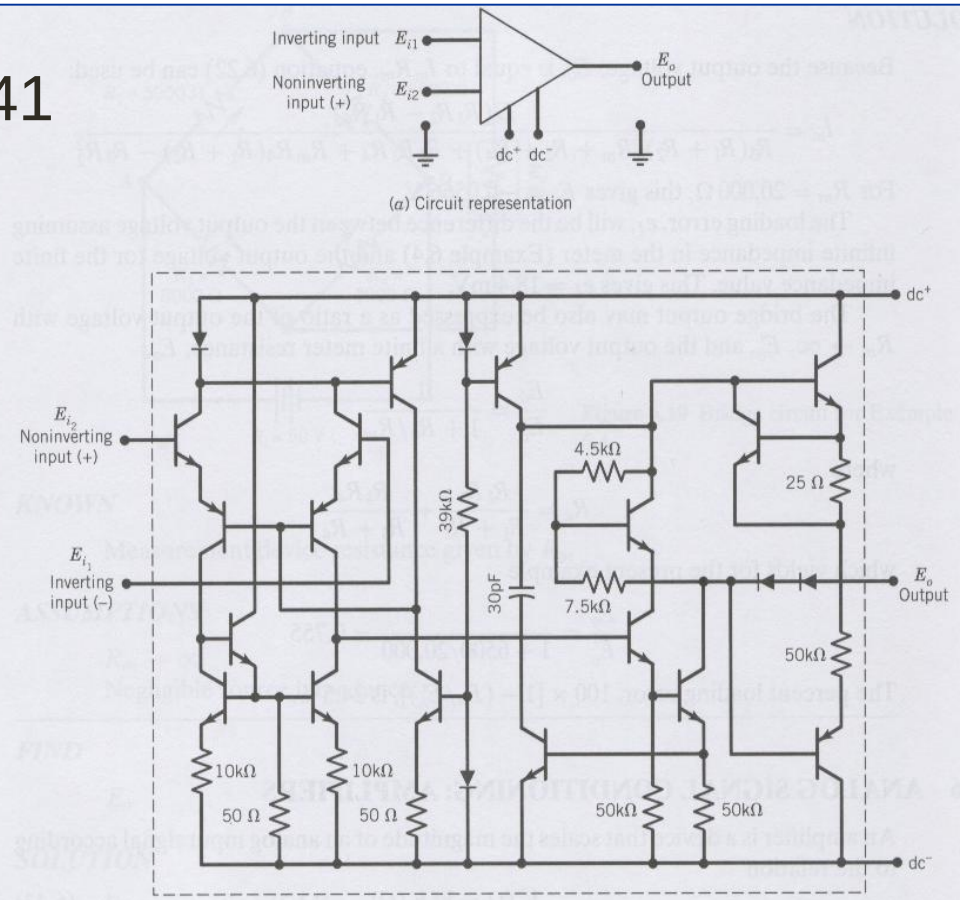

Figure 6.20 Operational amplifier.

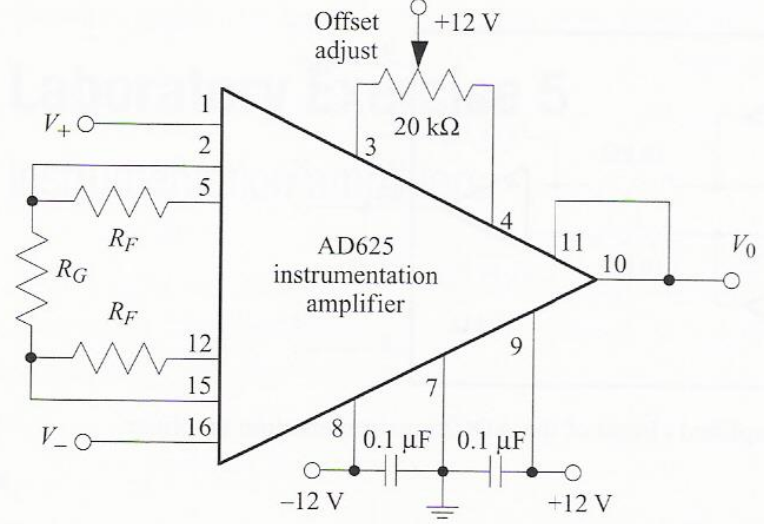

Laboratory Figure 5.2 AD625 instrumentation amplifier circuit. In the absence of common-mode gain, differential gain is given by $G_{\pm} = V_0/(V_+ - V_-) = 1 + 2R_F/R_G$.

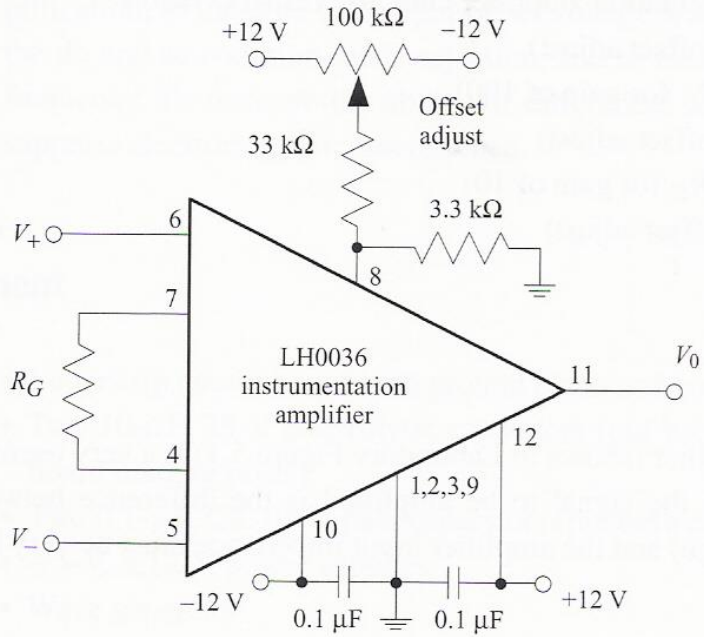

Laboratory Figure 5.3 LH0036 instrumentation amplifier circuit. In the absence of common-mode gain, differential gain is given by $G_{\pm} = V_0/(V_+ - V_-) = 1 + 50\,\text{k}\Omega/R_G$.

$$V_{out} = -\frac{R_F}{R_1} V_{SEN}$$

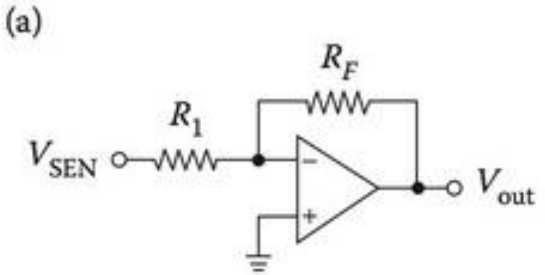

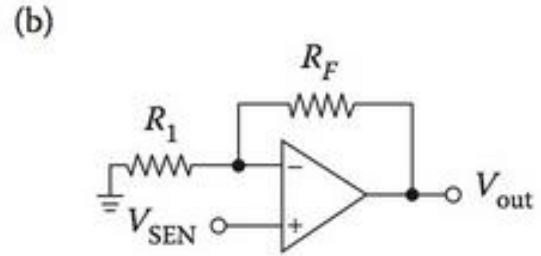

$$\text{Gain} = \frac{V_{out}}{V_{SEN}} = 1 + \frac{R_F}{R_1}$$

$$V_{out} = \frac{R_F}{R_1}(V_{SEN^+} - V_{SEN^-})$$

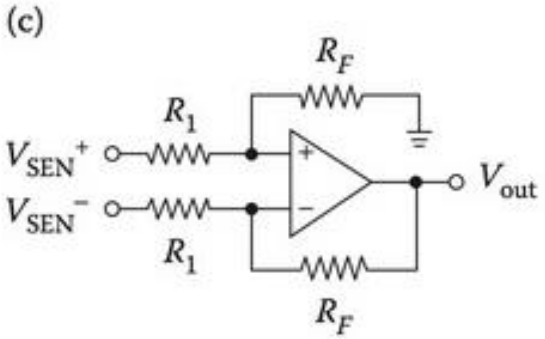

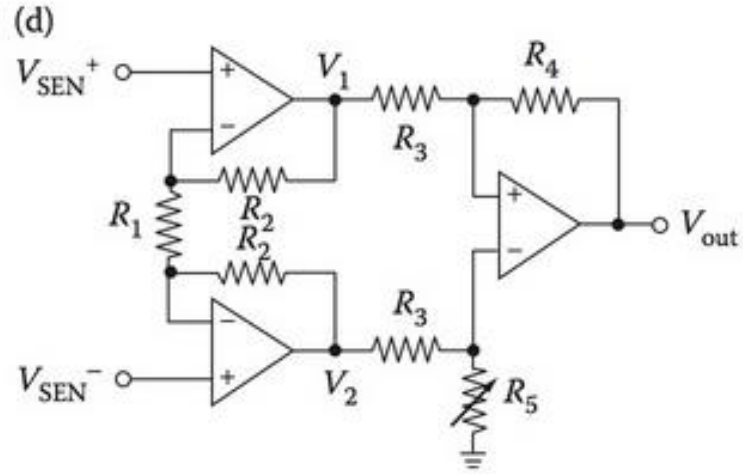

FIGURE 6.22 Four primary types of amplifier circuits: (a) inverting amplifier; (b) non-inverting amplifier; (c) differential amplifier; (d) instrumentation amplifier.

The merits of this amplifier are: it rejects common mode noise, allows large input voltage, and provides resistive isolation from the sensor signal source. A Wheatstone bridge output is often connected to this amplifier.

The instrumentation amplifier in Figure 6.22d is the most popular one. It maximizes the *Common Mode Rejection Ratio* (CMRR) by minimizing the common mode gain [32]. The left two amplifiers form a differential input/differential output amplifier; the right amplifier (a differential amplifier) rejects the common-mode voltage and converts the differential output of the first stage into a single-ended output. The output of each amplifier is [33]

(d)

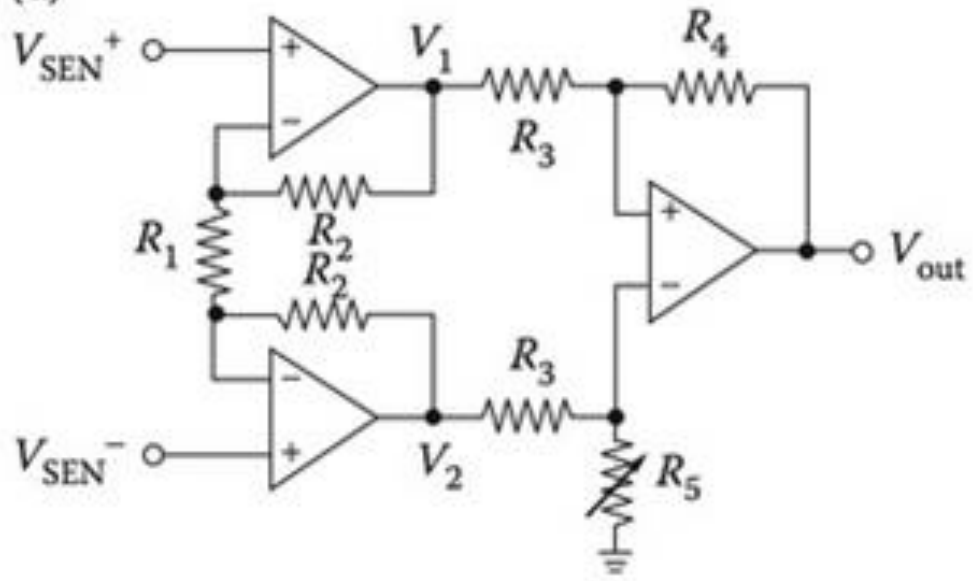

$$V_1 = \left(1 + \frac{R_2}{R_1}\right) V_{SEN^+} - \frac{R_2}{R_1} V_{SEN^-} \tag{6.59}$$

$$V_2 = -\frac{R_2}{R_1} V_{SEN^+} + \left(1 + \frac{R_2}{R_1}\right) V_{SEN^-} \tag{6.60}$$

$$V_{out} = \left[\frac{R_4}{R_3}\left(1 + 2\frac{R_2}{R_1}\right)\right](V_{SEN^+} - V_{SEN^-}) \tag{6.61}$$

For a common mode input, that is, $V_{SEN^+} = V_{SEN^-}$, Equation 6.61 yields a zero output voltage. Hence, the common mode gain is zero, and the CMRR is infinite if $R_5 = R_4$. In reality, the resistances are never an exact match, thus an adjustable resistor is used for R_5.

Filtros

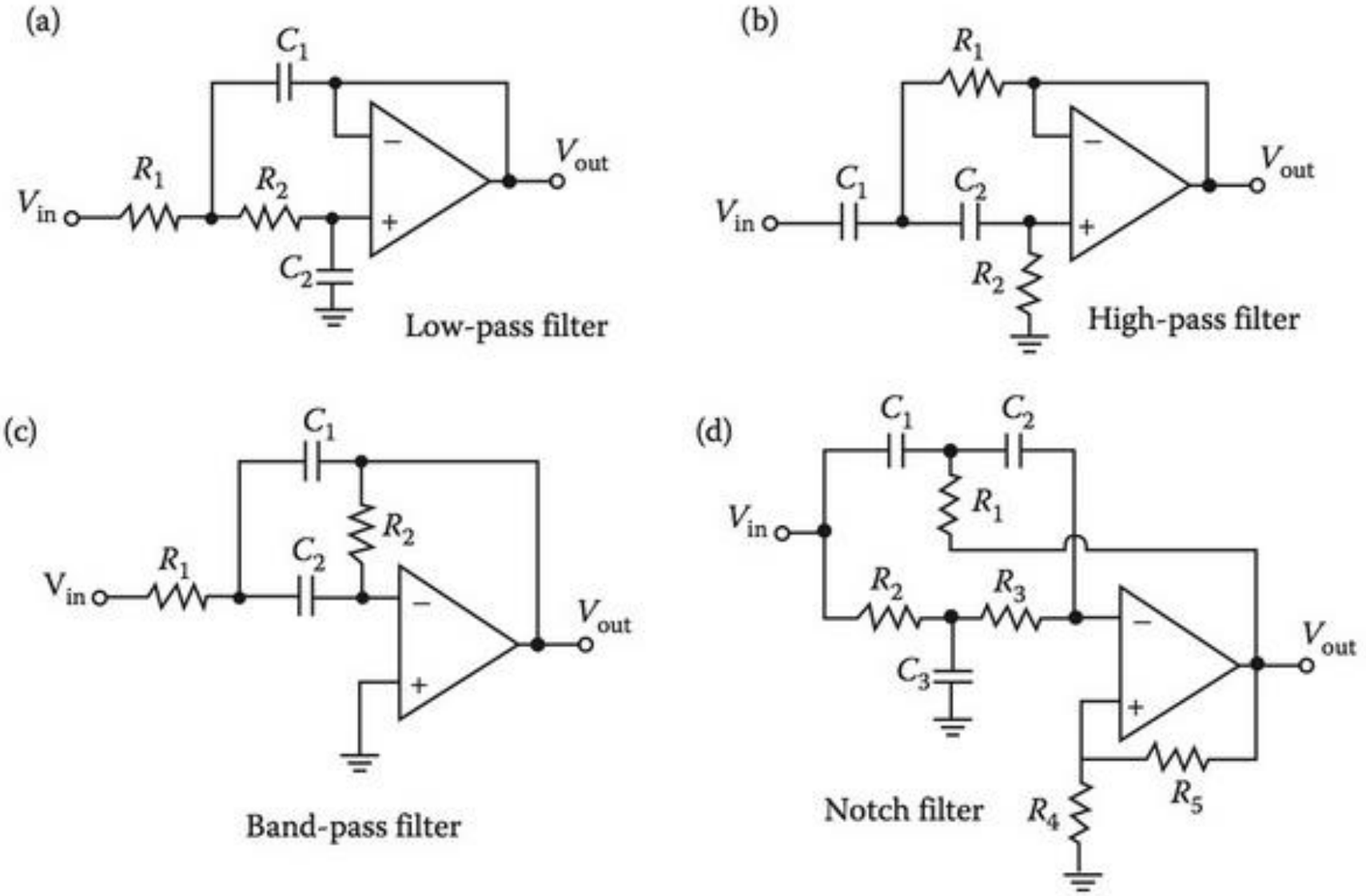

FIGURE 6.44 Examples of various active filters. (a) low-pass filter; (b) high-pass filter; (c) band-pass filter; (d) notch filter.

https://www.electronics-tutorials.ws/

EXEMPLOS DE USO DE EXTENSÔMETROS

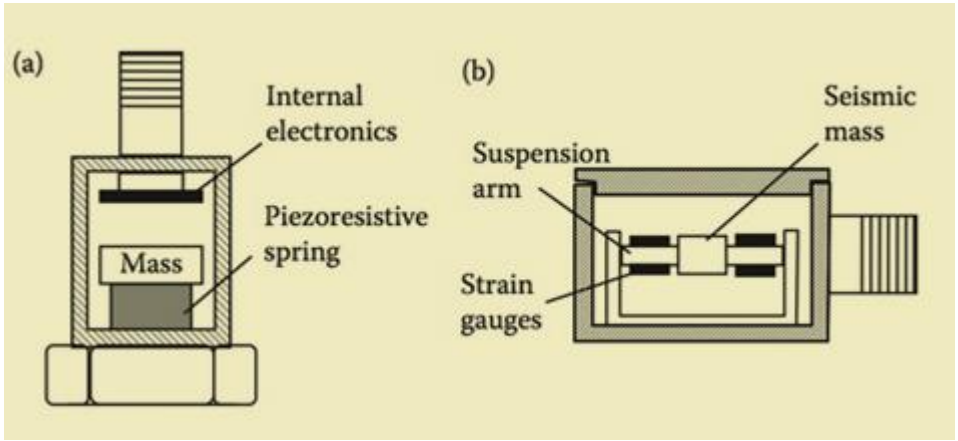

Acelerômetro

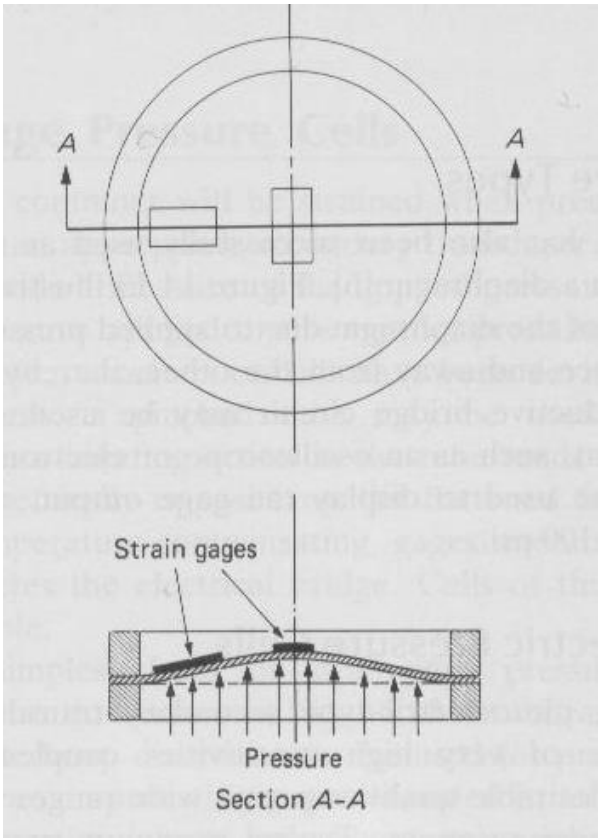

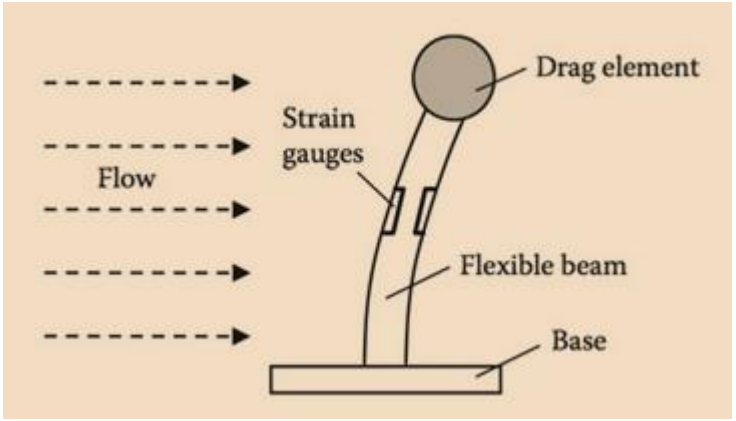

vazão

CÉLULAS DE CARGA

0.3kg Compression Load Cell, 15V dc, IP66

RS Stock No. **414-0821**
Brand Tedea Huntleigh
Mfr. Part No. **1004-00.3-JW00-RS**

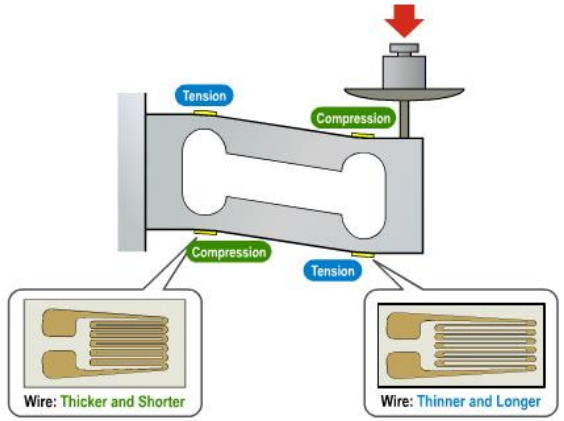

Load Sensor - 50kg
SEN-10245
$9.95

Load Cell - 50kg, Disc (TAS606)
SEN-13331
$56.95

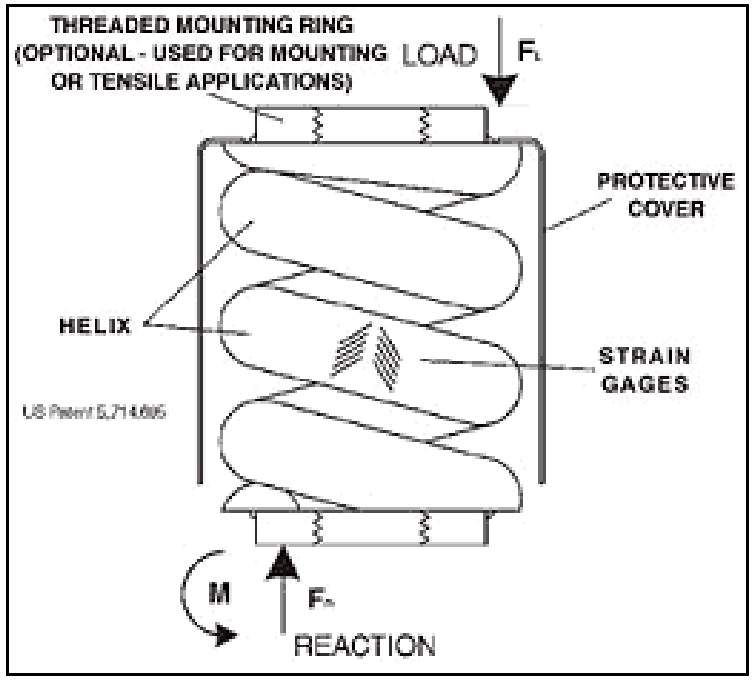

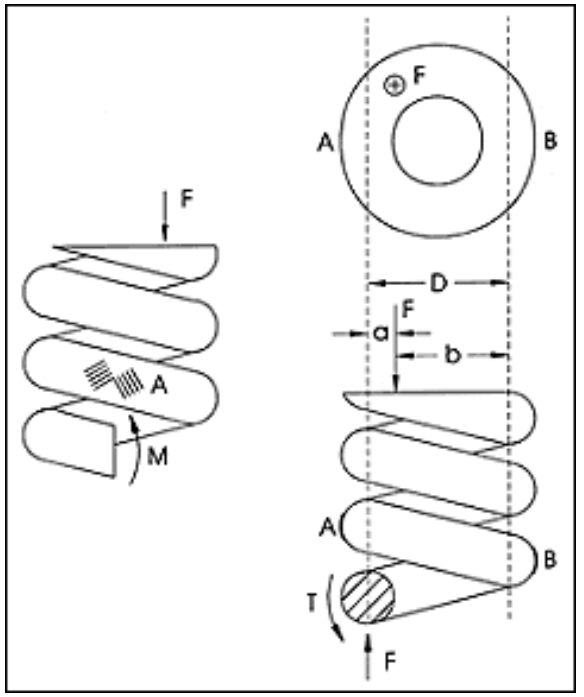

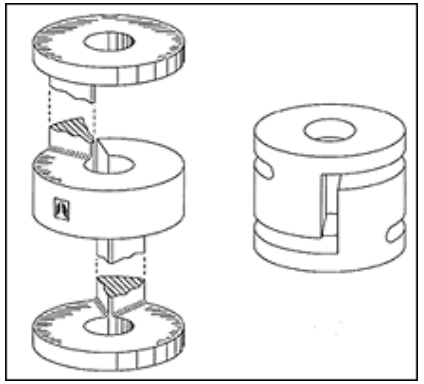

$$\tau = \tau_A + \tau_B$$

$$\tau = \frac{F}{A} - \frac{Far}{J} + \frac{F}{A} - \frac{Fbr}{J}$$

$$\tau = \frac{2F}{A} - \frac{FrD}{J} = kF$$

onde

$$k = \frac{2}{A} - \frac{rD}{J} = \text{constante geométrica (não depende do alinhamento)}$$

ANÁLISE DE UMA CÉLULA DE CARGA

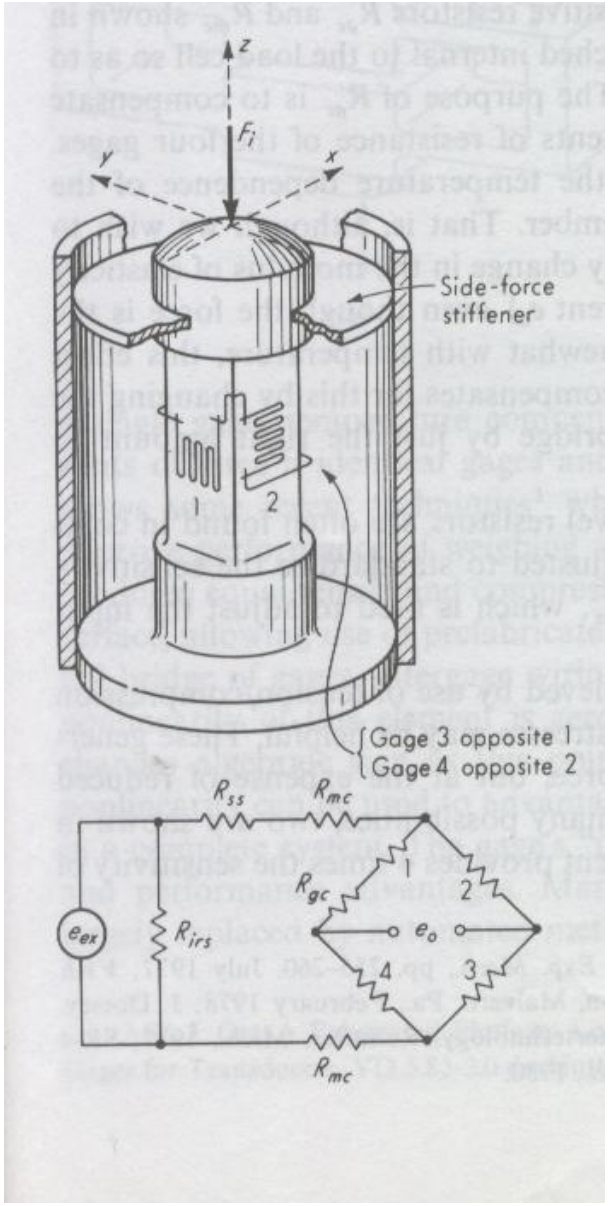

$$\varepsilon_{axial} = \frac{P}{AE} \qquad \varepsilon_{transv} = -\nu \frac{P}{AE}$$

$$\varepsilon_{axial} = \frac{\Delta R / R}{G.F.}$$

$$\frac{\Delta R_1}{R_1} = \frac{\Delta R_3}{R_3} = G.F.\ \varepsilon_{axial} \qquad \frac{\Delta R_2}{R_2} = \frac{\Delta R_4}{R_4} = G.F.\ \varepsilon_{transv}$$

$$e_0 = \frac{e_i}{4}\left(2G.F.\frac{P}{AE} + 2\nu\ G.F.\frac{P}{AE}\right)$$

$$P = \frac{AE}{(1+\nu)e_i} e_0$$

Este arranjo permite anular efeitos de temperatura, torção e flexão.

EXERCÍCIOS

2.[2 pontos] Considere um anel com os seguintes parâmetros geométricos: espessura h de 2 mm, largura b de 10 mm e raio médio R de 100 mm. Admita que o anel sofra a ação de uma força F conforme a figura 1.

a)A partir da modelagem indicada na figura 2, o elemento do anel em destaque estará sujeito a tensões de flexão e tração. Nesta situação, determine a razão entre a tensão máxima de flexão e a tensão de tração.

b) Pretende-se utilizar o anel como dinamômetro, colando-se 4 extensômetros elétricos, de resistência nominal 120 Ω, *gage factor* 2,0 , nos locais apresentados na figura 1, com a numeração correspondente à posição na ponte de Wheatstone. Considerando que o material do anel seja aço-carbono com limite de escoamento de 450 MPa, módulo de elasticidade de Young de 210 GPa e fator de segurança de 2,0, V_0 de 5 V, determine: a sensibilidade do dinamômetro (N/V sem amplificação) e sua capacidade.

Dados: $\frac{\Delta V}{V_0} = \frac{1}{4R_0}(-\Delta R_1 + \Delta R_2 - \Delta R_3 + \Delta R_4)$ G.F. =(ΔR/R) / ε_ℓ

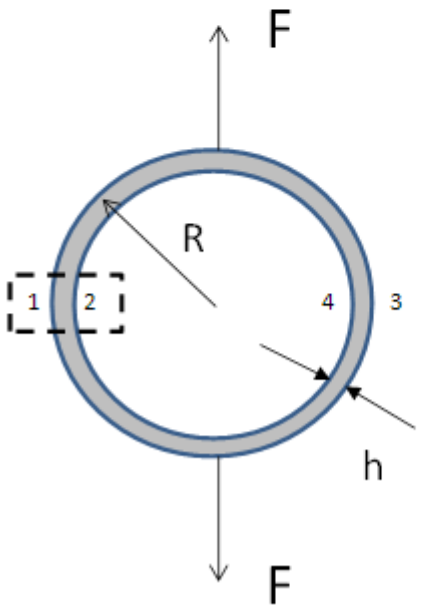

Fig.1 - Anel

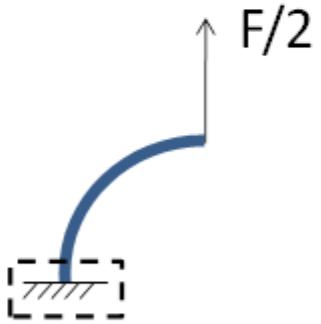

Fig.2 - Modelagem

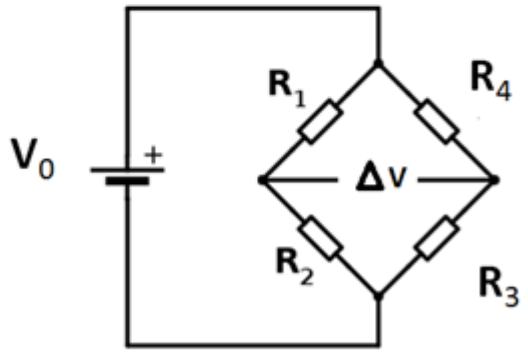

Fig. 3 Ponte de Wheatstone

ANALISE DE CELULA DE CARGA TIPO ANEL

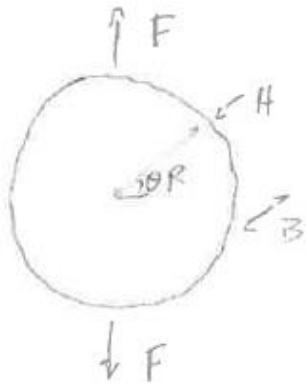

Posição $\theta = 0$

$$M = EIk \qquad \varepsilon = k y$$

$$M = \frac{EI\varepsilon}{y} = \frac{EBH^3}{12\,H/2}\,\varepsilon_M$$

$$\varepsilon_M = \frac{6}{EBH^2}\,\frac{F}{2}R = \frac{3R}{BH^2}\,\frac{F}{E}$$

$$\varepsilon_F = \frac{F/2}{BH\,E}$$

$$\varepsilon_M = \frac{3R}{BH^2}\,2BH\,\varepsilon_F \qquad \varepsilon_M = \frac{6R}{H}\,\varepsilon_F \qquad \begin{matrix} R=30 \\ H=3 \end{matrix} \qquad \boxed{\varepsilon_M = 60\,\varepsilon_F}$$

Logo, pode-se desprezar efeito de ε_F.

Deve-se usar flexão e desprezar deformação axial

Um modelo mais detalhado pode distinguir entre as deformações dentro e fora do canal

$$\varepsilon_M = \frac{M}{EI}\, y = \frac{3R}{BH^2}\,\frac{F}{E}$$

$$\varepsilon_F = \frac{1}{3BH}\,\frac{F}{E}$$

$$\varepsilon_i = \left(\frac{3R}{H} + \frac{1}{2}\right)\frac{F}{3HE}$$

$$\varepsilon_o = \left(-\frac{3R}{H} + \frac{1}{2}\right)\frac{F}{BHE}$$

mas o fator $1/2$ é pequeno frente a $\frac{R}{H}$ grande (0.5 em 30)

Ligações na ponte de Wheatstone

$$\frac{V_0}{V_i} = \frac{1}{4R}\left(\Delta R_2 - \Delta R_1 + \Delta R_3 - \Delta R_4\right) = \frac{\Delta \bar{R}}{4R}$$

Caso I - Todos SG na vertical

SG externos < 0

SG internos > 0

Internos 2, 3 externos 1, 4

$$\Delta \bar{R} = \Delta R_2 + \Delta R_3 - (-\Delta R_1) - (-\Delta R_4) = 4\Delta R$$

$$\frac{V_0}{V_i} = \frac{\Delta R}{R}$$

$$G_F = \frac{\Delta R/R}{\varepsilon}$$

$$\frac{V_0}{V_i} = G_f E_M$$

$$\frac{V_0}{V_i} = G_f \cdot \frac{3R}{BH^2} \frac{F}{E}$$

$$F = \frac{BH^2}{3R} \frac{E}{V_i} V_0$$

Note que o arranjo usado na ponte implica que as deformações axiais, sendo iguais, levam a

$\Delta R_1 = \Delta R_2 = \Delta R_3 = \Delta R_4 > 0$, ou seja, $\Delta \bar{R} = 0$, logo os efeitos já pequenos de F na deformação axial são anulados.

F_{max} deve ser tal que $\varepsilon_M < \varepsilon_y$

$$\varepsilon_M = \frac{3R}{BH^2} \frac{F_{max}}{E} = \frac{\sigma_{max}}{E S_g}$$

$$F_{max} \leq \frac{BH^2}{3R S_g} \sigma_{max}$$

$$F_{max} \leq \frac{10 \times 3^2}{3 \cdot 30 \times 3/2} \cdot 300 < \frac{10^{-3} \cdot 10^{-6} \times 10^6}{10^{-3}} \leq 200\,N$$

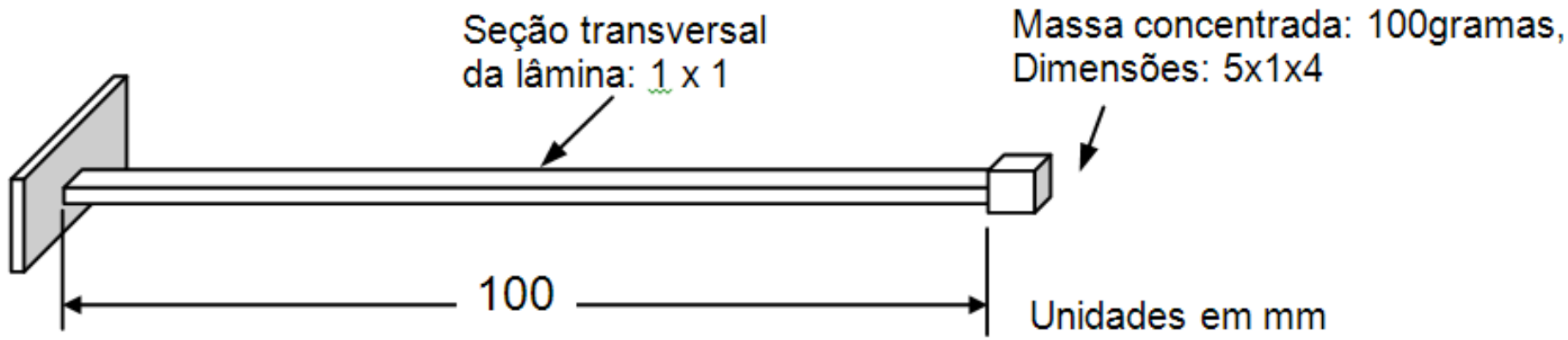

Quatro extensômetros são ligados no *acelerômetro* da Figura acima e posicionados em uma ponte de Wheatstone, com dois extensômetros ativos. A resistência nominal de todo eles é de 120 Ω. O *gauge factor* é 2.1 e a voltagem de entrada é 10 V. Material da lâmina: E=200GPa, γ=7850 Kgf/m^3, Escoamento = 250 MPa. A linha elástica da lâmina é dada por

$$v = \frac{Px^2}{6EI}(3L - x).$$

(a) Qual deve ser o arranjo de ligação destes extensômetros na ponte de Wheatstone e em que posição da lâmina eles devem ser colados? Justifique.

(b) Calcule a deformação quando a medição do desbalanceamento da ponte é 20 mV.

(c) Qual é o valor da deformação acusada pelos extensômetros para uma aceleração de 2g?

(d) O condicionador de sinais possui resolução de 1mV e amplificação máxima de 1000. Pergunta-se se o mesmo é adequado para a medição de acelerações na faixa de 1 a 5g.

a)Para produzir as maiores deformações possíveis, é recomendável fazer a lâmina trabalhar em flexão na direção da espessura. Neste caso, os extensômetros devem ser colados junto ao engaste, um de cada lado da espessura, alinhados com o comprimento e ligados em pernas adjacentes na ponte elétrica.
Obtém-se, com isso, o efeito adicional benéfico de ser o acelerômetro compensado a variações de temperatura.

b) Deformação

-Área da secção transversal : $A = (1cm).(1mm) = 10^{-5} m^2$

-Inércia à flexão : $I = (1cm).(1mm)^3 / 12 = (10^{-11} / 12) m^4$

-Módulo de resistência : $W = (1cm).(1mm)^2 / 6 = (10^{-8} / 6) m^4$

-Carga distribuída : $p = (2).(7850 kgf / m^3).A = 1.5386 N / m$

-Carga concentrada : $P = (2).(100 g).(9.8 m / s^2) = 1.96 N$

-Momento fletor no engaste : $M_f = P.L + p.L^2 / 2 = (1.96).(0.1) + (1.5386).(0.01) / 2$

$$M_f = 0.196 + 0.007693 = 0.203693 N.m$$

-Tensão normal : $\sigma = M_f / W = (0.203693) / (10^{-8} / 6) \cong 1.222 x 10^8 N / m^2$

$$\sigma = M_f / W \cong 122.2 MPa$$

-Deformação : $\varepsilon = \sigma / E \cong 122.2 MPa / 200 GPa \cong 0.611 x 10^{-3} = 611 \mu S$

c)Ponte

$\Delta R / R_0 = GF.\varepsilon = (2).(611 x 10^{-6}) = 1222 x 10^{-6}$

$\Delta V / V_0 = (\Delta R_1 - \Delta R_2 + \Delta R_3 - \Delta R_4) / (4.R_0) = (2.\Delta R) / (4.R_0) = 611 x 10^{-6}$

Assim, para uma alimentação $V_0 = 5 Volts$ obtem-se uma leitura de: $\Delta V \cong 3.06 mV$

d)Como o sinal pode ser amplificado até 1000 vezes:

$$2G \Rightarrow \Delta V = 3060 mV \qquad \begin{matrix} 1G \Rightarrow \Delta V = 1530 mV \\ 5G \Rightarrow \Delta V = 7650 mV \end{matrix}$$

resolução: $\Delta G = 2G.(1mV / 3060 mV) \Rightarrow \Delta G / G = 0.0654\%$

Assim, tanto em termos de fundo de escala como em resolução o condicionador parece adequado.

EXERCÍCIO EM GRUPO [PROVA]

Pretende-se desenvolver um acelerômetro a partir de uma viga engastada à base que sofre a aceleração e tendo no extremo livre uma massa concentrada.

Pergunta-se:

1. Considerando dois extensômetros ativos, onde eles devem ser colados e qual seu arranjo na ponte de Wheatstone?
2. Qual é a deformação na viga quando carregada pela massa e por seu peso próprio? Considere que a viga possa estar em qualquer posição do espaço e está sujeita a campo gravitacional da terra.
3. Qual é o valor da tensão de saída para o carregamento do item 2?
4. Qual é a deformação na posição dos extensômetros quando a base está sujeita a uma vibração harmônica de frequência ω e aceleração de amplitude A_i?
5. Qual é o diagrama de Bode deste sistema?

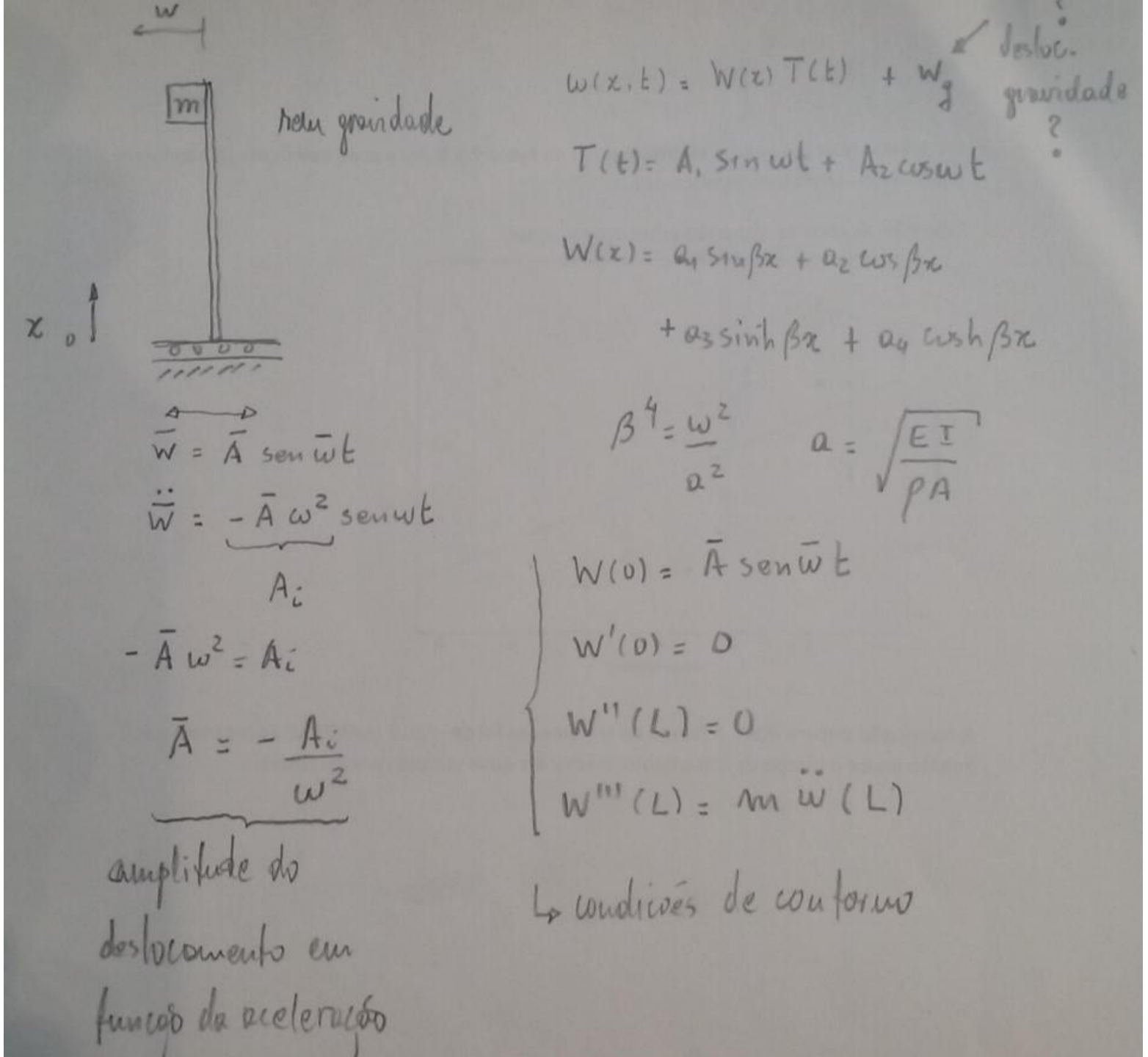
w
m
sem gravidade
x
0
$\bar{w} = \bar{A} \operatorname{sen} \bar{\omega} t$
$\ddot{\bar{w}} = -\bar{A}\omega^2 \operatorname{sen} \omega t$
A_i
$-\bar{A}\omega^2 = A_i$
$\bar{A} = -\frac{A_i}{\omega^2}$
amplitude do deslocamento em função da aceleração
$w(x,t) = W(x)\,T(t) + w_g$
desloc. gravidade
?
$T(t) = A_1 \operatorname{sen} \omega t + A_2 \cos \omega t$
$W(x) = a_1 \operatorname{sen} \beta x + a_2 \cos \beta x + a_3 \operatorname{sinh} \beta x + a_4 \cosh \beta x$
$\beta^4 = \frac{\omega^2}{a^2}$
$a = \sqrt{\frac{EI}{\rho A}}$
$W(0) = \bar{A} \operatorname{sen} \bar{\omega} t$
$W'(0) = 0$
$W''(L) = 0$
$W'''(L) = m\,\ddot{w}(L)$
↳ condições de contorno

SENSORES PIEZOELÉTRICOS

PIEZOELÉTRICOS

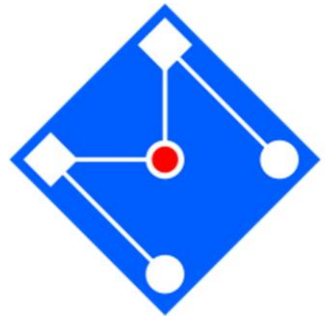

Atuadores

Coletores de Energia

Sensores

ATUADORES PIEZOELÉTRICOS

APC International, Ltd.

State of the art of co-fired low voltage actuators

Piezo actuators are electro-mechanical "motors", based on the solid state piezo-mechanical deformation effect of piezo-ceramics (PZT lead ["plumb"] zirconium titanate). Highlights are unlimited positioning sensitivity (sub-nanometers), high load capability and high force generation resulting in utmost mechanical dynamics with reaction times down to micro seconds. Only piezo actuation allows top innovations in mechatronics like nano-positioning or high pressure common rail fuel injection.

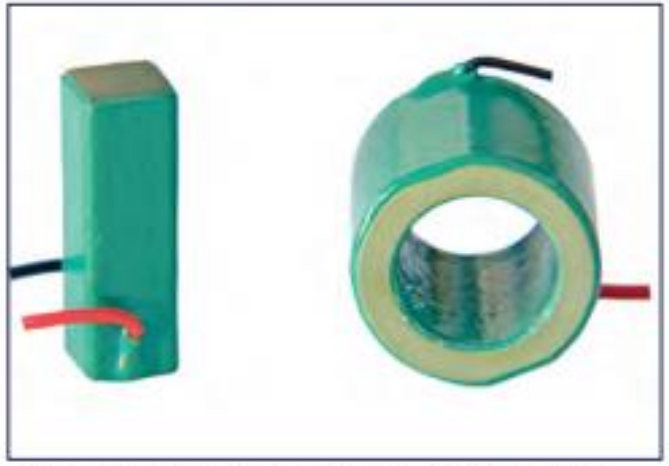

Fig.12: Massive stack actuator and hollow ring-actuator

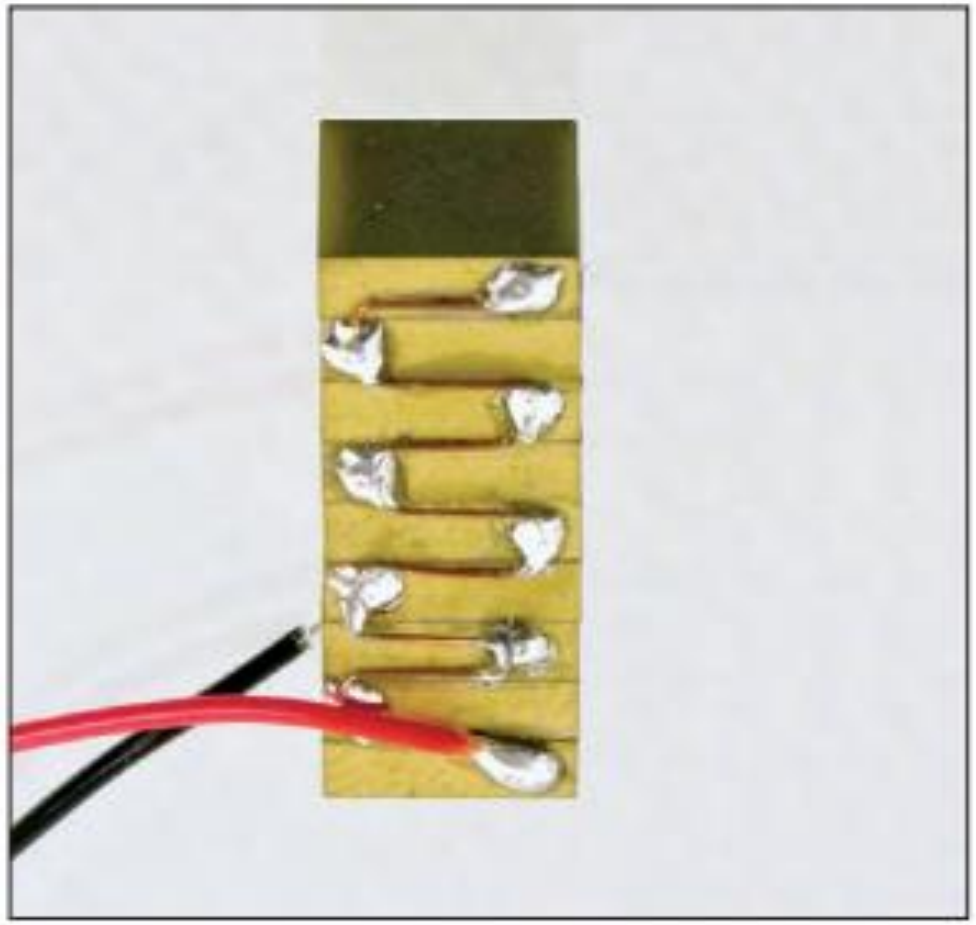

Fig. 8: Chip-based piezo-stack

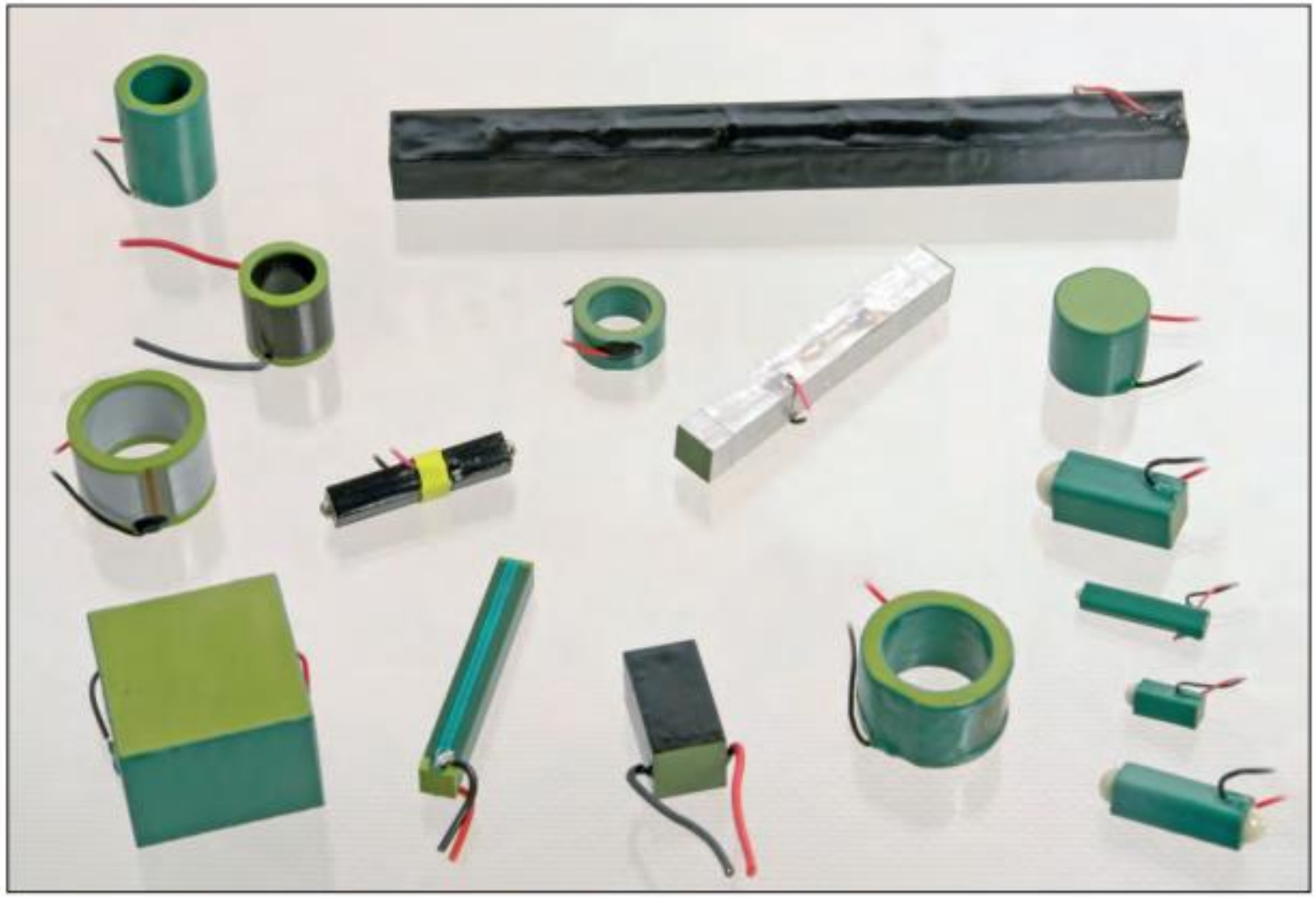

Fig. 21: Piezo-stacks PSt 150 and piezo-rings HPSt 150 in unsurpassed osi-technology

Fig. 25: piezo actuator with casing and internal preload, using PSt 150hTc (check also main catalogue)

COLETORES DE ENERGIA

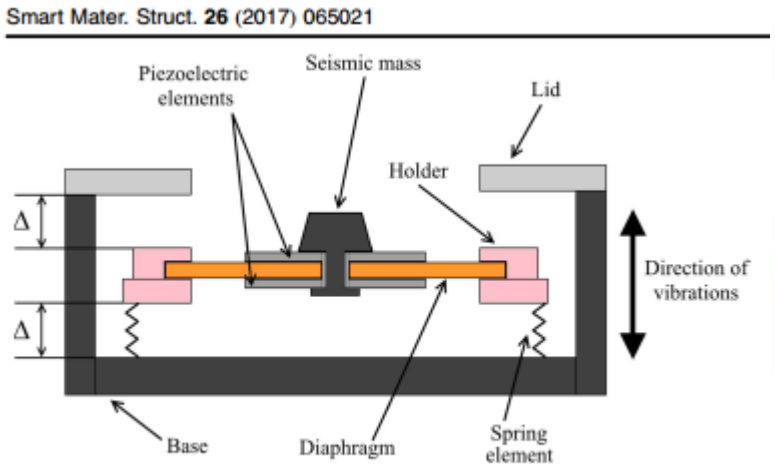

Figure 2. Schematic view of the mechanical design of the harvester. The drawing is not to scale.

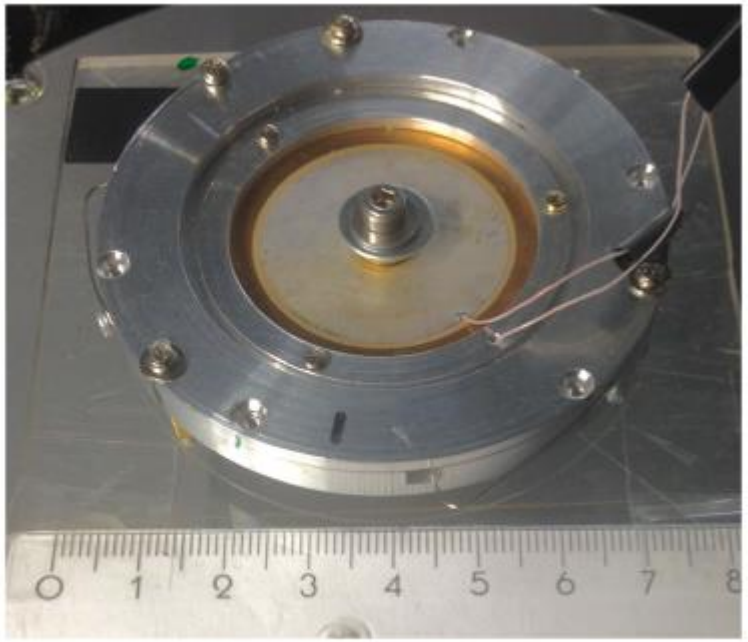

Figure 5. Photograph of the mechanical setup.

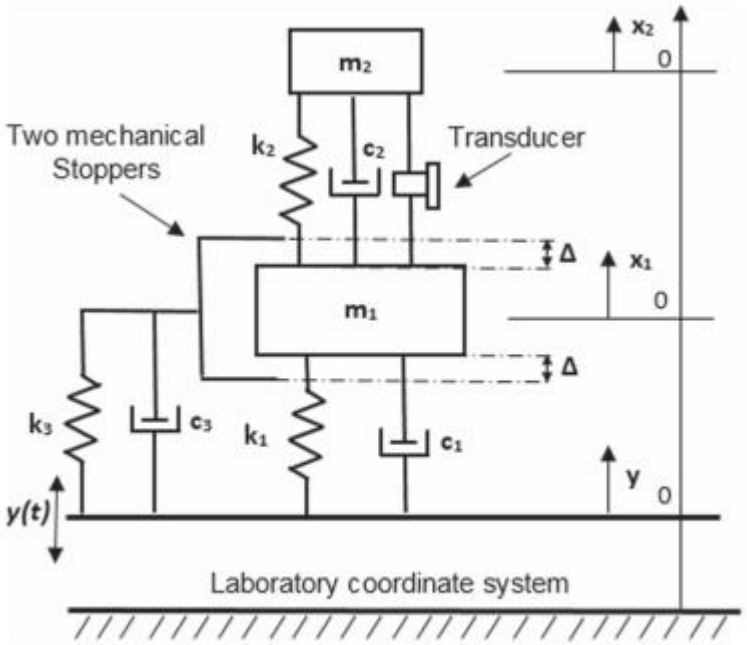

Figure 6. Picewise linear model of the system.

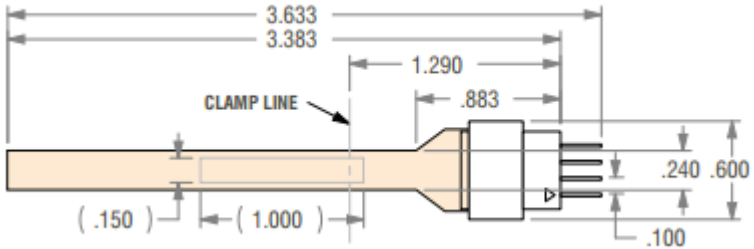
3.633
3.383
1.290
.883
CLAMP LINE
.240
.600
.100
(.150)
(1.000)

V22BL

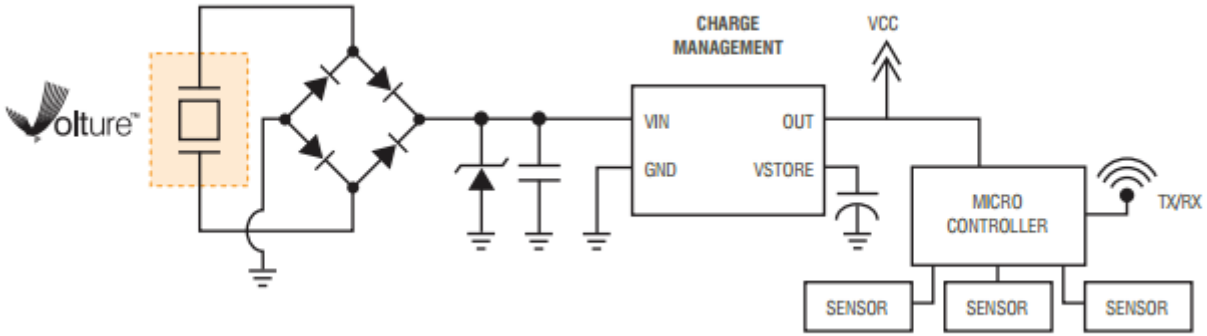
Volture
CHARGE MANAGEMENT
VCC
VIN
OUT
GND
VSTORE
MICRO CONTROLLER
TX/RX
SENSOR
SENSOR
SENSOR

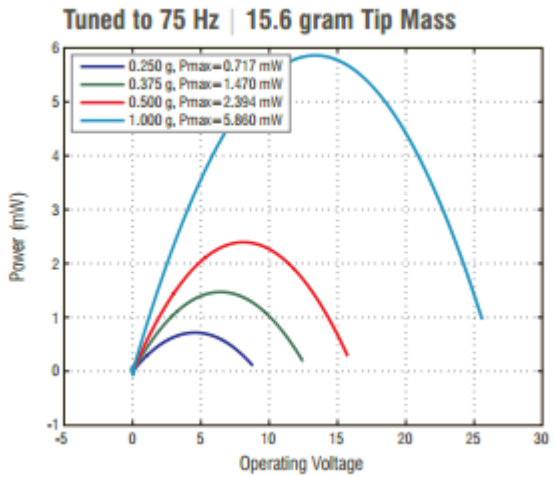
Tuned to 75 Hz | 15.6 gram Tip Mass
0.250 g, Pmax=0.717 mW
0.375 g, Pmax=1.470 mW
0.500 g, Pmax=2.394 mW
1.000 g, Pmax=5.860 mW
Power (mW)
Operating Voltage

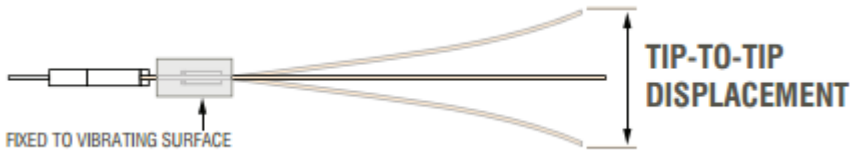
FIXED TO VIBRATING SURFACE
TIP-TO-TIP DISPLACEMENT

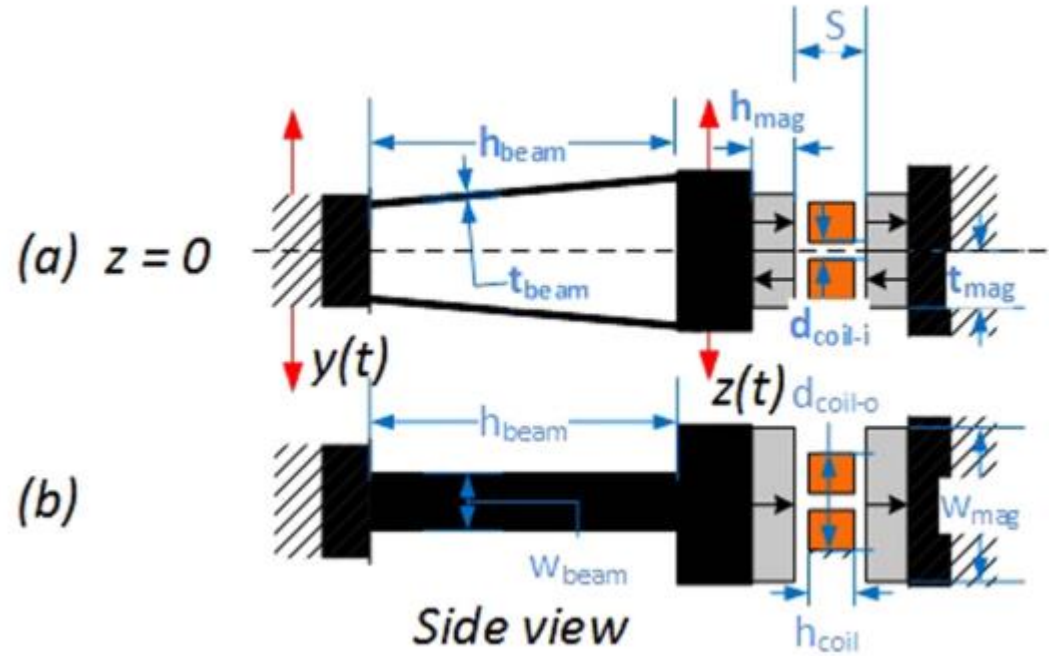
(a) z = 0
(b)
S
h_mag
h_beam
t_beam
t_mag
d_coil-i
y(t)
z(t)
d_coil-o
h_beam
W_mag
W_beam
h_coil
Side view

PIEZO SYSTEMS, INC.
65 Tower Office Park Woburn, MA 01801 USA
Tel: 781-933-4850 Fax: 781-933-4743 email: sales@piezo.com

Find
Search for a product or category

PIEZOELECTRIC ENERGY HARVESTING KIT

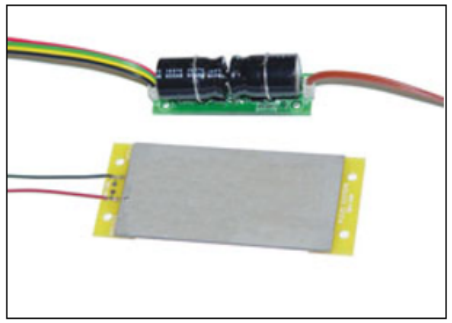

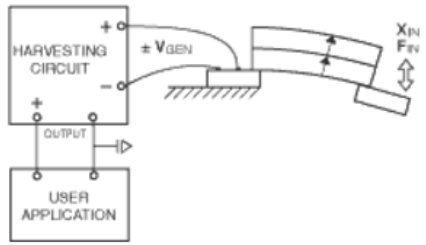

Bender & Circuit.

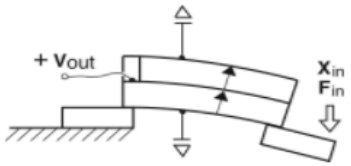

Bender mounted as a cantilever.

Print this Page: from © Piezo Systems, CATALOG #8 (2011), pages 20 & 21.

Part Number: KEH-007 *(Bender & Circuit)* **Prices**

ROHS: Piezo Exempt. Product compliant.

Description: When a piezoceramic trandsucer is stressed mechanically by a force, its electrodes receive a charge that tends to counteract the imposed strain. This charge may be collected, stored and delivered to power electrical circuits or processors.

The Piezo Bending Generator
When the Energy Harvesting Bender is flexed, one layer is compressed while the other is stretched, resulting in power generation. It may be excited by intermittent pulses or continuously from low frequency to resonant frequency (where rated displacement is achieved at the lowest force level). The Energy Harvesting Bender is a pre-mounted and pre-wired Double Quick-Mount Bending Generator designed to attach easily to sources of mechanical strain. Its double ended design lends itself to being mounted either as a cantilever or a simple beam. Dimensions for the standard -503 size Double Quick-Mounts are shown below.

Piezo Energy Harvesting Circuit
The self powered Piezo Energy Harvesting Circuit collects intermittent or continuous energy input from the piezo generator and efficiently stores their associated energy in an on-board capacitor bank. During the charging process, the capacitor voltage is continuously monitored. When it reaches 5.2V the module output is enabled to supply power to an external (user) load. At this point 55 mJ of energy are available. When generator energy input is high, the output voltage remains ON continuously. Capacitor voltage is clamped at 6.8V. If external power demand exceeds generation, the output voltage decreases. When the output voltage drops to 3.1V, power to the load is switched OFF and is not turned on again until the capacitor bank has been recharged to 5.2V. The circuit accepts input voltages from 0V to ±500V AC or DC and input currents to 400 mA.

Piezo Energy Harvesting Kit
The Energy Harvesting Kit consists of one Double Quick-Mount Harvesting Bender and one Energy Harvesting Circuit.

See an Introduction to Benders Used as Sensor (Generator) Elements.

SENSORES PIEZOELÉTRICOS

- The piezoelectric effect was discovered by Pierre and Jacques Curie in the latter part of the 19th century.
- They discovered that minerals such as tourmaline and quartz could transform mechanical energy into an electrical output.
- The voltage induced from pressure (Greek: piezo) is proportional to that applied pressure, and piezoelectric devices can be used to detect single-pressure events as well as repetitive events.
- Still, the ability of certain crystals to exhibit electrical charges under mechanical loading was of no practical use until very-high-input impedance amplifiers enabled engineers to amplify the signals produced by these crystals.
- Most electronic applications use quartz since its growth technology is far along, thanks to development of the reverse application of the piezoelectric effect; the quartz oscillator.
- Sensors based on the piezoelectric effect can operate from transverse, longitudinal, or shear forces, and are insensitive to electric fields and electromagnetic radiation. The response is also very linear over wide temperature ranges, making it an ideal sensor for rugged environments. For example, gallium phosphate and tourmaline sensors can have a working temperature range of 1,000°C.

https://www.digikey.com/en/articles/techzone/2011/dec/fundamentals-of-piezoelectric-shock-and-vibration-sensors

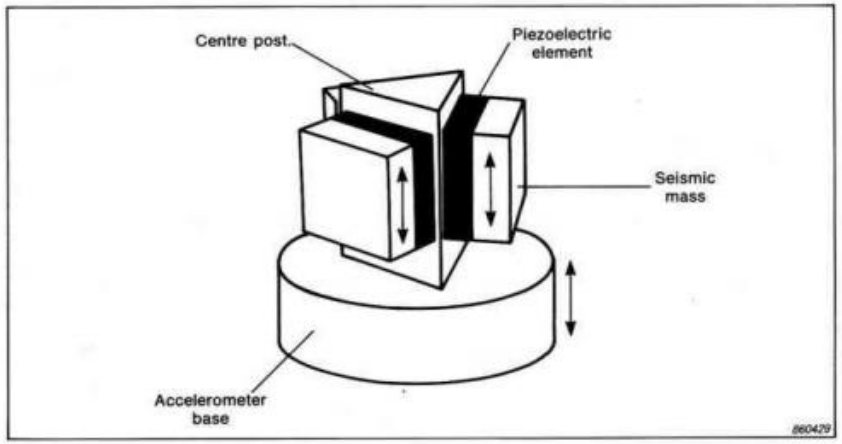

Fig. 2.1. Schematic of a Brüel & Kjær Delta Shear® piezoelectric accelerometer

PIEZOELECTRIC ACCELEROMETER AND VIBRATION PREAMPLIFIER HANDBOOK

by

Mark Serridge, BSc

and

Torben R. Licht, MSc

The piezoelectric accelerometer is widely accepted as the best available transducer for the absolute measurement of vibration. This is a direct result of these properties:

1. Usable over very wide frequency ranges.
2. Excellent linearity over a very wide dynamic range.
3. Acceleration signal can be electronically integrated to provide velocity and displacement data.
4. Vibration measurements are possible in a wide range of environmental conditions while still maintaining excellent accuracy.
5. Self-generating so no external power supply is required.
6. No moving parts hence extremely durable.
7. Extremely compact plus a high sensitivity to mass ratio.

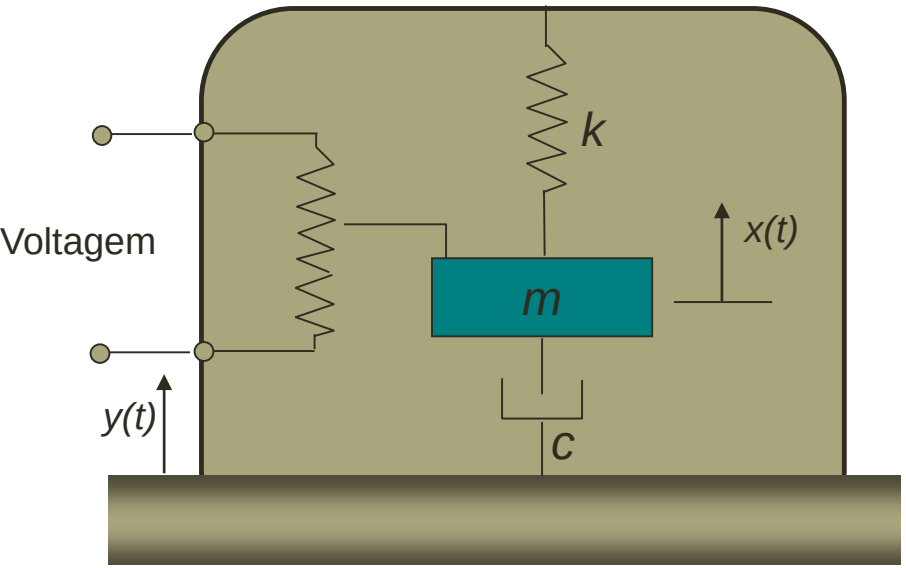

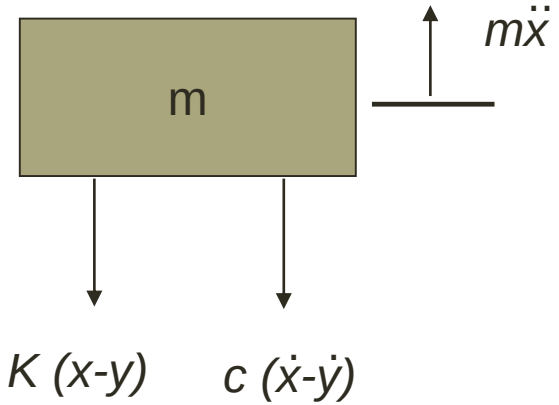

y(t): movimento da estrutura

$$m\ddot{x} = -c(\dot{x} - \dot{y}) - k(x - y)$$

$$z = x - y, \qquad y = Y \operatorname{sen} \omega\, t$$

$$m\ddot{z} + c\dot{z} + kz = m\omega^{2} Y \operatorname{sen} \omega\, t$$

$$z(t) = \frac{(1/\omega_n^{\,2}) Y \omega^2 \cos(\omega\ t - \phi(\omega))}{\sqrt{\left[1 - (\omega/\omega_n)^2\right]^2 + (2\xi\omega/\omega_n)^2}}$$

$$\omega_n^{\,2} z(t) = M(\omega)\ddot{y}$$

compressão do piezoelétrico

aceleração

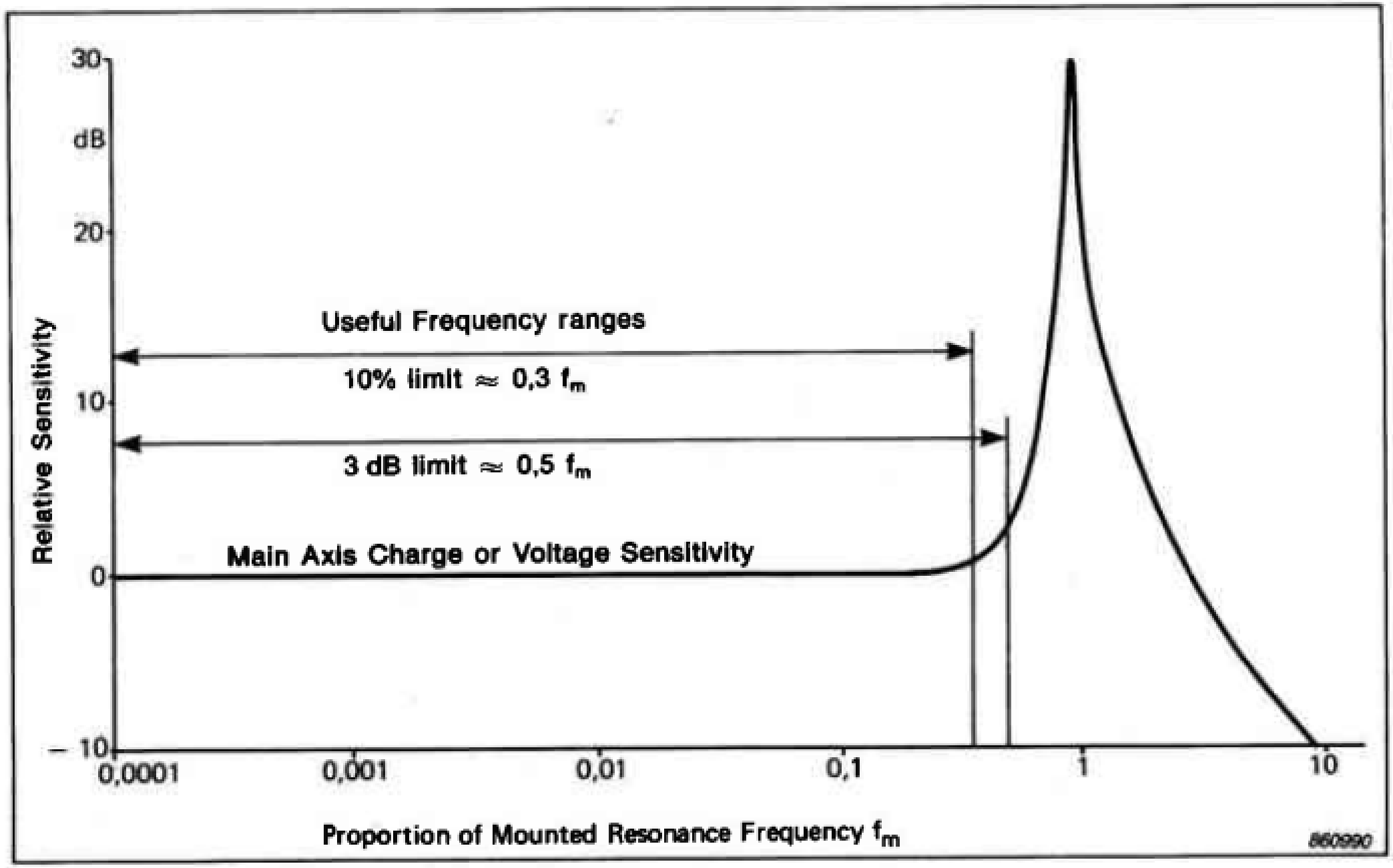
30
dB
20
10
0
– 10
Relative Sensitivity
Useful Frequency ranges
10% limit ≈ 0,3 f_m
3 dB limit ≈ 0,5 f_m
Main Axis Charge or Voltage Sensitivity
0,0001
0,001
0,01
0,1
1
10
Proportion of Mounted Resonance Frequency f_m
860990

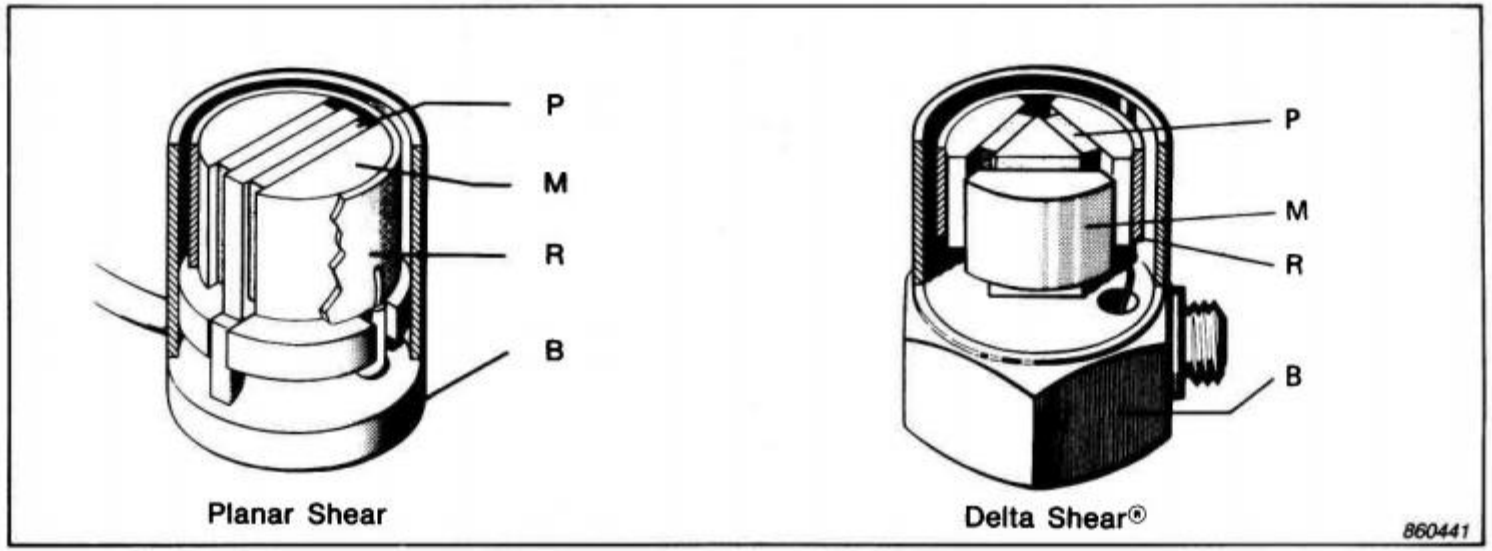

Fig. 2.5. Planar Shear and Delta Shear® designs. M=Seismic Mass, P=Piezoelectric Element, R=Clamping Ring and

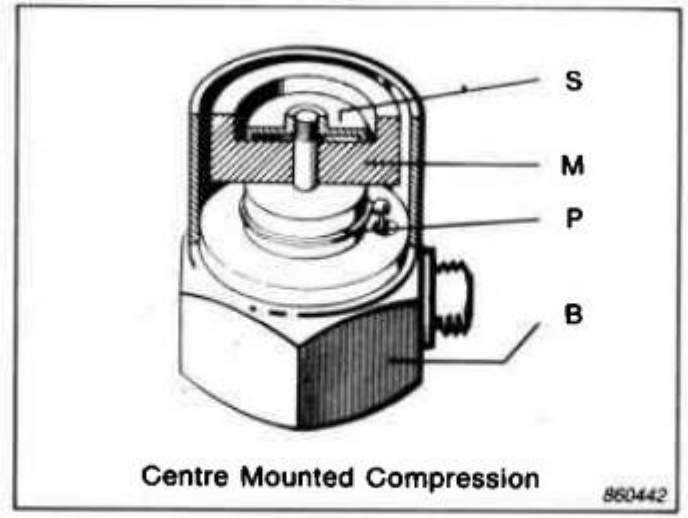

Fig. 2.6. Traditional Compression Design. M=Seismic Mass, P=Piezoelectric Element, B=Base, and S=Spring

2.5.1. Line-drive Accelerometers

These accelerometers contain a built-in preamplifier. A line-drive accelerometer is shown in Fig. 2.7. The accelerometer part of this design is identical to the Delta Shear® construction mentioned above. The electronic part utilizes thick film micro-circuitry techniques to produce a preamplifier with excellent performance characteristics. Chapter 3 includes a description of the operation of the preamplifier section.

Line–drive accelerometers require an external power supply for their operation. The built-in preamplifier is supplied by a constant voltage and the vibration signal is transmitted back to the external supply unit in the form of the modulated power supply current. This system is also described in Chapter 3.

The piezoelectric accelerometer can be regarded as either a charge source or a voltage source. The piezoelectric element acts as a capacitor C_a in parallel with a very high internal leakage resistance, R_a, which, for practical purposes, can be ignored. It may be treated either as an ideal charge source, Q_a in parallel with C_a and the cable capacitance C_c or as voltage source V_a in series with C_a and loaded by C_c, as shown in Fig. 2.8. The equivalent circuits for both models are shown in Fig. 2.8. Both models can be used independently according to which model yields the easiest calculations.

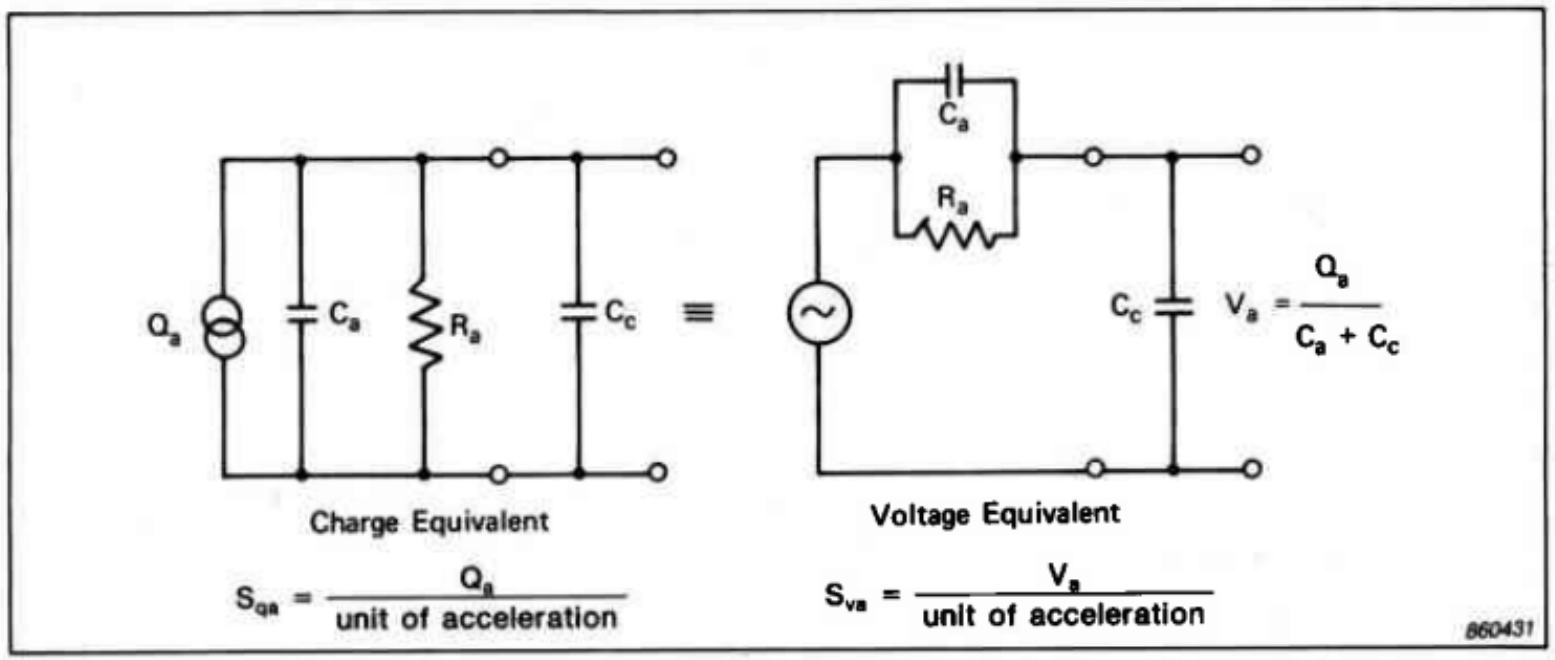

Fig. 2.8. Equivalent electrical circuits for piezoelectric accelerometer and connection cable

The choice of accelerometer preamplifier depends on whether we want to detect charge or voltage as the electrical output from the accelerometer.

The charge sensitivity, S_{qa}, of a piezoelectric accelerometer is calibrated in terms of charge (measured in pC) per unit of acceleration:

$$S_{qa} = \frac{\text{pC}}{\text{ms}^{-2}} = \frac{\text{pC}_{\text{RMS}}}{\text{ms}^{-2}_{\text{RMS}}} = \frac{\text{pC}_{\text{peak}}}{\text{ms}^{-2}_{\text{peak}}}$$

Likewise, the voltage sensitivity can be expressed in terms of voltage per unit of acceleration:

$$S_{va} = \frac{\text{mV}}{\text{ms}^{-2}} = \frac{\text{mV}_{\text{RMS}}}{\text{ms}^{-2}_{\text{RMS}}} = \frac{\text{mV}_{\text{peak}}}{\text{ms}^{-2}_{\text{peak}}}$$

It can be seen from the simplified diagrams that the voltage produced by the accelerometer is divided between the accelerometer capacitance and the cable capacitance. Hence a change in the cable capacitance, caused either by a different type of cable and/or a change in the cable length, will cause a change in the voltage sensitivity. A sensitivity recalibration will therefore be required. This is a major disadvantage of using voltage preamplification and is examined in greater detail in Chapter 3. Charge amplifiers are used nearly all the time nowadays.

Vibration Preamplifiers perform the essential role of converting the high impedance output of the piezoelectric accelerometer into a low impedance signal suitable for direct transmission to measuring and analyzing instrumentation.

In addition to this, the preamplifier may also perform some, or all, of the following roles:

1. Matching measuring instrumentation input sensitivity to that of the accelerometer output.

2. Amplification of the vibration signal to obtain a desired overall system sensitivity.

3. Integration of the accelerometer output to obtain velocity and displacement signals.

4. Warning of overload at both the input and output of the preamplifier.

5. Low and high frequency filtering to reject unwanted signals.

There are two basic types of preamplifiers which may be used with piezoelectric accelerometers.

1. Charge Preamplifiers. These produce an output voltage proportional to the input charge. They do not amplify charge!
2. Voltage Preamplifiers. These produce an output voltage proportional to the input voltage.

Charge preamplifiers are generally used in preference to voltage preamplifiers. This is reflected in the current range of Brüel & Kjær preamplifiers where only the Type 2650 offers both a charge and voltage input. This preamplifier is designed for use in accelerometer calibration rather than general vibration measurements. The distinct advantage of charge amplifiers is that both very short and very long cables can be used without changing the overall sensitivity of the system. However, when a voltage preamplifier is used a change in cable length will necessitate a recalibration of the system sensitivity. This is discussed in section 2.6.1.

Fig. 3.2. shows an equivalent circuit for a piezoelectric accelerometer connected to a charge preamplifier. The nomenclature below refers to this figure.

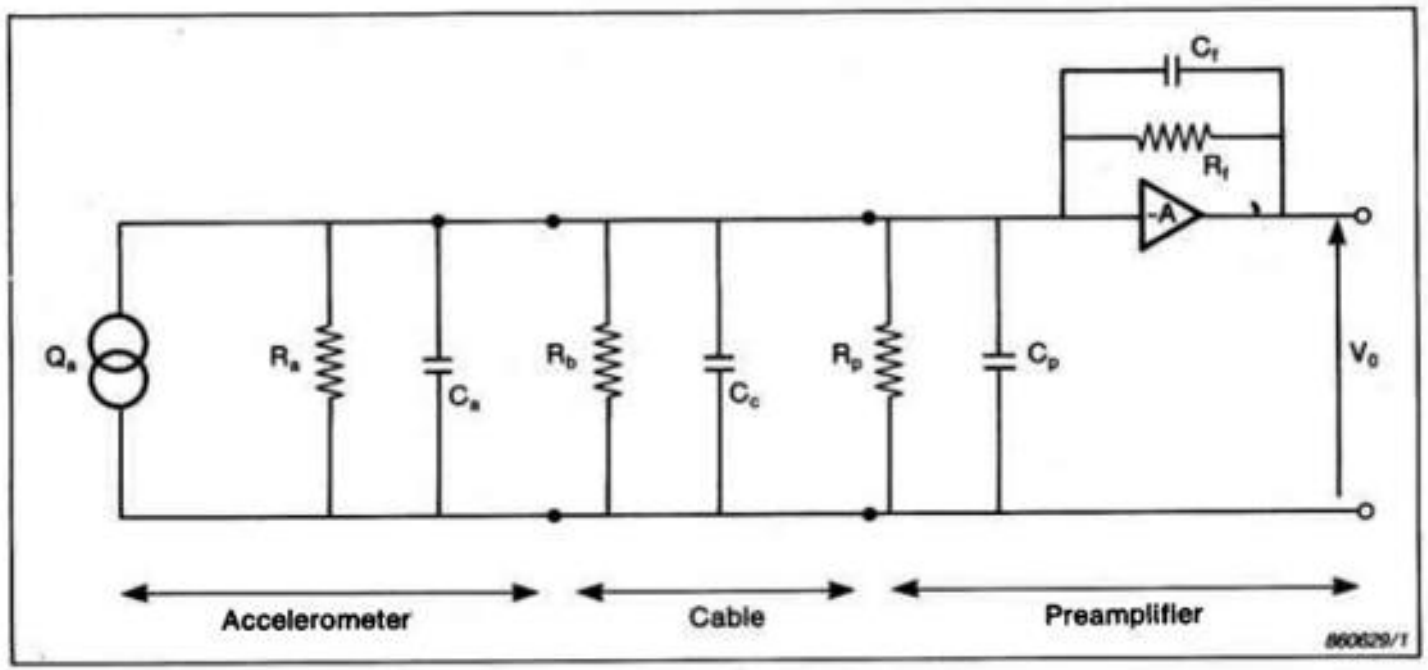

Fig. 3.2. An equivalent circuit for an accelerometer and cable connected to a charge amplifier

Q_a	=	charge generated by the piezoelectric elements (proportional to the applied acceleration)
C_a	=	capacitance of accelerometer
R_a	=	resistance of accelerometer
C_c	=	capacitance of cable and connectors
R_b	=	resistance between cable screen and centre conductor
C_p	=	capacitance of preamplifier input
R_p	=	resistance of preamplifier input
C_f	=	feedback capacitance
R_f	=	feedback resistance
A	=	gain of operational amplifier
V_o	=	voltage output of the preamplifier

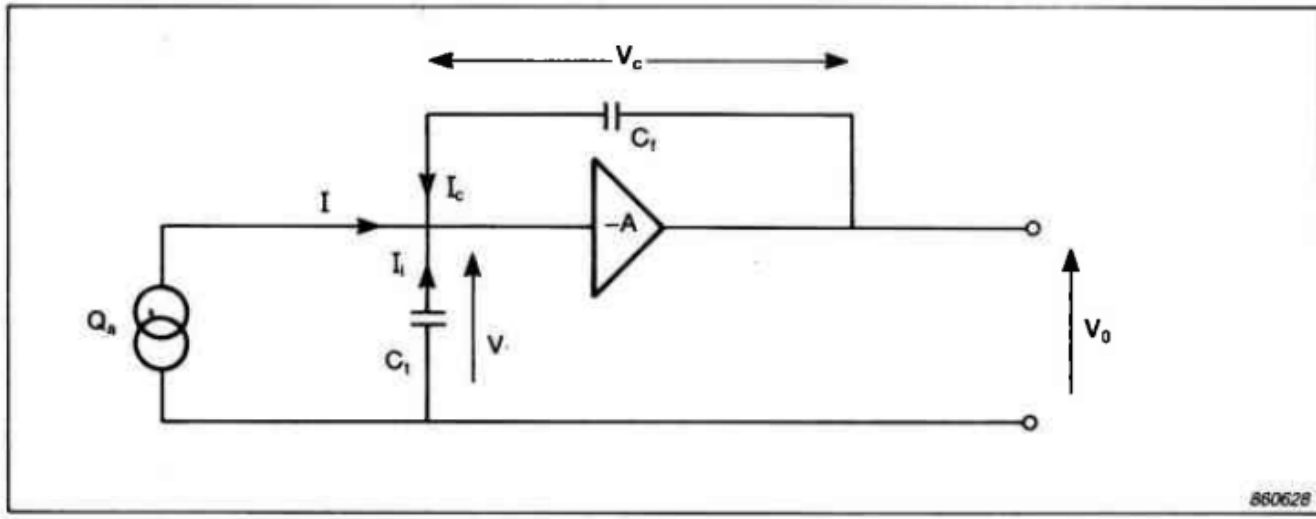

Fig. 3.3. Simplified equivalent circuit of an accelerometer connected to a charge preamplifier

Normally the resistances of the accelerometer, preamplifier input and feedback path can be kept very high. Consequently the circuit in Fig. 3.2 can be reduced to the one shown in Fig. 3.3 where the total capacitance and currents flowing are shown

C_t = $C_a + C_c + C_p$
I = total current flowing out of the accelerometer
I_i = current from C_t
I_c = current in the feedback loop of the operational amplifier
V_c = voltage across feedback capacitance

The input and output voltages, V_i and V_o are related by the equation

$$V_o = -A\,V_i$$

Furthermore V_c can easily be calculated since

$$V_c = V_o - V_i = V_o - \frac{V_o}{-A} = \left(1 + \frac{1}{A}\right) V_o$$

An ideal amplifier has zero input current. Kirchhoff's laws apply to the currents shown in Fig. 3.3.

$$I + I_f + I_c = 0$$

These currents can be defined in terms of other circuit parameters. I is related to the charge produced by the piezoelectric elements.

$$I = \frac{dQ_a}{dt}$$

$$I_c = C_f \frac{dV_c}{dt} = \left(1 + \frac{1}{A}\right) C_f \frac{dV_o}{dt}$$

$$I_i = -C_t \frac{dV_i}{dt} = \frac{1}{A} C_t \frac{dV_o}{dt}$$

By substituting these expressions into Kirchhoff's equation the current from the accelerometer is found

$$\frac{dQ_a}{dt} = -\left(1 + \frac{1}{A}\right) C_f \frac{dV_o}{dt} - \frac{1}{A} C_t \frac{dV_o}{dt}$$

This equation can be solved by integration. Constants corresponding to any DC offset voltage initially present at the amplifier output are assumed to be zero. Such offsets will disappear rapidly as the preamplifier is in use. The solution to the equation then becomes

$$V_o = -\frac{Q_a}{\left(1 + \frac{1}{A}\right) C_f + \frac{1}{A} C_t} \qquad (1)$$

When the magnitude of A is considered ($\approx 10^5$) the solution can be further reduced to the simple expression

$$V_o = -\frac{Q_a}{C_f} \qquad (2)$$

It is clear from this that the output voltage is proportional to the input charge and therefore to the acceleration of the accelerometer. The gain of the preamplifier is determined by the feedback capacitance.

The input capacitance has no effect on the resulting output voltage because, in the ideal case ($A \rightarrow \infty$), the input voltage is zero.

$$V_I = -\frac{V_o}{A} = 0$$

Consequently, the finite input resistance has no effect on the output voltage. This means that only the currents from the accelerometer and the feedback capacitor flow at the input point and these currents are equal in magnitude but are of opposite polarity. It now appears that all the charge flows from the accelerometer to the feedback capacitor.

3.3. VOLTAGE PREAMPLIFIERS

The output voltage of a voltage preamplifier is proportional to the voltage input and the accelerometer is treated as a voltage source. Changes in the cable capacitance cause a change in the overall sensitivity. Changes in the input resistance can cause a change in the low frequency performance.

3.3.1. Voltage Sensitivity

Fig. 3.14 shows the equivalent circuit for an accelerometer connected to a voltage preamplifier. By comparing this circuit with that shown in Fig. 3.2 it can be seen that they are identical except for the connection of the operational amplifier. In this case the operational amplifier is connected as a voltage buffer with a gain of 1 ($V_o = V_i$). The very high input impedance is represented by C_p and R_p. The nomenclature is the same as in Fig. 3.2 and Fig. 3.3.

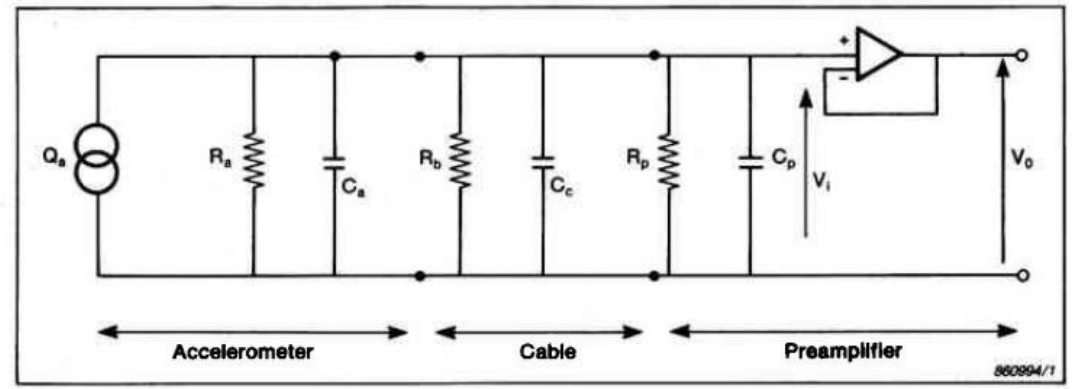

Fig. 3.14. Equivalent circuit of a voltage amplifier using a piezoelectric accelerometer as a voltage source

In Fig. 2.8 it was shown that when the accelerometer is not loaded by a cable and preamplifier it produces an output voltage, V_a equivalent to

$$V_a = \frac{Q_a}{C_a}$$

R_a is a very high parallel resistance and can therefore be ignored. From section 3.2.2 the voltage at the preamplifier input can be written directly

$$V_i = \frac{Q_a}{C_a + C_c + C_p}$$

and therefore

$$V_o = V_i = V_a \frac{C_a}{C_a + C_c + C_p}$$

This expression can be expressed in terms of the charge sensitivity S_{qa} [pc/ms^{-2}] and voltage sensitivity S_{va} [mV/ms^{-2}]

$$S_{va} = \frac{S_{qa}}{C_a + C_c + C_p}$$

$$= S_{va(open)} \frac{C_a}{C_a + C_c + C_p}$$

Where $S_{va(open)}$ is the open circuit (unloaded) accelerometer voltage sensitivity.

Because S_{qa}, the charge sensitivity and C_a are accelerometer constants the voltage sensitivity, S_{va} is dependent on the cable capacitance. This is obviously an undesirable situation because an accelerometer can only be used with the cable with which it was factory calibrated if quoted voltage sensitivities and voltage preamplifiers are used. If the cable is changed then a recalibration is required. A short example will help to illustrate this.

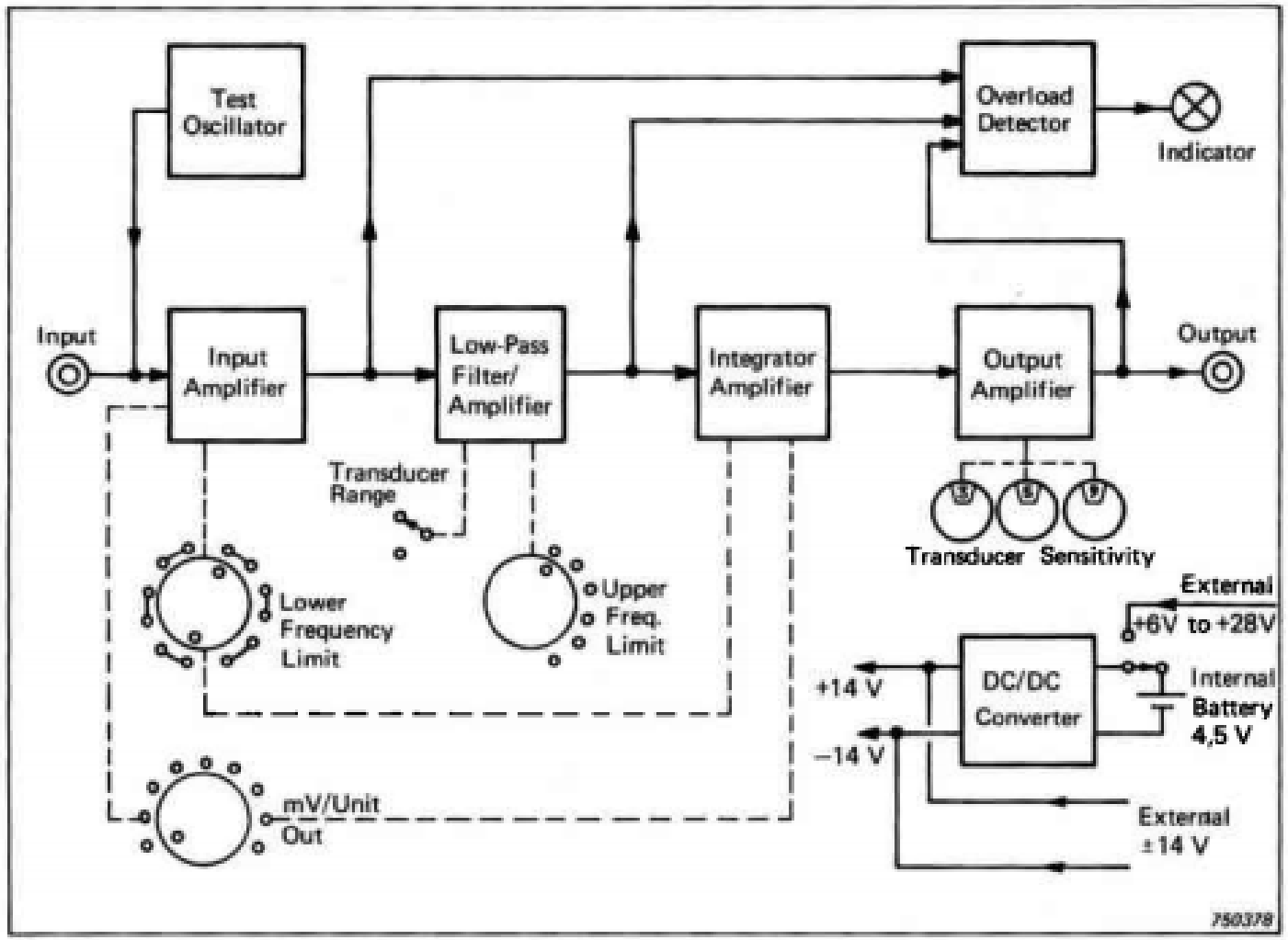

Fig. 3.25. Block diagram showing the arrangement inside a Brüel & Kjær charge amplifier

Let the acceleration signal be represented by a sine wave expressed by

$$a = a_0 \sin \omega t$$

where

a = acceleration at time t
a_0 = acceleration amplitude
ω = frequency in radians per second.

The first integration will yield velocity v

$$v = \int a\, dt$$
$$= \frac{-a_0}{\omega} \cos \omega t$$
$$= v_0 \cos \omega t$$

where

$$v_0 = \frac{-a_0}{\omega}$$

It can be seen that the constant of integration has been taken as zero. This is not true when transient signals are integrated.

The second integration yields the displacement signal, x

$$x = \int v\, dt$$
$$= \frac{-a_0}{\omega^2} \sin \omega t$$
$$= x_0 \sin \omega t$$

where

$$x_0 = \frac{-a_0}{\omega^2}$$

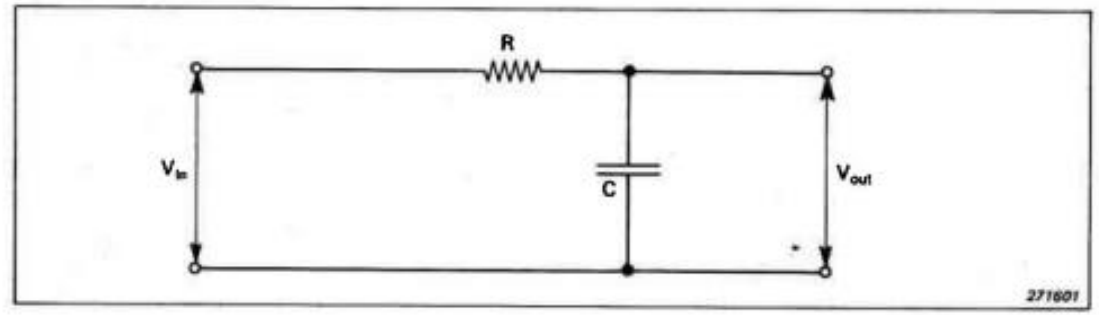

Fig. 3.26. A simple RC integration network

This simple analysis has demonstrated that integration is achieved by dividing the acceleration by a factor proportional to the frequency to obtain velocity, and by a factor proportional to the square of the frequency to obtain displacement.

Electronic integration, at its most basic level can be achieved using a electronic network similar to that shown in Fig 3.26.

When the voltage V_{in} from the accelerometer and preamplifier is applied to the input, the voltage across the capacitor V_{out} can be shown to be

$$V_{out} = \frac{V_{in}}{1 + j\omega RC}$$

when $\omega RC >> 1$ then

$$V_{out} \approx \frac{1}{jRC} \frac{V_{in}}{\omega}$$

By comparing this expression with the previous integration analysis it can be seen that an electronic integration has taken place. The factor 1/RC can be taken care of in the internal calibration. A double integration is achieved by using a second integration network to yield displacement information.

EFEITO DO TIPO DE MONTAGEM

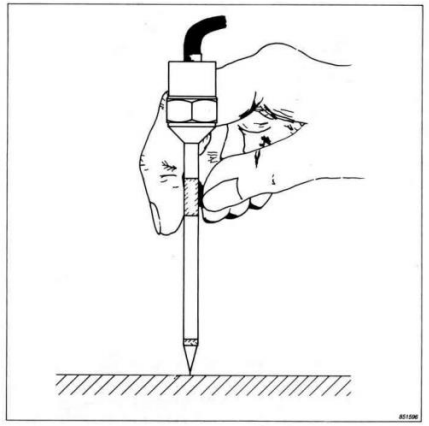

Fig. 4.19. The use of the Hand Probe YP 0080 for rapid vibration measurements

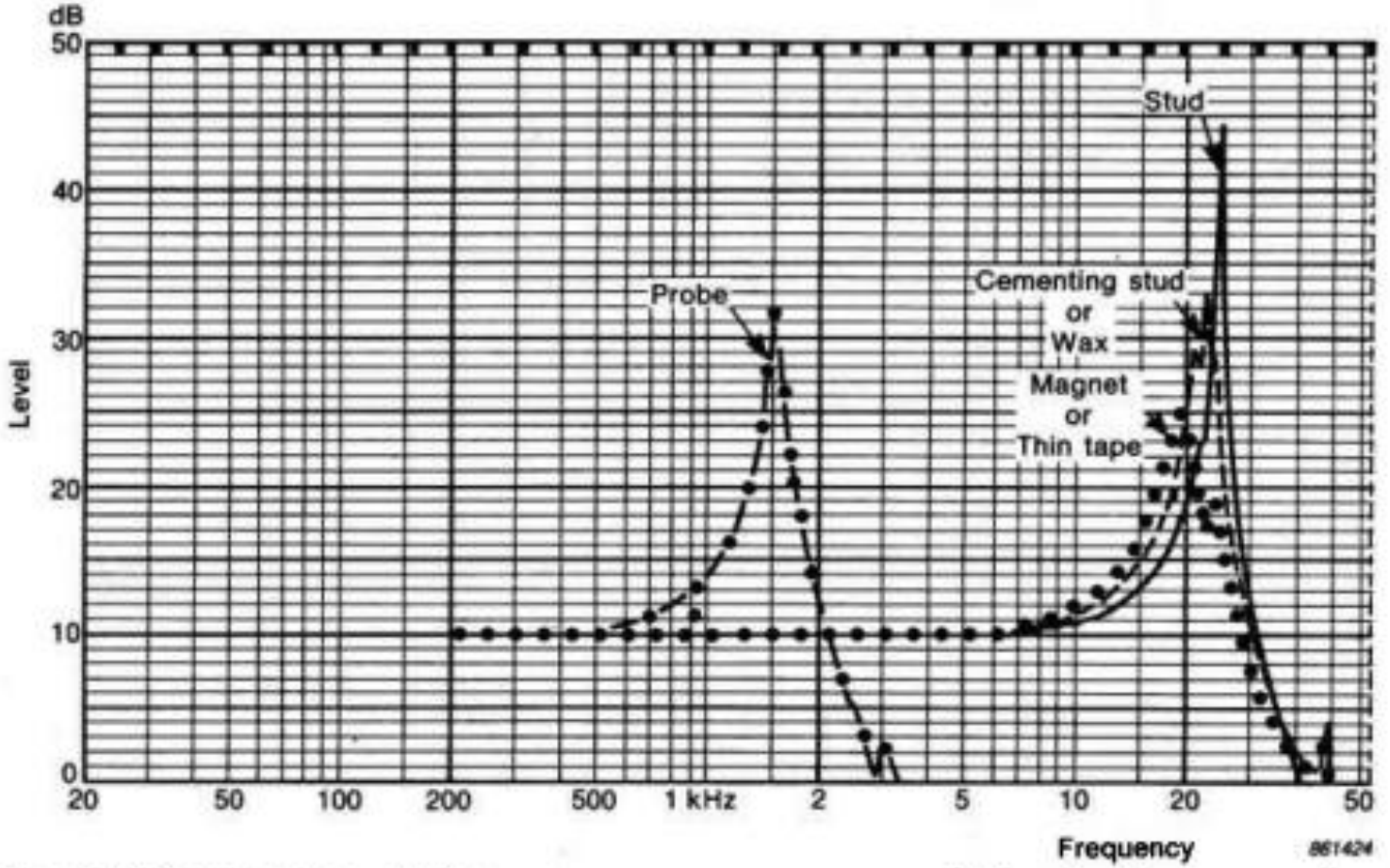

Fig. 4.7. Comparison of frequency response curves obtained using several accelerometer mounting techniques

Piezoelectric sensors require some precautions when connecting to sensitive electronic components. First and foremost, the voltage levels created by hard shock can be very high, even around 100-V spikes.

More than likely, an op amp will be used to interface these sensors to an A/D converter, either discrete or on a microcontroller. One tip is to choose a high-input-impedance op amp to minimize current. One possible candidate is the Linear Technology JFET input dual op amp. It has 10^{12} Ω input resistance and a 1 MHz gain bandwidth product, good enough to easily handle the vibration ranges of piezoelectric sensors.

Another suitable part is the TLV2771 from Texas Instruments. This rail-to-rail low-power op-amp also has a 10^{12} Ω differential input resistance and a 5 MHz unity-gain bandwidth. Signal conditioning in a single stage can prepare the input from the shock sensor directly into an A/D converter (Figure 3).

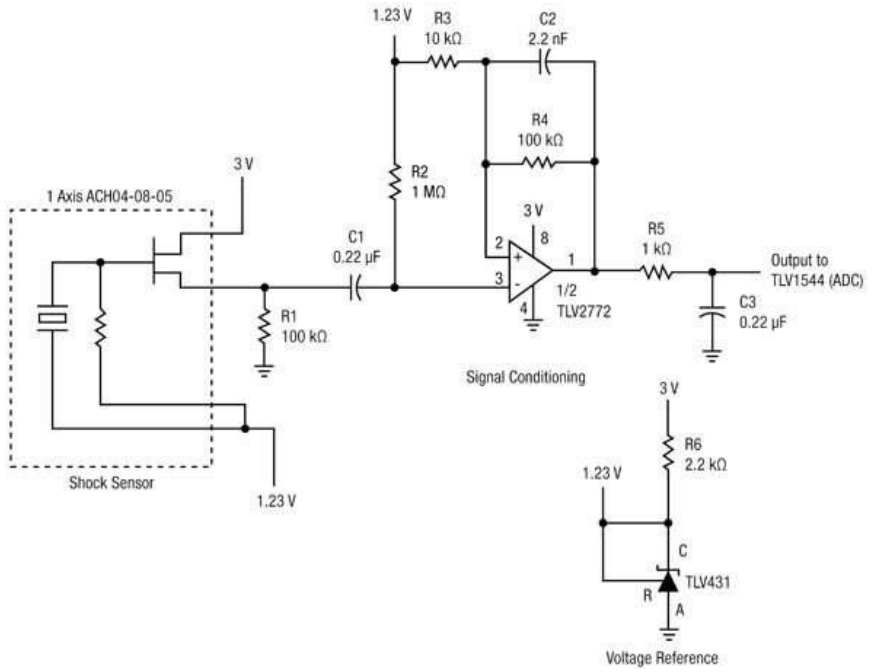

Figure 3: Op amps such as the TI TLV2772 feature high input impedances to help minimize current from the potentially high-voltage inputs from the piezoelectric sensors.

Op-amp circuits can be designed to operate in voltage mode or charge mode. Charge mode is used when the amplifier is remote to the sensor. Voltage mode is used when the amplifier is very close to the sensor.

6.7.3 Charge Output Circuits

Some sensors (e.g., piezoelectric film sensors) measure or detect charge variation. When using this type of sensors, care must be taken since stray capacitance can shunt the sensor output to ground. The capacity of the cable from the sensor to the amplifier and the input impedance of the amplifier are also critical. If the impedance is too small, any small resistance can easily shunt the input sensor signal, resulting in large errors. Special amplifiers called charge amplifiers are available to condition these types of sensor signals. A charge amplifier has very high input impedance, and a capacitor is inserted into the input stage. It is not as sensitive to distributed capacity as a normal operational amplifier (op-amp) would be.

A sensor's charge output can be converted into a voltage using a circuit shown in Figure 6.25. R_1 and C_1 create a high-pass filter (HPF); R_1 also provides a bias path to prevent the inverting input of the op-amp from drifting over time. Any change in charge, Q_{SEN}, will appear almost exclusively across C_1, providing an accurate measurement of sensor output, Q_{SEN}. Thus, the sensor's charge output Q_{SEN} is converted into an output voltage V_{out}. This layout also rejects the common mode noise.

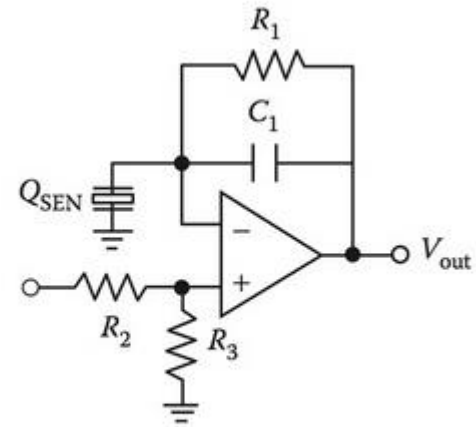

An amplifier circuit for a charge output sensor.

DEMONSTRAÇÃO DE UM SENSOR + TRANSDUTOR

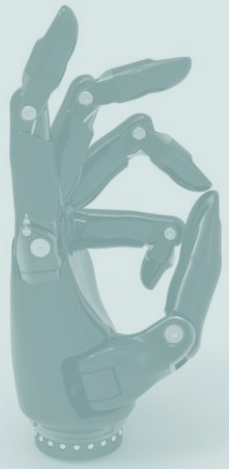
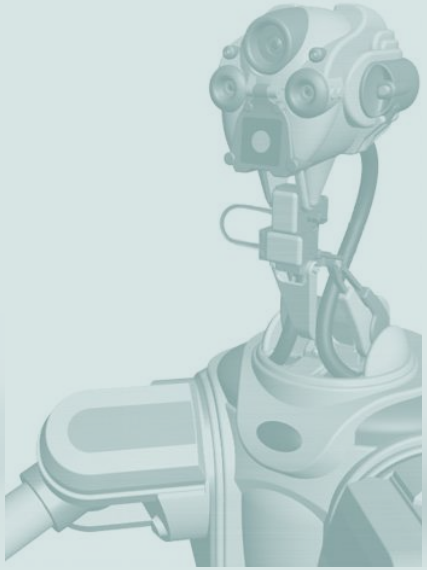
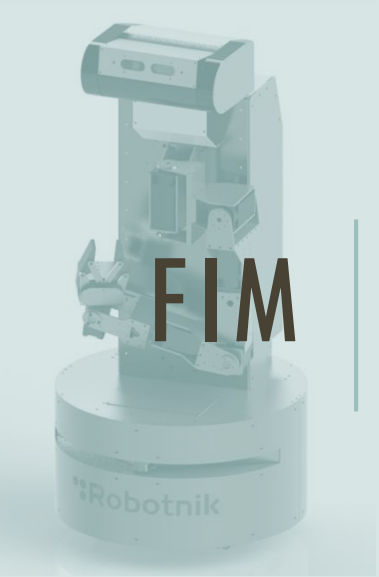

FIM